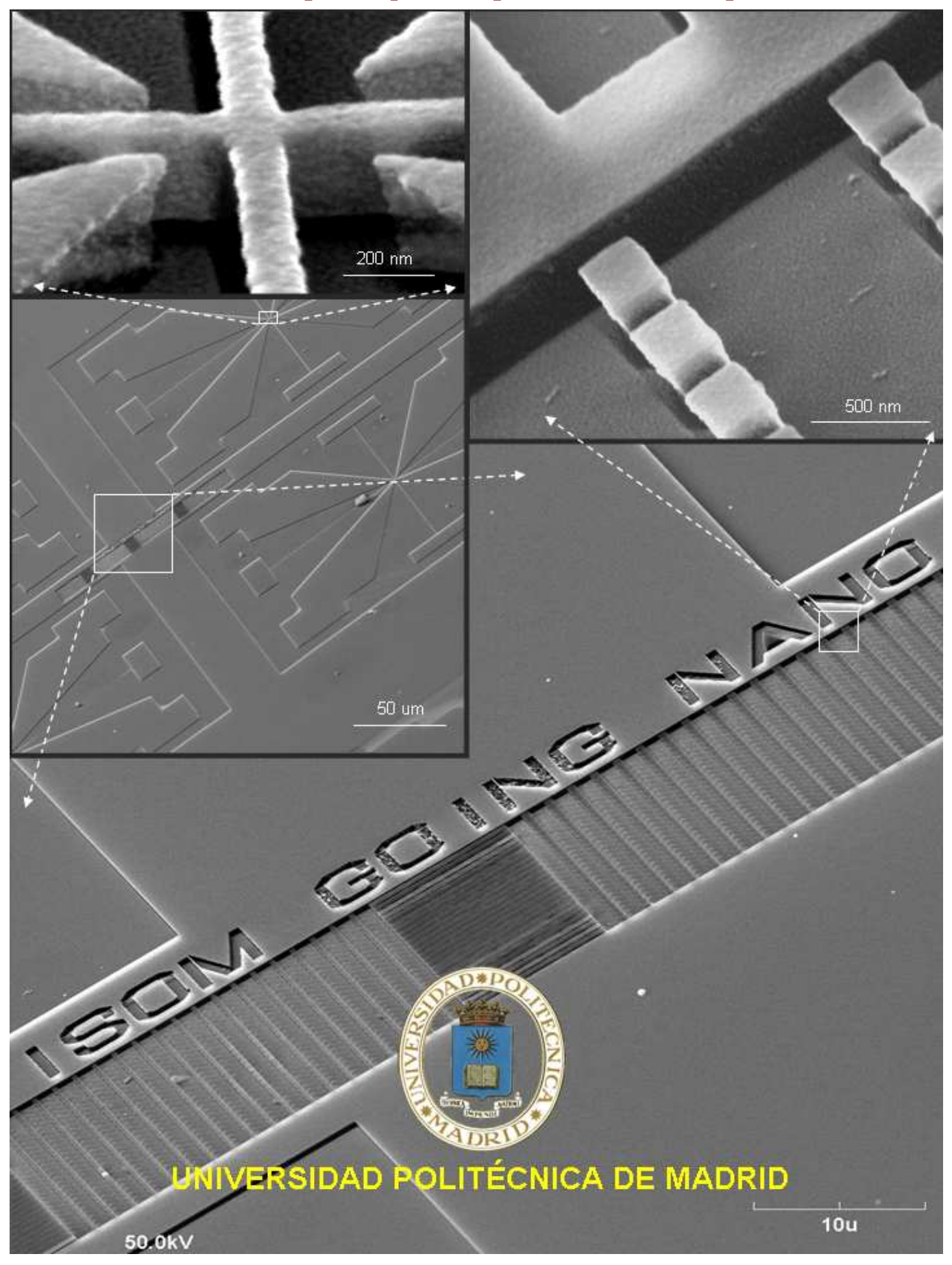


INSTITUTO DE SISTEMAS OPTOELECTRÓNICOS Y MICROTECNOLOGÍA

(INSTITUTE FOR SYSTEMS BASED ON OPTOELECTRONICS AND MICROTECHNOLOGY)

Activity Report (2004-2006)



Different picture zooms of a lithographic pattern on a 500 nm thick resist. The center-left picture shows a panoramic view of four terminal device lithographies with their contact pads. The top-left picture is a zoom of the center area with cross junctions and four 'concentrators' adjacent to the junction. The potential of the lithography even for thick resists is very clear in this picture. Thinner tracks in the cross junction are easily achievable. The bottom picture shows the logo of the lithography and on the top right there is a zoom into that logo, showing some nano-square pillars.



Instituto de Sistemas Optotelectrónicos y Microtecnología

(INSTITUTE FOR SYSTEMS BASED ON OPTOELECTRONICS AND MICROTECHNOLOGY)

Universidad Politécnica de Madrid

Activity Report

2004-2006

E.T.S. Ingenieros de Telecomunicación Ciudad Universitaria s/n 28040, Madrid

Teléfono: (34) 91 336 6832 Fax: (34) 91 336 6832

http://www.isom.upm.es

PREFACE

The Institute for Systems based on Optoelectronics and Microtechnology (ISOM) is devoted to research and development activities in information and communication technologies based on III-V semiconductors, magnetic and non-metallic materials. This report summarizes the technical and scientific activities carried out at ISOM in years 2004-06, inclusive. Looking back, this period has been key in the growth and consolidation of ISOM scientific staff, in installing new technical facilities and in carrying out leading research activities. Complementing the research teams of Semiconductor Devices and Magnetic Devices, which founded ISOM in Y2000, a new group from the Chemistry Department of UPM, led by Prof. Manuel Laso and devoted to the simulation of non-metallic materials, joined ISOM in Y2005. We are very proud of joining forces with such world class team, giving ISOM new strengths in the area of materials for information technology and nanostructures.

UPM launched in 2005 a program aiming to provide tenure research positions to young researchers with outstanding scientific curricula. This UPM program, plus the national Ministry of Education (MEC) program for postdoctoral fellows (Ramón y Cajal), has allowed ISOM to gain five experienced research members, already leading some new research activities.

In 2006 UPM institutes underwent a scientific evaluation by external committees, for the first time. ISOM was evaluated in June 2006, with a very favourable final report by the evaluation committee. As we tried to emphasize already in the cover plate, in this period ISOM moved to nanofabrication and nanoengineering by decisive steps. A new MBE system for III-nitrides growth, granted by the Madrid Regional Administration, started operating in 2004. A second key nanotechnology facility, an electron beam nanolithography system, funded by the Spanish Ministry of Education was installed and set in operation in the fall of 2006.

Research on semiconductor materials and devices at ISOM has been largely based on binary and ternary compounds containing nitrogen (group III nitrides), leading to either wide or narrow band-gap heterostructures. These compounds show quite interesting properties, many scientific challenges and important applications. Progresses in optical sensors based on nitride QD and QW, nanocavity structures for quantum computing and nanoemitters, IR lasers based on dilute nitrides, acoustic wave devices, high temperature electronics, and in understanding the surface physicochemical properties of AlGaN/GaN transistors, have been made in this period. In the area of magnetic materials, research has been focused on nano and microstructured soft materials, multilayer microsystems, hybrid systems and magnetic nanoparticle fabrication, structures to be used in multifunctional sensors and biomedical imaging.

The research period covered by present report shows ISOM significant participation in European Union research programs, in both the VI Framework Program and through the newly formed European Defence Agency. A new line of research on photonic devices based on slot-waveguides was initiated in 2006 as a participation in an EU FP6 project. Besides, the association of ISOM with CSIC-IMB-CNM also led to a joint international project.

As summarized in this report, ISOM participated significantly in national and regional research programs. Rapid

developments in information, communication and nanotechnologies moved us to seek and to obtain the participation in

frontier research areas as nanotechnology, biosensors and MEMS. ISOM cooperation with Spanish industries and

institutions has been reinforced in this period. Direct contracts with companies, and joint projects funded by the Spanish

Administration (PROFIT projects) have supported such cooperation.

Although in 2001 the Technology Center of ISOM was acknowledged as a Scientific and Technological

Singular Facility (ICTS) by the Spanish MEC, it has been in 2005 when the mechanisms for providing technological

services to external academic labs were defined by MEC. We consider this activity of ISOM as having a clear priority in

the institute strategy and objectives.

Finally, I wish to thank all ISOM scientific staff members, PhD students and support personnel for their

commitment and continuous efforts through these years. We acknowledge the support of the various funding institutions

for their confidence in our activities. Thanks also are given to the Electronic Engineering, Applied Physics and

Chemistry Departments, to the ETSIT and ETSII Directors and to the UPM Rector for their continuous support and

understanding. Special credit has to be given to Pedro Sánchez, Marco Maicas and Montse Juárez for their dedication

and efforts to make this report to be possible.

Madrid, January 2007

Elias Muñoz Merino

Director

V

Activity Report 2004-2006

CONTENTS

1	PR	RESENTATION AND OBJECTIVES	8
2	OK	RGANIZATION CHART	12
3		TS (SCIENTIFIC AND TECNOLOGICAL SINGULAR INFRAESTRUCTURE, XTERNAL ASSISTANCE)	
	3.1	Description of the ICTS: "CT-ISOM"	18
	3.2	Services offered by the CT-ISOM	19
4	TE	ECHNOLOGICAL AND CHARACTERIZATION FACILITIES	20
	4.1	Materials Growth and Processing Systems	22
	4.2	Characterization Systems	22
	4.3	ISOM going nano	24
5	RE	ESEARCH LINES	28
	5.1	Microsystems and Nanotechnology	30
	5.2	Optical Sensor Systems	30
	5.3	Optical Communications	31
	5.4	Systems with Magnetic Sensors	31
	5.5	Simulation of Non-Metallic Materials	31
6	RE	ESEARCH REPORTS	32
	6.1	Group III-nitride-based photodetectors: new functionalities and advanced structures	34
	6.2	Quantum Dot structures for IR detectors and 1.3 µm lasers	38
	6.3	MBE growth of III-V-N quantum structures for optoelectronic devices	42
	6.4	III-Nitride Nanocolumnar heterostructures	46
	6.5	Lasing Characteristics of 1.3-1.52 µm GaInNAs/GaAs QW Laser Diodes: Degradation Mechanisms	

6.6	Characterization of InN layers and nanocolumns grown on Silicon (111) by Plasma Molecular Beam Epitaxy	
6.7	AlGaN/GaN High Electron Mobility Transistors	58
6.8	SAW and PSAW Devices in Nitride Heterostructures: Characteristics and Novel Applications	62
6.9	Photonic devices based on slot-waveguides	66
6.10	An approach to an integrated magnetic sensor	70
6.11	New RFID system of low frequency that avoids screening magnetic problems	74
6.12	Domain walls and exchange-interaction in Permalloy/Gd films	78
6.13	Nanocavity oscillation and collapse in viscoelastic fluids	82
6.14	Bijective-mapping min-map Monte Carlo for chain molecules	86
7 R	ESEARCH PROJECTS	90
7.1	International Public Funding	92
7.2	National and Regional Public Funding	93
7.3	Funding from companies and institutions:	96
8 D	ISEMINATION OF THE SCIENTIFIC ACTIVITY	98
8.1	Papers in Scientific Journals and Books	100
8.2	Conferences and Meetings	108
8.3	Invited Talks	116
8.4	Ph.D. Thesis	118
8.5	B.Sc. Thesis	120
8.6	Patents	121
9 R	&D COLLABORATIONS, SERVICES AND SEMINARS	122
9.1	International	124
9.2	National	125
9.3	Cooperation and Services	126
9.4	Stays abroad of ISOM members	129
9.5	Programme Committees Membership	130
9.6	Invited Seminars held at ISOM	132
9.7	Internal Seminars by ISOM members	135
9.8	Scientific workshops and meetings organized by ISOM members	138
10 F	UNDING INSTITUTIONS	140
11 14	TEMPEDS	144

1 PRESENTATION AND OBJECTIVES



The *Instituto de Sistemas Optoelectrónicos y Microtecnología* (ISOM) is an interdepartmental research institution of *Universidad Politécnica de Madrid* (UPM). ISOM was created on March 16th, 2000. ISOM technological facilities are located in the basement of the *López Araujo* building at the *Escuela Técnica Superior de Ingenieros de Telecomunicación* (ETSIT) of UPM (*Ciudad Universitaria* campus). These facilities include a 400 m² clean room and 300 m² of characterization and system development laboratories. Simulation activities of non-metallic materials are carried out at the *Escuela Técnica Superior de Ingenieros Industriales* (ETSII) of UPM (*Nuevos Ministerios* location). The institute has presently 42 researchers, 1 computer manager, 1 clean room engineer, 3 technicians and 1 administrative assistant. Researchers from Electronics, Physics and Chemistry Departments are combining their research efforts in a truly multidepartment and pluridisciplinar R&D institute.

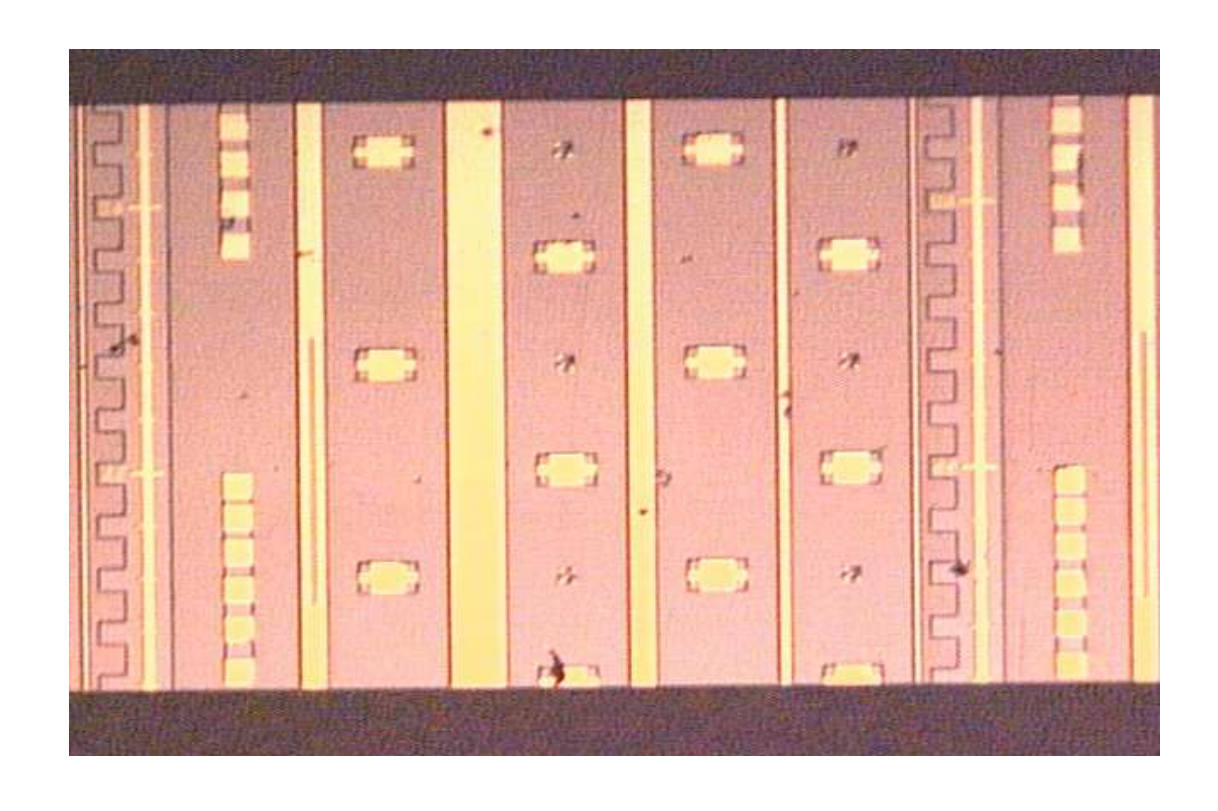
The mission of ISOM is to perform research in the fields of detection, processing, transmission and recording of information by means of micro and nanotechnologies based on the optical, electronic, magnetic and chemical properties of materials and structures. As a university institute, education and training of innovative professionals and scientists is a first priority, to be accomplished through their participation in research and development activities seeking new knowledge, and through graduate education programs.

The Technology Centre of ISOM was awarded the recognition as a "Scientific and Technological Singular Facility" (ICTS) by the Spanish Ministry of Education in 2001. Through periodic public calls, ICTS-ISOM offers its services on technology, processing and characterization to the Spanish and EU scientific and technical community.

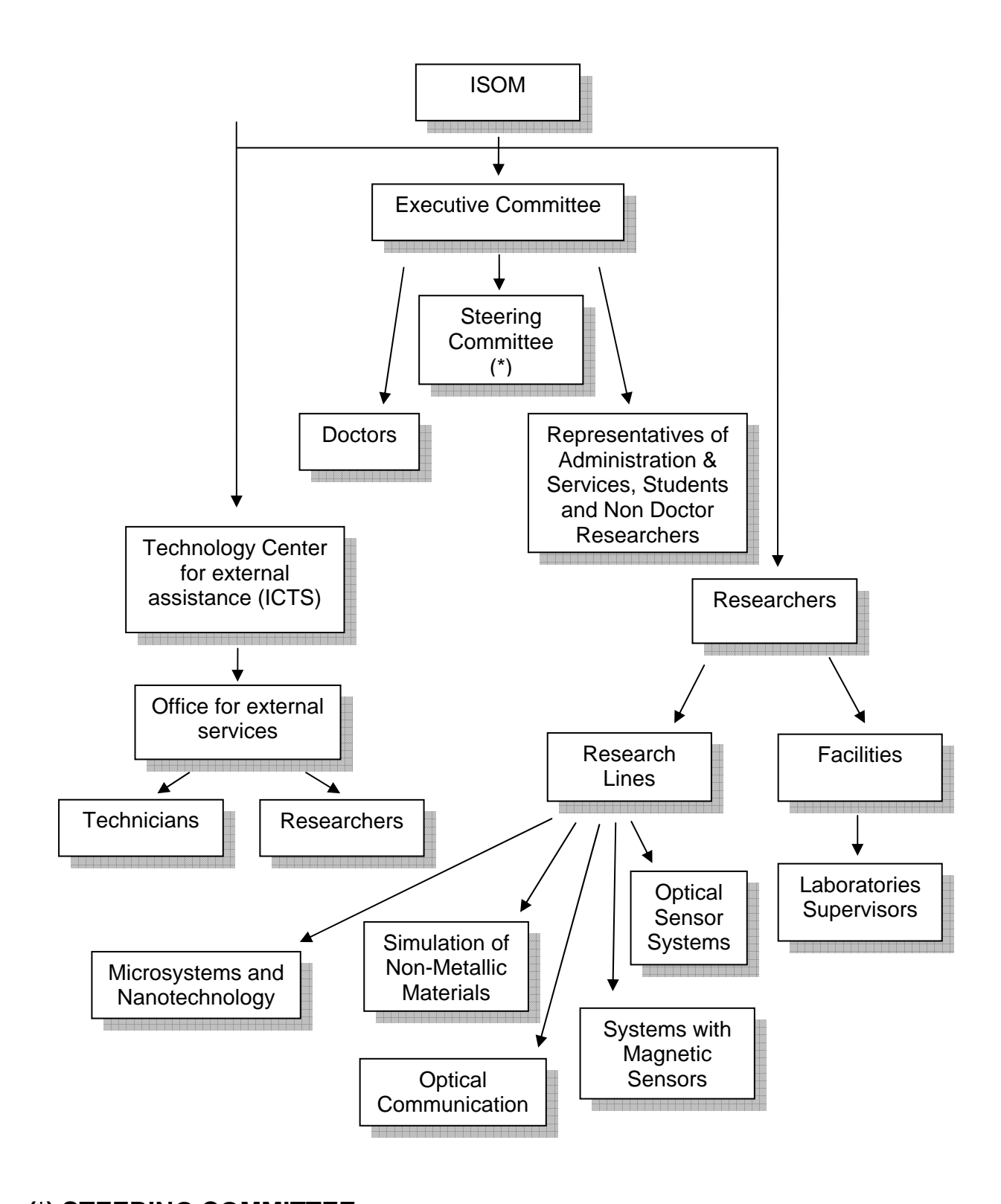
The transfer of R&D results to the industry, the cooperation with external laboratories and institutions, are very important objectives pursued by the institute. ISOM seeks to be a R&D laboratory able to participate and to lead research projects at the European Union and international level. ISOM aims to be a centre of excellence, a reference research laboratory, and a singular scientific and technological facility that openly provides assessment and services to other academic and non-academic entities. The institute intends to contribute to the generation of spin-off companies by means of temporary agreements on usage of clean room space and processing equipment as well as by providing its R&D expertise.

Since 2002, ISOM is an Associate Unit of *Consejo Superior de Investigaciones Científicas* (CSIC), through IMB-CNM (*Instituto de Microtelectrónica de Barcelona, Centro Nacional de Microtelectrónica*).

2 ORGANIZATION CHART



Plane view picture of a series of processed edge-emitting Galn(N)As/GaAs quantum well laser diodes (vertical stripes), grown by MBE on n-GaAs. These lasers are broad area laser diodes with Fabry-Perot cavities defined by cleavage and widths ranging from 10 to 100 μ m. Their emission wavelengths can be tuned from 1 to 1.55 μ m, thus covering the 1.3 and 1.55 μ m windows for optical fiber communications applications.



(*) STEERING COMMITTEE:

Director: Elías Muñoz Merino
Vice-director and ICTS coordinator: Pedro Sánchez Sánchez

Secretary: Adrián Hierro Cano

Technical coordinator: Claudio Aroca Hernández-Ros

Administrator: Enrique Calleja Pardo

from January 2007 : Alvaro de Guzmán Fernández González

3 ICTS (Scientific and Tecnological Singular Infraestructure, for external assistance)



High Resolution Electron Beam Lithography System (CRESTEC CABL-9500C)

3.1 Description of the ICTS: "CT-ISOM"

At the end of 2001, the "Technology Center of ISOM" (CT-ISOM) was acknowledged as a Large Scientific Infrastructure (GIC) by the Spanish Ministry of Science and Technology. Recently (BOE June 16th 2006) the GIC were renamed as "Singular Scientific and Technological Infrastructure" (ICTS). This title acknowledges the important material and human resources of the Centre that are open to offer scientific and technological services and assistance. Thanks to these resources, we are able to develop state of the art technology and to establish scientific links with other top research centres, both inside Spain and overseas, in the fields of Micro and Nanotechnology. We should highlight that our institute is presently the only ICTS in Spain belonging to a University.

The CT-ISOM has both a Clean Room and different Laboratories for devices and materials characterization. In these installations researchers, technicians and administrative personnel work to sustain our research lines and to provide external services. In particular, the research groups of the ISOM have participated in the last 15 years in a large number of European projects.

The facilities at the CT-ISOM allow the fabrication of different materials, technological processing, and implementation of different devices and integrated electric, optic, optoelectronic and magnetic structures. Indeed CT-ISOM has the capacity to develop and fabricate laser diodes for instrumentation, environment and optical communications; high power and high temperature microwave transistors; infrared detectors for military and non-military applications; ultraviolet detectors to monitor the UV radiation from the sun and for military applications; visible light detectors for biophotonic applications; magnetic sensors for all sort of applications and also SAW RF filters for sensors and mobile phones, nanooptical cavities, etc. The range of possibilities of the CT-ISOM covers not only the micrometric scale, but also the nanometric frontier thanks to the newly acquired e-beam lithography system. This tool allows a line resolution of about 10 nm.

The CT-ISOM has developed processing and fabrication protocols that allow a control of the incidences and of the final quality of the structures. Each processing order gets a "processing form" where all the individual processes and their incidences are recorded. This gives us a feedback for future processing so we can improve it or to reproduce it. The information from these processing forms is later incorporated to the Specific Fabrication Protocols of the CT-ISOM.

3.2 Services offered by the CT-ISOM

The CT-ISOM offers external services within the research lines (Chapter VI) and capabilities of the Institute (Chapter V), from a simple characterization to the complete device fabrication (sensors, actuators, transistors, integrated structures, filters, optical emitters, etc). The CT-ISOM has the capability to fabricate and optimize a designed structure, thanks to its technology line, design and fabrication of masks, deposition of many types of materials and characterization of the final product/device.

These external services are offered to the industry and to all scientific community, national and international.

The academic researches interested on using the facilities of the CT-ISOM have now the possibility of doing it free of charge under the call "Ayudas financieras para la mejora de las Infraestructuras Científicas y Tecnológicas Singulares (ICTS) y para el acceso a las mismas" (BOE 04/08/06). Find details in our website:

http://www.isom.upm.es

- CT-ISOM: Singular Scientific and Technological Infrastructure.
- Services offered by the CT-ISOM.

This initiative from the Ministerio de Educación y Ciencia (MEC) has the following objective:

"to promote the access of new research groups or individual investigators to ICTS, for the acquisition of new knowledge, their formation on the technology available at the Installation or for the completion of their research work"

The selection of applications that could benefit from the terms of this service is first done by an internal CT-ISOM committee. In this evaluation, the Institute determines the viability of the research requested and selects a number of proposals. Further, an External Committee, formed by prestigious national investigators, chooses and ranks among the proposals selected.

Today, the equipment needed for micro and nanotechnology is very expensive and requires an expensive maintenance. Therefore a national policy from MEC has been launched to allow ALL researchers to have access to the equipment available at the various ICTS, so they are able to complete their research.

4 TECHNOLOGICAL AND CHARACTERIZATION FACILITIES



Compact21S RIBER MBE system dedicated to the growth of III-Nitrides materials (GaN, AIN, InN and their alloys). The MBE system has 7 source ports, including a central flange for the installation of the radio-frequency plasma source to activate the nitrogen. Introduction of samples is implemented by the use of a loadlock chamber. The system is also provided with standard in-situ real-time characterization techniques such as RHEED (reflection high energy electron diffraction) and RGA (residual gas analyzer).

4.1 Materials Growth and Processing Systems

- Molecular Beam Epitaxy (MBE) (3 systems)
- Magnetron Sputtering system (3 systems)
- Chemical Vapour Deposition (CVD and PE-CVD)
- Metal Deposition (Joule, e-beam) (5 systems)
- Electron Beam Nanolithography (resolution ~ 10 nm)
- Electron Beam Lithography (resolution ~ 0.2 μm)
- UV Photolithography (resolution $\sim 1 \mu m$) (2 systems)
- Reactive Ion Etching (RIE)
- Standard and Rapid Thermal Annealing (RTA)
- High precision disk sawing systems and diamond Scriber
- Ultrasonic and Thermocompression Microsoldering (2 systems)

4.2 Characterization Systems

A) Surface and Structural properties

- High Resolution X-Ray Difractometers (HR-XRD) (2 systems)
- Thickness Profiler (DekTak)
- Atomic Force Microscope (AFM)
- Scanning Electron Microscope (SEM) with EDAX

B) Electric and Magnetic properties

- Electrical and Optical Characterization Systems under Hydrostatic Pressure.
- Carrier Traps and Defect Analysis Techniques (DLTS, AS, etc.)
- Two-port and microstrip probes for RF analysis (up to 20 GHz)
- Electrical Characterization (transistor curve tracer, I-V parametrizer, impedance bridges up to 1GHz, sampling oscilloscopes, nanovolt generators, lock-in amplifiers, boxcar amplifiers, low noise amplifiers, system analyzer, etc.)
- Hall Effect System (including cryostat)
- Magnetic Characterization (VSM, including cryostat)
- Magnetic Force Microscope (MFM)

C) Optical properties

- VIS and IR Fourier Transform Absorption Spectrometer (FTIRS)
- High Resolution Nomarski Optical Microscope
- Ellipsometry System
- Cryogenic Systems (5 systems)
- UV, VIS and IR Luminescence (PL) (4 systems)

D) Device characterization

- Probing Stations (Low Capacitance) for VLSI and discrete devices (2 systems)
- Probing Station for RF measurements
- VIS-IR Optical Spectrum Analizer (OSA) for LEDs and Lasers
- Electrical Characterization Systems for Transistors and Devices up to 20 GHz (C-V, I-V, C-f, 1/f noise, T, etc.)
- Image Capture and Analysis System
- Optical characterization for detectors (from IR to UV)
- High temperature device assessment chamber

4.3 ISOM going nano

Our institute has recently installed an e-beam nano-lithography tool (high resolution electron beam lithography, HREBL), CRESTEC CABL-9500C (see Figure 1). This is the second HREBL from this manufacturer in operation in Europe after the one in the university of Magna Grecia and before the one recently acquired by the University of Cambridge.

Perhaps the best characteristics of this tool is the minimum line width, which can go below 10 nm and its outstanding stability, in both beam current and beam position.

The system performances are listed below

Writing method: Vector and raster scanning using Gaussian distribution electron beams.

Stage-movement: Using stepping motors.

X and Y axes: Laser interferometer for positining. Resolution: 0.6 nm.

Z axe: Semiconductor laser displacement for height control.resolution 200 nm.

Wafer size: 2,3,4,5,6,8 inch wafers and irregular pieces.

Electron beam scanning areas: 60,120,300,600 microns.

Minimum lithography line width. 10 nm. Minimum electron beam diameter: 2 nm.

Beam current: 5 pA to 800 nA.

Beam current stability: Less than 1% / 5 h (at ± 0.1 °c temperature stability).

Beam current homogeneity: Less than 0.5 %

Beam position stability: ±30 nm/5h.

Stiching accuracy:

 $50~\text{nm}~(\text{mean} + 3\sigma)$ for $500~\mu\text{m}$ scanning area.

 $35~nm~(mean + 3\sigma)$ for $100~\mu m$ scanning area.

20 nm (mean + 3σ) for 50 μ m scanning area.

Overlay accuracy:

50 nm (mean + 3σ) for 500 μ m scanning area. 35 nm (mean + 3σ) for 100 μ m scanning area.

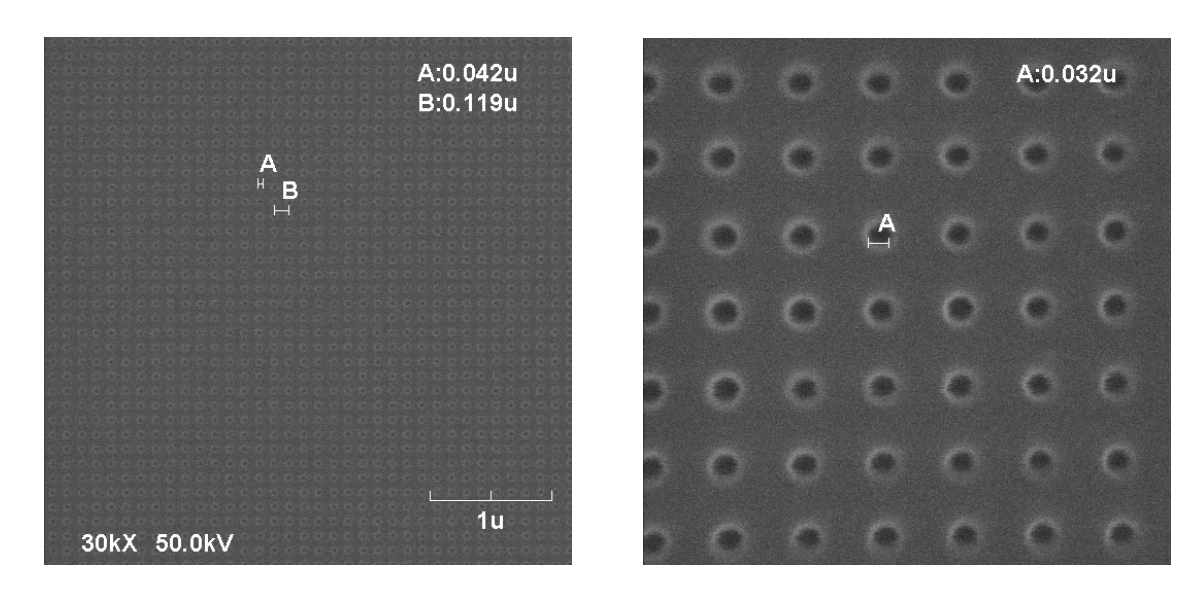
20 nm (mean + 3σ) for 50 μ m scanning area.



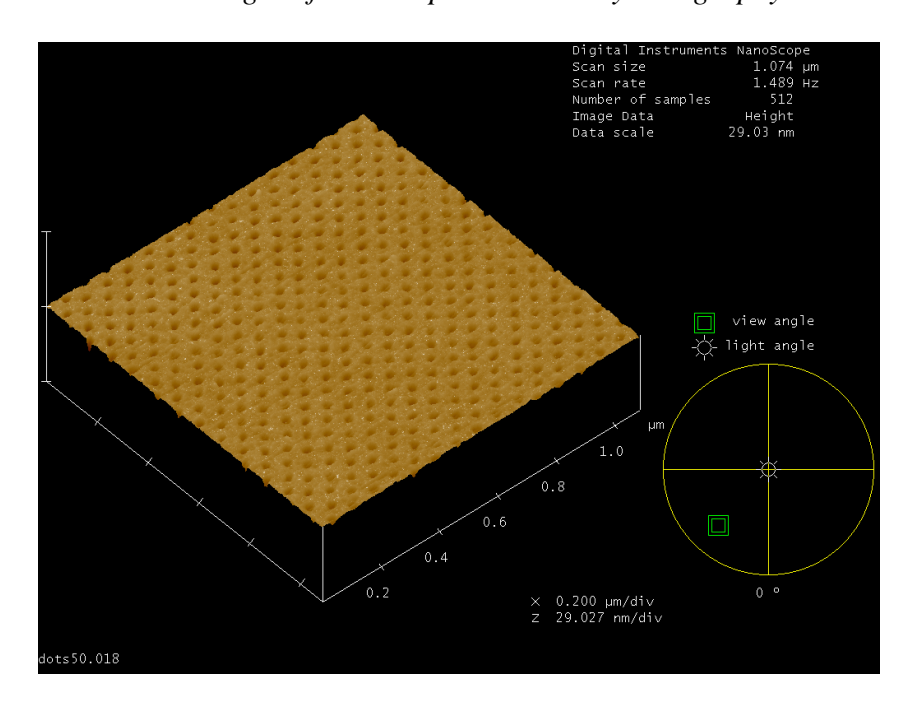
Some examples of preliminary achievements and applications already obtained at ISOM are shown below:

- Dots Arrays

In future optical and magnetic recording, quantum dots and nanocolumns fabrication have to form an ultrahigh packed fine dots arrays (2.5 x 10¹¹ dots/cm²). HREBL has a potencial to form these structures. ISOM is already able to generate challenging patternings for nanodots arrays. Some of the applications will be the deposition of magnetic nanodots for medical applications with very controlled characteristics, regular patterning for nanocolumnar growth, micro and nano LED's, photodetector arrays, etc. The image below shows the pattern of dots transferred to the Si substrate through a dry etching technique.



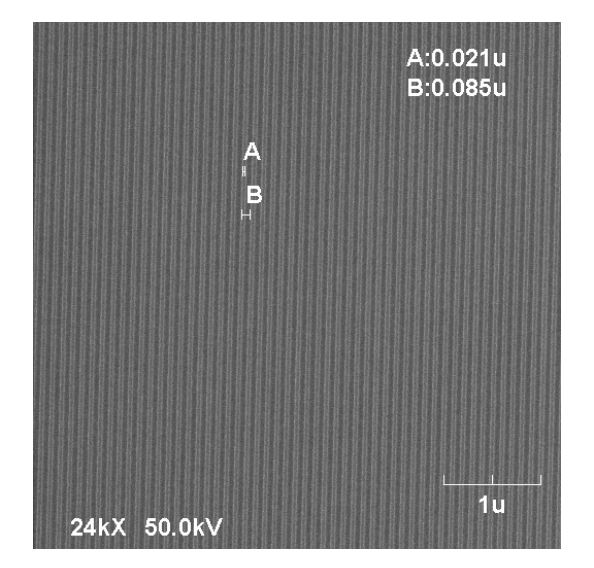
SEM images of 120 nm pich hole array lithography.



Atomic force microscopy image of 50 nm pitch holes etched on silicon.

- Line Arrays

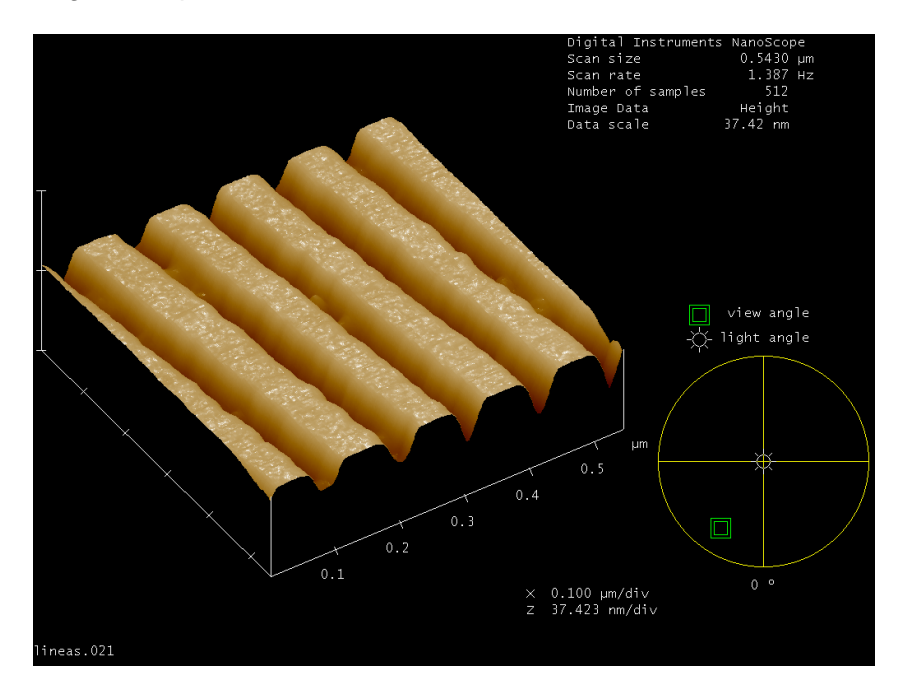
There is a wide range of applications for diffraction gratings for opto-electronics. From the generaration of polarized modes in lasers to difractive optics.





SEM images of linear and circular gratings lithography.

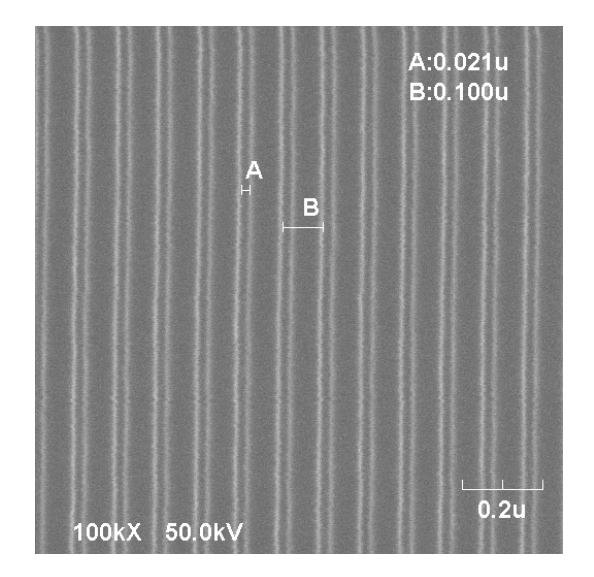
Below we show the picture of some lithographed lines transferred to a Si substrate through a conventional etching technique.

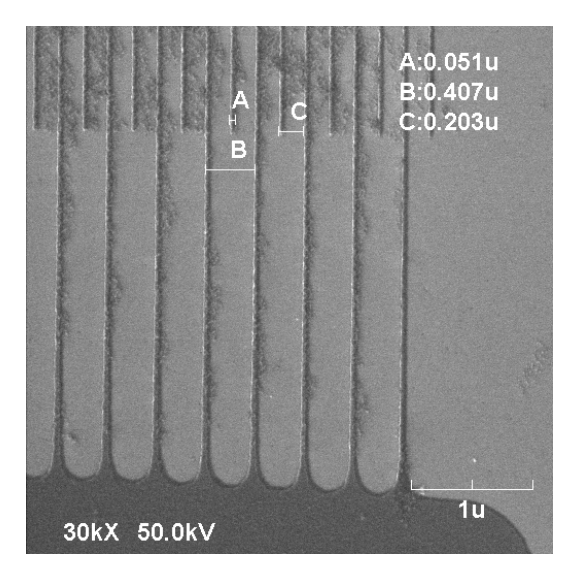


Atomic force microscopy image of 100 nm pitch linear grating etched on silicon

- SAW devices

SAW technology has evolved to the GHz range in recent years and now routinely covers the frequency range of up to 3 GHz. Nowadays, in order to reach this frequency band and higher (10-20 GHz) High Resolution Electron Beam Lithography technique is required.

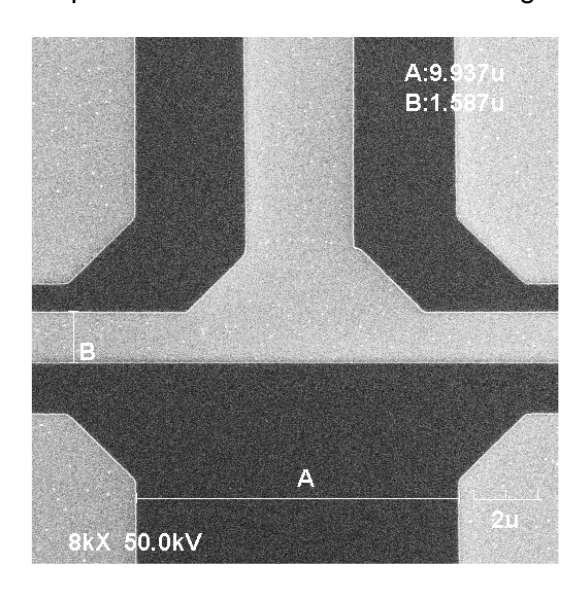


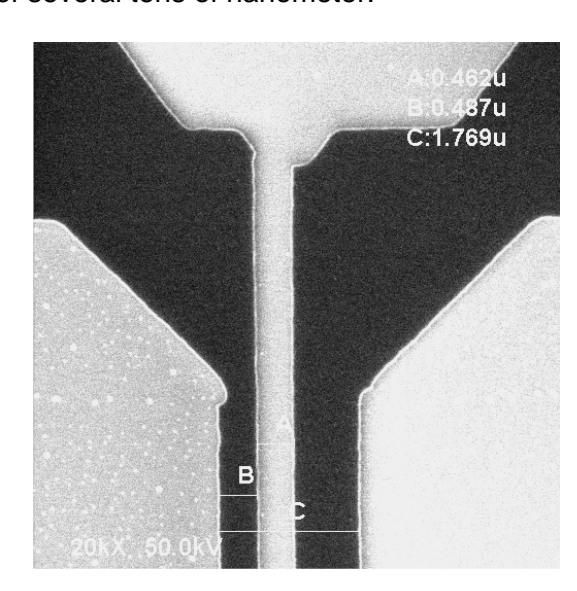


Letf. SEM imagen of IDT with 100 nm period lithography. Right. Ti/Au metallization of IDT with 400 nm period

- Transistors

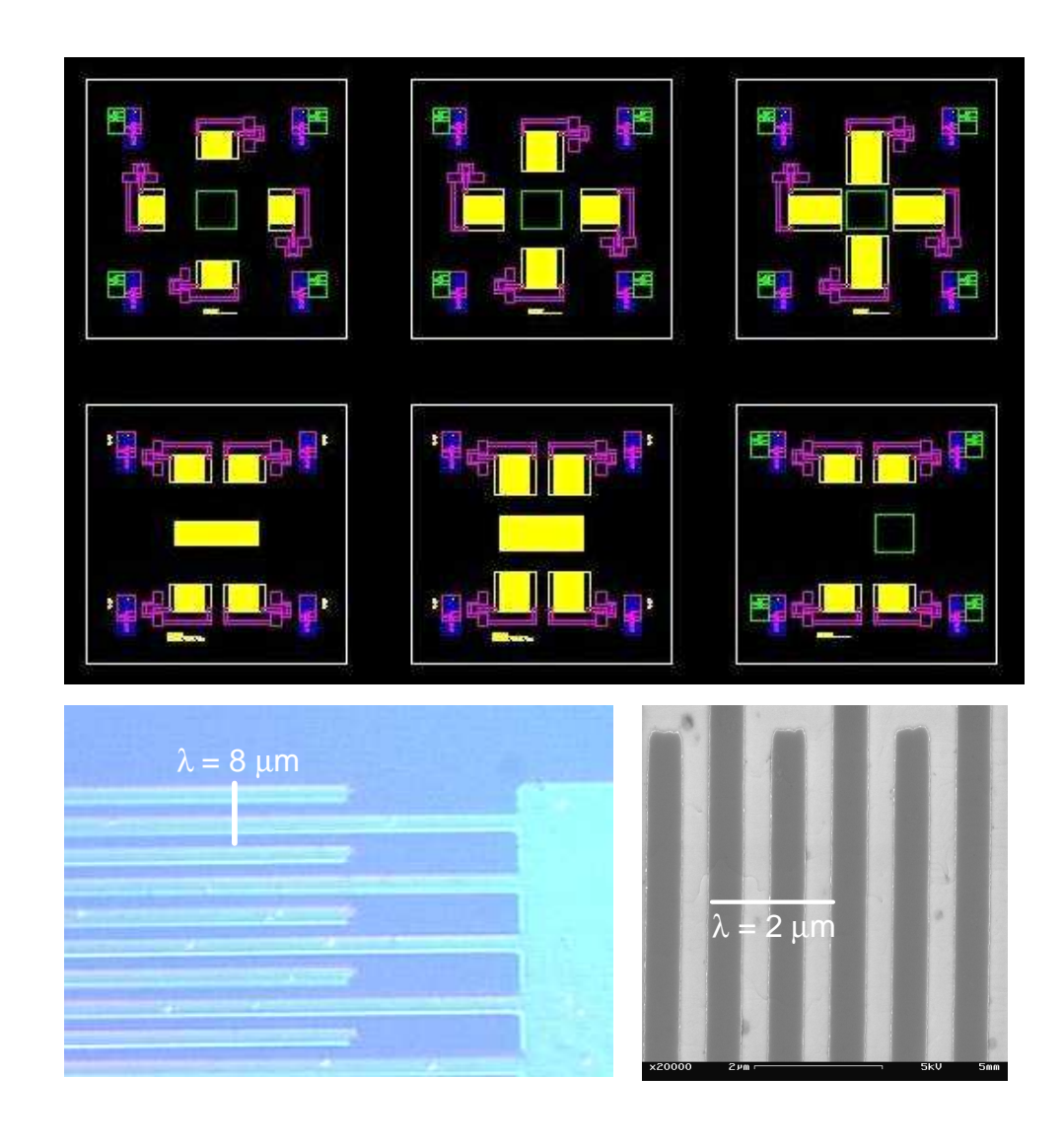
The availability of overlay tecnique allow the integration of photolithography and electron beam lithography with accuracy below 20 nm. This tecnique is crucial for transistors development which combine pads of hundred of microns with a gate of several tens of nanometer.





Overlay of ohmics contacs and gate in HEMT transistor based on AlGaN/GaN

5 RESEARCH LINES



Top: Orthogonal and parallel surface acoustic wave (SAW) delay lines.

Bottom: Nomarsky (left) and scanning electron (right) micrographs, showing details of interdigital transducers transferred by optical and e-beam lithographies (pitches of 2 and 0.5 μ m, respectively).

Several devices were developed using nitride-based structures, including remote UV photodetectors assisted by SAWs (with undoped, non-conductive layers) and voltage controlled SAW filters and oscillators (on 2DEG structures).

5.1 Microsystems and Nanotechnology

- Semiconductors-Optoelectronics-MOEMS
 - InGaAs(N) Quantum Dots and QWs, grown by MBE
 - Fabrication of IR emitters with InGaAs(N) QDot and QW layers
 - Optical Properties of nanostructures for quantum information systems (Single Photon Emitters)
 - GaN, InN, AlGaN e InGaN on Si(111) and Si(100) Nanocolumns growth
 - Growth of AlGaInN QW and quantum discs
 - Optical properties of diluted and Nitrides-III Nanostructures
 - Planar and Columnar InGaN/AlGaN microcavities, including Bragg reflectors
 - Nanovision: single photon detectors in the VIS and near UV

• Semiconductors- Nanoelectronics-MEMS

- Electron transport in AlGaN/GaN hetero-junctions: high frequency effects
- Submicron HEMT transistors for microwave applications and high T operation
- Opto-acousto-electronic interactions in SAW structures based on GaN/AlGaN
- Optoelectronics, physico-chemical and biological sensors based on SAW
- Multifunction sensors based on HEMTs and magnetic gate layers
- SAW filters for high frequency and high temperature.
- High temperature microsystems based on GaN
- Polymer deposition for molecular electronics
- Atomic force and electron lithography. Force microscopy control

Magnetic Microsystems-MEMS

- Magnetic multilayer structures. Applications to sensor production and spintronics
- Layered systems for magnetic anisotropy induction
- Nanodots and magnetic MEMS. Applications to sensors and magnetic recording
- Magnetic Nanoparticles

5.2 Optical Sensor Systems

- Ultraviolet and visible tunable photo-detection
 - UV-B solar radiation monitoring systems
 - UV and VIS integrated systems for fluorescence applications
 - Fire detection systems based on UV detection
 - High temperature AlInGaN photodetectors: combustion control applications by optical detection and analysis of flame emissions.
 - UV imaging in Astrophysics
 - Biosensors based on AlInGaN devices for water contaminants detection

- Infrared photo-detection with multispectral response (QWIPs)
 - Multispectral integration. Associated electronics
 - Environmental applications of IR detection
 - Quantum dots detectors

5.3 Optical Communications

- Medium-power lasers from 0.9 to 1.3 micron (InGaAs/GaAs) and 1.3 to 1.55 micron (InGaAsN)
- Resonant cavity emitters (LED, 510-570 nm) for transmission through plastic optical fibres (POF)
- LEDs in the visible range for displays and white indoor lighting

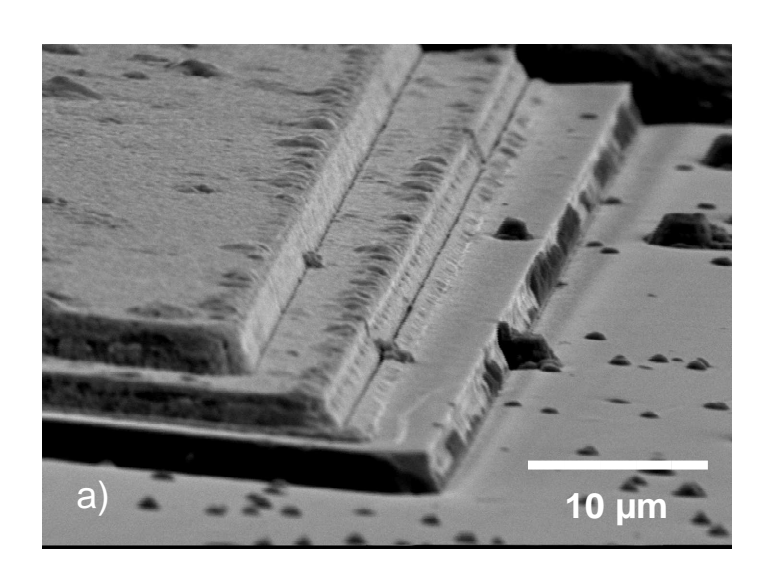
5.4 Systems with Magnetic Sensors

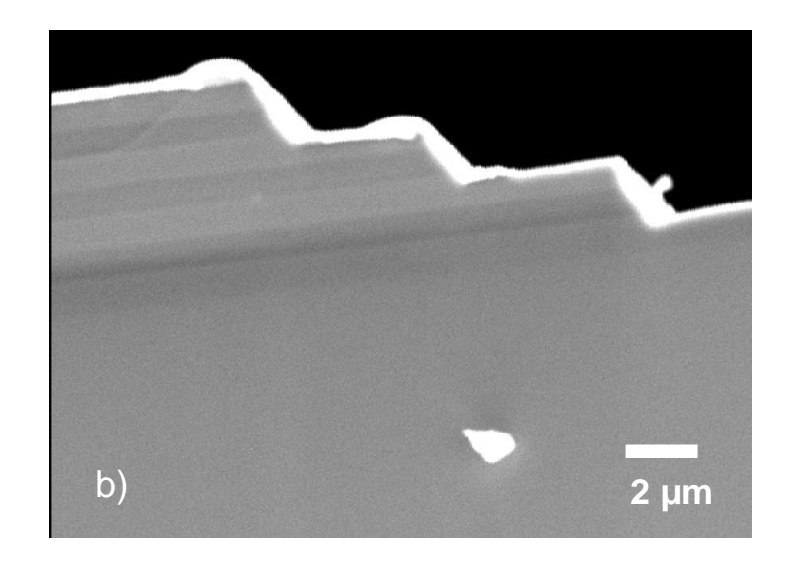
- Magnetometric sensors for low magnetic field measurements: fluxgates, piezoelectric, magnetostrictive, magnetoresistive and magnetoptic sensors
- Multisensors
 - Ground airplane control and guiding
 - Applications to monitoring large battery complexes
- Planar devices. Applications to planar inductors for commuting sources and antennas
- Low frequency intelligent cards with magnetic sensors

5.5 Simulation of Non-Metallic Materials

- Simulation of Non-Metallic Materials and Complex Fluids
 - nanocavity oscillation and collapse in viscoelastic fluids
 - rheomechanical modelling of biological membrane-complex fluid interaction
 - micro-macro calculation of complex non-newtonian flows (CONNFFESSIT + level set techniques)
- Advanced Monte Carlo and Molecular Dynamics
 - bijective-mapping min-map Monte Carlo for chain molecules
 - high-density and jammed chain fluids via multiple-bridging Monte Carlo
- Nanostructured Materials and Adsorption
 - self-organized nanostructured interfaces for biological sensors
 - nanoindentation of *Staphylococcus Aureus* via atomic force microscopy

6 RESEARCH REPORTS





SEM micrograph of a three-color quantum IR detector:

- a) Mesa etching carried out in three stages in order to isolate each one of the active zones.
- b) Cross section showing the active regions (in dark) in contrast with the conductive layers used as ohmic contacts. The mesa etching isolates perfectly the mentioned active regions.

6.1 Group III-nitride-based photodetectors: new functionalities and advanced structures ¹

The ISOM has maintained during the last ten years an intense research activity on group III-nitride-based photodetectors. In contrast to previous research, current efforts have been focused on the development of devices based on low dimensional systems and on advanced new structures. In addition to this device development activity, attention has been paid to some basic aspects in such low dimensional and novel devices, with the double objective of understanding the physics involved and to propose new detection concepts [1][2].

I. Quantum-Well-based photodetectors

There are two main motivations for using multiple-quantum-well (MQW) photodetectors, one is from technological origin and the other from a basic origin. The technological motivation is related to the interest in covering the full spectral range in photodetection, from ultraviolet (UV) to the visible (VIS) range. From a basic point of view, group III-nitride semiconductors exhibit potential advantages over other materials, such as the possibility to tune the absorption edge from UV to VIS ranges or a theoretically expected lower noise. In order to extend III-nitride detection range to the VIS regions, In alloys must be used. Our initial experiments showed that (In,Ga)N-bulk photodetectors had high dark currents, and MQW-based photodetectors have been studied as an alternative. MQW-based photodetectors additionally offer new functionalities not present in bulk-based devices. These functionalities, properly engineered, can be exploited to improve the photodetection response.

Structures studied as photodetectors were photoconductors, Schottky barrier (SB), metal-insulator-semiconductor (MIS) and p-i-n photodiodes with (In,Ga)N/GaN quantum wells embedded in their active region (i.e. the space charge region).

Samples were grown on c-face sapphire substrates by both molecular beam epitaxy (MBE) and metalorganic vapour phase epitaxy (MOCVD). The most interesting results were achieved in p-i-n and SB photodiodes. In the first case, high detectivities and UV/VIS contrasts were measured, allowing narrow band detection for back-illuminated configuration. It was also shown that detectivity in these devices was higher than for commercial Si photodiodes at high temperatures [3]. In the second case, a large gain under positive bias was obtained at low dark current levels [4].

The photoresponse characteristics of p-i-n devices as a function of applied voltage, In content and number of QWs were reported in detail in Ref. 5. Figure 1(a) shows the spectral response of two different samples with 10 and 20% In content, respectively. A high contrast in excess of 10³ between QW response above and below the absorption edge is observed in this figure. It is also worth noting that, although quantum efficiency was not optimized, the peak detectivity was determined to be higher than 1.2×10^{12} cmHz^{1/2}W⁻¹ in 9-mm² devices, which is comparable to standard bulk-based photodetectors. The spectral response for the back-illuminated configuration shown in the inset of Fig. 1(a) corresponds only to QW photodetection. These devices have successfully been used in flame detection, combustion monitoring and biophotonics [6][7]. We

¹ Contact person: Elias Muñoz: elias@die.upm.es

have also demonstrated that the transport mechanism of photogenerated carriers, either diffusion or drift, is critical to improve QW photodetection. Namely, the collection efficiency for QWs increases dramatically as the QWs move from the quasi-neutral region to the space charge region. Photocapacitance and photocurrent measurements support our model as shown in Fig. 1(b). In Fig. 1(b), each photocurrent step is related to a change in the current transport mechanism from diffusion to drift as the width of the space charge region increases. Fig. 1(c) displays the photodetector layer structure.

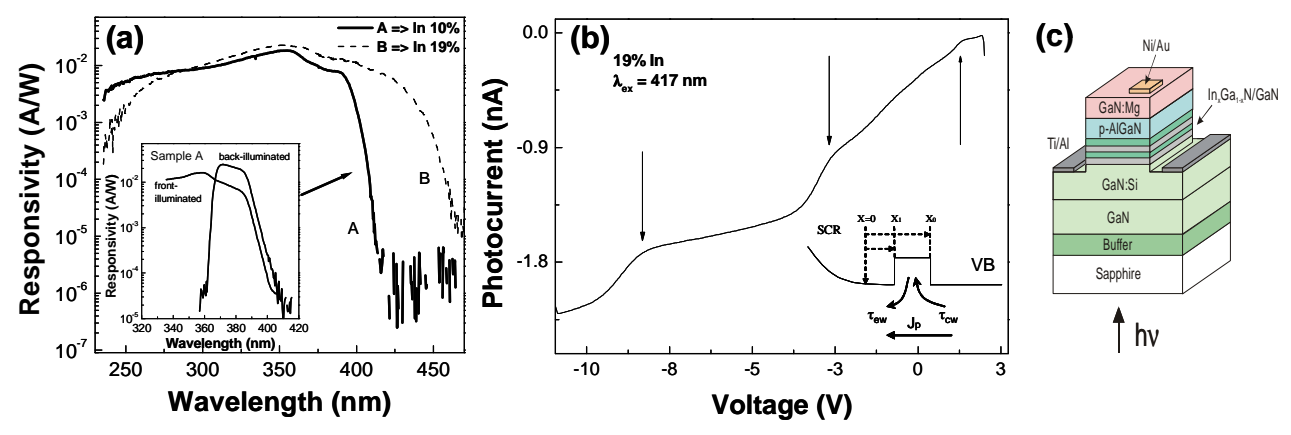


Figure.1. (a) Spectral response of 10% and 19% In samples operating in photovoltaic mode.(b) Photocurrent under optical excitation in the QWs. The inset shows a schematic of the processes involved in the photocurrent model.(c) Device layer structure.

We have recently proposed that the large gain associated to SB devices is caused by the negative average electric field (NAF) region formed as a result of the piezoelectric fields present in the quantum wells [8]. In this work, we explain that an additional barrier for carrier transport can appear at the boundary of the quantum well region under certain conditions (applied voltage, In content,...). Photocurrent gain appears when this barrier height is modulated by photogenerated carrier screening. This novel gain mechanism is intrinsic of piezoelectric materials. Measured responsivities were higher than 1 A/W at forward voltage, whereas that dark current was below 10 nA/mm². Specific detectivities in the range of 10¹¹ cmHz^{1/2}W⁻¹ were measured at 1.5 V, providing a far superior performance than typical III-nitride-based photoconductors. Moreover, the parameters of the device (e.g. wells width) can be designed to customize the range of optical excitation for optimum operation. These devices are suggested as an alternative to avalanche structures for high sensitivity applications.

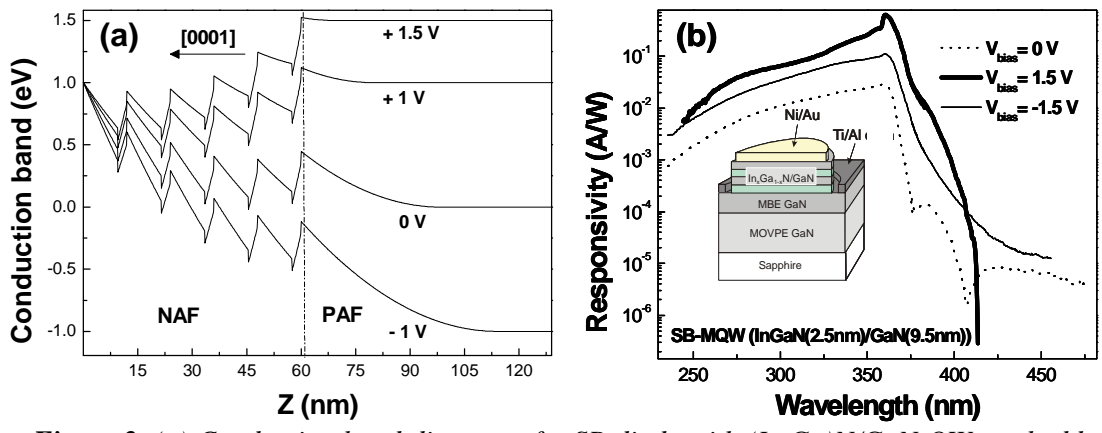


Figure.2. (a) Conduction band diagram of a SB diode with (In,Ga)N/GaN QWs embedded within the space charge region at different voltages.(b) Photoresponse at different applied voltages. Inset: Device layer structure. A gold semitransparent Schottky contact is used for front-illumination.

The conduction band diagram of the SB devices is shown in Fig. 2(a). We can observe that the piezoelectric field effect on the potential envelope divides the space charge region into two electric field domains at forward voltage. In this case, light can be used to screen the electric field in the QW region, thus modulating the effective barrier height. The spectral response of a representative (In,Ga)N/GaN MQW-based SB device as a function of applied voltage is shown in Fig. 2(b), and its inset shows the layer structure of the detector. The shift in the absorption edge and the change in the shape of photoresponse seem to be related to NAF effects.

II. Polarization-sensitive photodetectors

The growth of group III-nitride compounds along non-polar directions has attracted much attention for its potential application to QW-based emitters (both laser and light emitting diodes), but also in polarization-sensitive detectors and dichroic filters. More precisely, Ghosh *et al.* proposed the use of the in-plane asymmetry enhanced by the anisotropic strain generated by the lattice mismatch between the nitride film and the substrate to fabricate polarization-sensitive photodetectors [9]. These photodetectors can be used in data storage, optical communications, biophotonics and other sensing applications.

GaN films are usually grown on C-plane sapphire in their hexagonal-phase (wurtzite), leading to C-plane oriented surfaces along the c-axis. Hence, these GaN films exhibit in-plane symmetry which cannot be broken under isotropic strain. However, the use of other growth orientations such as in the case of M-plane or A-plane GaN films results in a reduced in-plane symmetry [see the inset of Fig. 3(a)]. The in-plane asymmetry affects both the electrical and optical properties of the film. For the realization of polarization-sensitive photodetectors we will be interested in the effect of the in-plane asymmetry on the optical properties of the film.

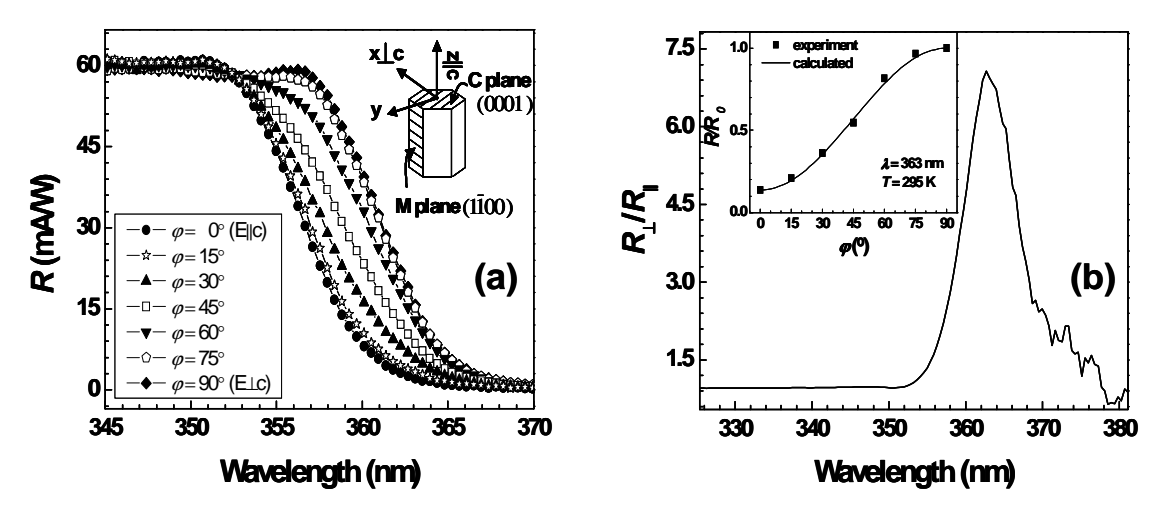


Figure.3. (a) Photocurrent spectra for different in-plane polarization angles □under normal incidence at room temperature. Inset: The unit cell of the wurtzite crystal structure of GaN. (b) Contrast of the responsivities for polarization perpendicular and parallel to the c-axis. Inset: Responsivity as a function of the in-plane polarization angle (squares) and fit (solid line).

Birefringence and dichroism were found in M-plane GaN films grown on γ -LiAlO₂ (100). In these films where c-axis lies in the in-plane, besides the intrinsic in-plane asymmetry, an anisotropic strain is generated between GaN and the LiAlO₂ substrate. Theoretical and experimental works have demonstrated that the separation between the two topmost valence bands increases under anisotropic compressive strain. At the same time, the two interband transitions in

the vicinity of the energy gap become almost completely polarized either parallel $(E \parallel c)$ or perpendicular to the c-axis $(E \perp c)$. Therefore, it is possible to use the in-plane anisotropy to detect the polarization state of light in $E \parallel c$ and $E \perp c$ directions.

The work carried out in the ISOM consisted of the design, fabrication and characterization of polarization-sensitive photodetectors based on *M*-plane GaN films grown on LiAlO₂ substrates. Films were grown in the Paul-Drude Insitute for Solid State Electronics (Berlin, Germany). Both SB and MIS nitride-based structures have been used as polarization-sensitive photodetectors for the first time [10].

These photodetectors show particular characteristics for their sensitivity to the polarization state of light. We have defined two new figures of merit to represent the specific characteristics of this type of photodetectors, namely the polarization-sensitive bandwidth and the contrast between the detection of light polarized perpendicular and parallel to the *c*-axis (hereafter referred as contrast). Firstly, since the valence band anisotropy is produced in the vicinity of the energy gap, the polarization sensitivity appears at the band gap energies where only the first topmost transition is possible [see Figs. 3(a) and 3(b)]. For higher energies, both bands absorb light, so that no polarization sensitivity is found. Nevertheless, it would be possible to extend the polarization-sensitive bandwidth to other wavelengths from infrared to vacuum ultraviolet by using (In,Ga)N or (Al,Ga)N compounds. The polarization-sensitive bandwidth is related to the valence band splitting. Secondly, the maximum contrast depends on the amount of light absorbed for each polarization at the peak wavelength.

From our results, we have proposed general design rules to improve the response of this type of photodetectors through film thickness [10]. Both polarization-sensitive bandwidth and contrast depends on film thickness, since it determines the strain state and the total absorption at a certain wavelength. Signal to noise ratio was also included in our design considerations to obtain reasonable values of contrast and polarization-sensitive bandwidth without affecting significantly to specific detectivity. Currently, we are trying to optimize the electrical characteristics of detectors to reduce the leakage current at reverse voltage.

- [1] C. Rivera, U. Jahn, T. Flissikowski, J. L. Pau, E. Muñoz, H. T. Grahn, Phys. Rev. B 74, 15 December (2006).
- [2] C. Rivera, J. L. Pau, E. Muñoz, T. Ive, O. Brandt, Phys. Stat. Sol. (c) 3, 1978 (2006).
- [3] A. Navarro, C. Rivera, R. Cuerdo, J. L. Pau, J. Pereiro, E. Muñoz, Phys. Stat. Sol. (a) 204, 262 (2007).
- [4] C. Rivera, J. L. Pau, J. Pereiro, E. Muñoz, Superlattices Microstruct. 36, 849-857 (2004).
- [5] C. Rivera, J. L. Pau, A. Navarro, E. Muñoz, IEEE J. Quantum Electron. 42, 51-58 (2006).
- [6] J. L. Pau, J. Anduaga, C. Rivera, A. Navarro, I. Álava, M. Redondo, E. Muñoz, Appl. Optics 45, 7498 (2006).
- [7] GaNano Project (EU STREP 505641-1 project, 2005-07), Furtursen Project (Comunidad de Madrid, AMB/0374, 2006-08)
- [8] C. Rivera, J. L. Pau, E. Muñoz, Appl. Phys. Lett. 89, 25 December (2006).
- [9] S. Ghosh, O. Brandt, H. T. Grahn, K. H. Ploog, Appl. Phys. Lett. 81, 3380-3382 (2002).
- [10] C. Rivera, J.L. Pau, E. Muñoz, P. Misra, O. Brandt, H.T. Grahn, K.H. Ploog, Appl. Phys. Lett. 88, 213507 (2006).

6.2 Quantum Dot structures for IR detectors and 1.3 µm lasers ²

Since its creation in 2000, the Institut for Systems based on Optoelectronics and Microtechnology (ISOM) has an active research line focused on the growth by Molecular Beam Epitaxy (MBE), fabrication and characterizacion of Quantum Well (QW) based structures for Infrared (IR) detection and lasing applications. Within this framework, several devices were developed using different material systems including GaAs/AlGaAs, GaAs/InGaAs as well as the so-called dilute nitrides GaAs/(In)GaAsN. Besides, different crystal orientations were considered for these studies, in particular GaAs(111)B surfaces, where we have fabricated to our knowledge the first GaAs/InGaAsN QW laser with operation in 1.2 µm at room temperature [1]. On the other hand, another original contribution of the ISOM is the development of InGaAsN/AlAs/GaAs QW intraband IR detectors for the 3-5 µm atmospheric windows [2]. In this case, due to the high effective mass of the InGaAsN, similar to that of the AlAs, and depending on the QW thickness, it is possible to confine more than two levels in the QW, giving rise to a multicolor detection [3].

In parallel with this investigation, in 2004 the ISOM initiated the study of quantum dot (QD) layers to be used as the active regions of both IR detectors and lasers. The physical properties of these zero dimensional (0D) structures are of great interest, in particular to improve the characteristics of such devices with the temperature. Furthermore, in comparison with the QW IR detectors, QD IR detectors have a lower dark current and a higher photoresponse resulting from longer carrier capture and relaxation times. Thus, stacked self-assembled QDs, instead of MQWs, have been employed as a possible solution for overcoming these problems. All this, leads to the fact that in theory it is possible to fabricate QD detectors with operation at room temperature which is not yet possible using QW structures. However, many problems still exist in controlling the size, homogeneity, and distribution of QDs, which significantly affect the tunneling transport of carriers. The ISOM is now researching how the different growth conditions and growth techniques affect the surface distribution and homogeneity of the QD layers, as well as their influence in the photoluminescence (PL) emission. The materials we use for such QD are mainly InAs or more recently InAsN.

Among the different techniques employed to fabricate these 0D nanostructures, we have chosen the so-called Stranski-Krastanov growth mode. This mode is an intermediate case in between the island growth and the layer by layer growth modes. After forming a few monolayers of material (in our case InAs or InAsN on GaAs), subsequent layer growth is highly strained, and thus, islands are formed on top of this intermediate layer (normally called "wetting layer"). The most important point is to control the first nucleation of these islands on the wetting layer in order to achieve self-ordered distribution of the QDs (fig 1).

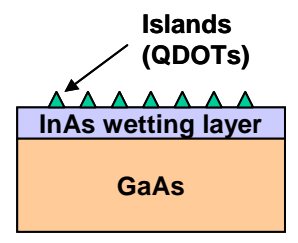


Figure 1. Stranski-Krastanov growth mode. InAs quantum dots are formed on top of a InAs wetting layer.

.

² Contact person: Alvaro de Guzmán Fernández: guzman@die.upm.es

All the samples described in this report were grown in a RIBER 32 MBE reactor equipped with a valved cracker As cell and an Oxford Applied RF plasma source for supplying the N species. After the native oxide desorption at 580°C we grew a 1 µm GaAs buffer layer at approximately 600° calibrated to the GaAs congruent sublimation temperature at 640°C and the mentioned oxide desorption at 580°C. This layer helps the surface to smooth and to be prepared for the growth of the quantum dot structures. Afterwards, the temperature of the substrate was dropped down to a value below that of the transition from the (2x4) to the c(4x4) surface reconstructions. Then, the In shutter was open in order to grow the wetting layer. In situ reflection high energy electron diffraction (RHEED) patterns were used to monitor the transformation from two-dimensional to three-dimensional growth. This transition occurred after the deposition of several monolayers of InAs, indicating the onset of islanding, and hence quantum dot growth. Finally, some of the samples were capped with a 50nm GaAs layer in order to bury the QD to allow the photoluminescence studies to be carried out. The samples without capping were studied using SEM and AFM to estimate the surface density of QD and the QD size.

After an exhaustive scan of the growth conditions (V/III flux ratio, growth temperature, InAs growth rate and number of InAs monolayers deposited) we observed a clear improvement of the QD surface density as well as of the PL emission when we used a V/III ratio of \sim 60, a growth rate of 0.14 ML/s, a substrate temperature 40°C below the (2x4) to c(4x4) transition and 20 sec. growth (2,8 ML). For these conditions a surface density of \sim 5·10¹⁰ cm⁻² of pyramidal 30nm x 30nm in width and 5 nm in height QD can be achieved. These values are the current state of the art for this type of layers. In fig. 2 we show AFM images of the surface of several samples grown under different growth conditions, it can be observed how the growth evolves from pure isolated islands of InAs to a high density of QDs.

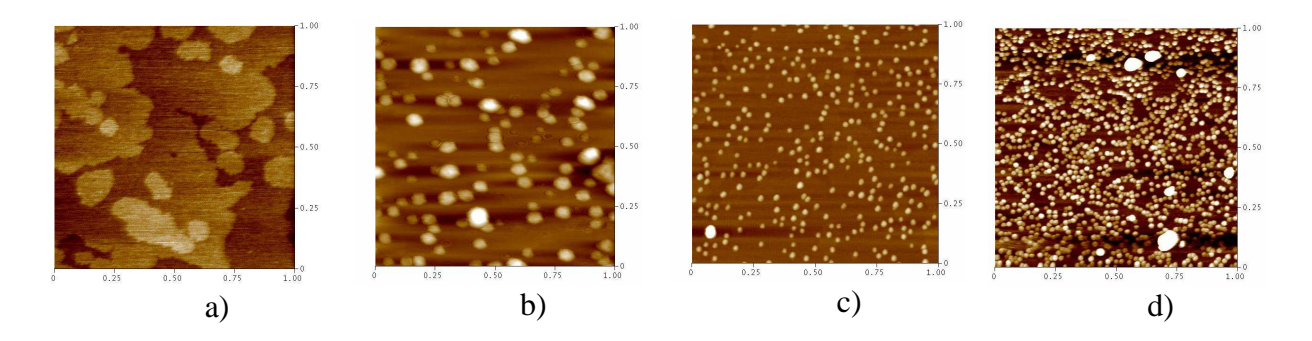


Figure 2. AFM images (1x1 μ m) of different QD layers. a) No QD are formed, big islands reveal a layer by layer 2D growth. b) Low density of big QD (120 nm wide). c) moderate density of small QD (30 nm wide). d) High density of small QD (optimum conditions)

Another approach to grow these QD layers is the patterning of the surface prior to the InAs deposition. This, normally requires the sample to be unloaded from the MBE reactor, processed using some nanolithography and etching techniques and then introduced again in the growth chamber to carry out the final growth of the QD. Due to the different roughness at the bottom of the etched holes compared to that on the surface, the dots tend to nucleate in such holes, giving rise to a higher level of order in the QD distribution. One of the original contributions of the ISOM in this area is the development of an *in-situ* pre-patterning technique using dilute nitrides on GaAs(111)B surfaces [4]. Since step-flow is the main growth mode for these surfaces it is very difficult to obtain a transition from a 2D growth to a 3D growth. We demonstrated that the different

migration coefficients of the N and As species over the surface of the sample gives rise to the formation of a regular distribution of self-organized holes. High definition AFM images show an interruption of the step flow growth mode due to the presence of the N that creates such holes on the surface (fig.3 a,b). Afterwards, the above mentioned holes can be used as patterns to grow standard InAs QD (see fig. 3 c) without unloading the sample from the growth chamber. In addition, controlling the amount of InAs ML deposited o top of the dilute nitride layer, it is possible to cover completely or partially the hole, thus providing an easy way to tailor the height of the QD obtained (fig 3. d,e).

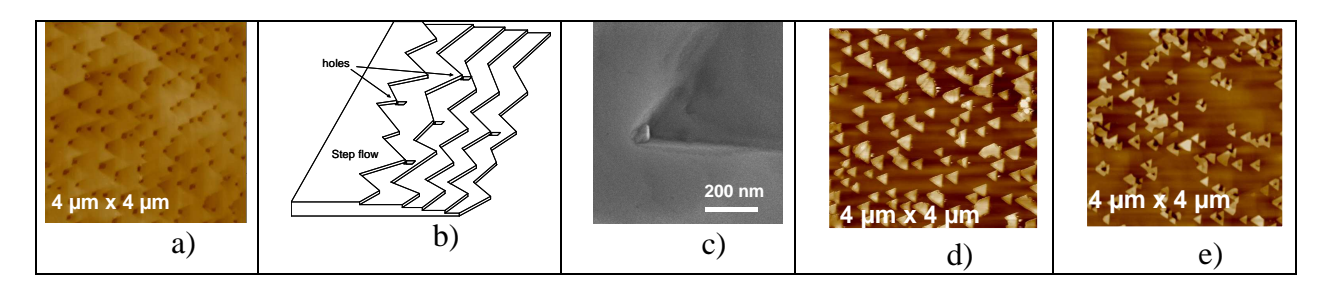


Figure 3. In-situ pre-patterned surfaces. a) A few GaAsN ML on GaAs(111)B, the presence of N produces the interruption of the step-flow growth mode creating holes. b) Schematic showing the generation of the holes. c) SEM image showing a QD grown inside one of the mentioned holes. d) High density of holes completely covered by InAs QD, e) High density of holes partially covered by InAs QD

However, in order to use the QD layers as the active region of an intraband detector it is necessary to introduce some doping species in the QD. In this case the carrier transitions take place from a ground level bound in the quantum dot to a second level. The carriers promoted to this latter, may escape if a bias voltage is applied, giving rise to a net photocurrent at the contacts. To ensure the presence of carriers in the ground level, it is necessary to introduce n-type or p-type doping species near the quantum dots layer. Due to the fact that the quantum dots have a reduced density of states (the ground level can only accommodate 2 electrons) it is critical to have an accurate control of the doping concentration introduced (the surface doping concentration must be at most twice the density of QD). If the doping level is lower, the performance is reduced, but if this limit is exceeded, the second level starts to populate, thus reducing the response of the device. In our case we have introduced the doping species (Si for n-type doping) in the GaAs barrier with an spacer of 10 Å. Since our QD surface density is ~5·10¹⁰ cm⁻², we have introduced a doping level of ~10¹¹ cm⁻². We grew weveral samples with different doping levels around the theoretical limit to optimize the final response of the devices involved.

Finally, the performance of the device is improved if more than one QD layer is grown. This increases the total responsivity reducing moreover the dark current. We grew samples with different number of QD layers (5,10,17 and 25) [5] in the active region separated by GaAs layers 100 nm wide and further sandwitched between two AlGaAs barriers in order to reduce more the total dark current of the device (see fig. 4). As you can see in the figure, we have achieved good PL emission, compared to that of a In_{0.3}Ga_{0.7}As 3nm thick QW. The responsivity of one of these devices is also shown as a function of the temperature. It can be observed how the detector can operate from low temperature to 150K. The measurement of the responsivity above this limit is difficult since the dark current increases drastically making it hard to separate from the photocurrent. We are now developing a low noise amplifier capable of removing the dark current

from the photosignal. With this equipment we will probably be able to operate this device at higher temperatures.

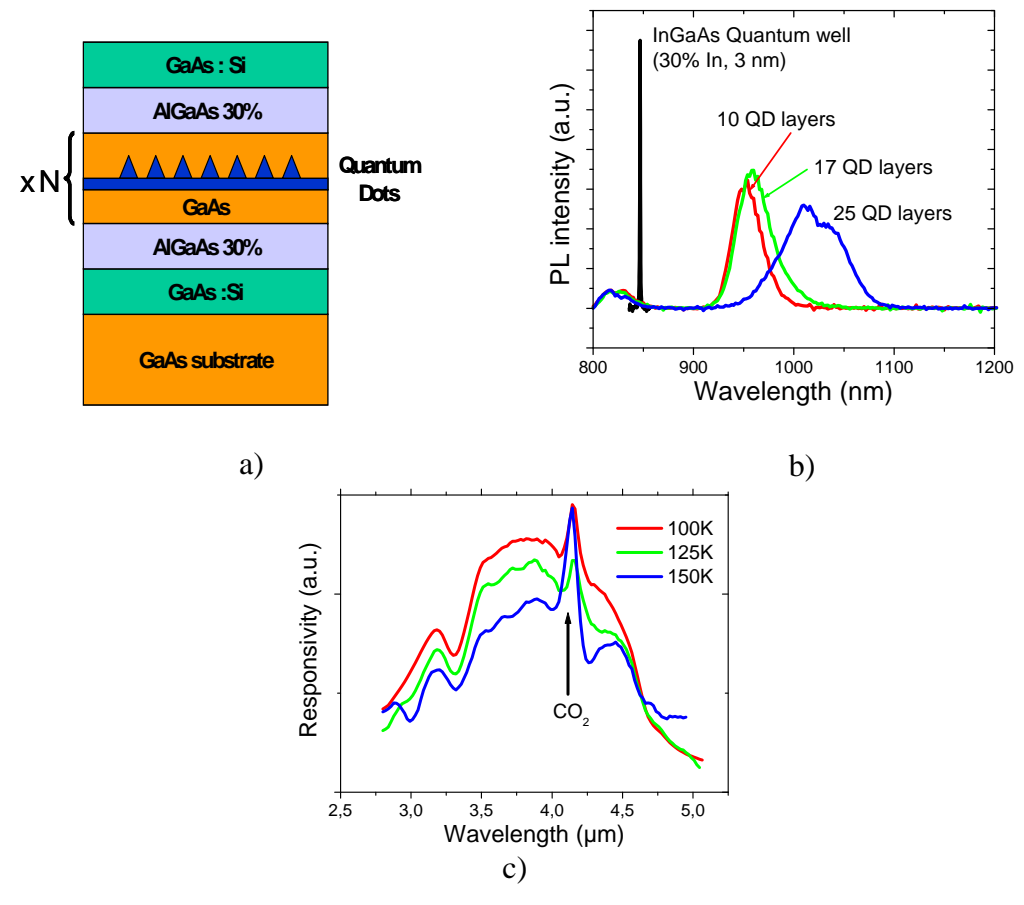


Figure 4. Quantum Dot IR Photodetectors (QDIPs) a) Layer structure. b) Photoluminescene spectra for three different QDIPs with 10, 17 and 25 QD layer. c) Responsivity of the QDIPs, it can be measured from low temperature to 150 K, above this limit the dark current is too high to separate it from the photosignal.

In conclusion, we have explored the possibilities of the InAs QD to achieve high temperature detectors. We developed devices operating at temperatures as high as 150K. In the future, our main interest is to use these QD layers to fabricate lasers and to use the material system InAsN to increase the wavelength to $1.3~\mu m$.

- [1] J. Miguel-Sánchez, A. Guzmán, J. M. Ulloa, M. Montes, A. Hierro, E. Muñoz. IEEE Photonics Technology Letters, Vol. 17, No. 11, Nov. 2005, 2271-2273.
- [2] E. Luna, M. Hopkinson, J.M. Ulloa, A. Guzmán and E. Muñoz, Applied Physics Letters 83 (15), 13 Oct. 2003. 3111-3113.
- [3] A. Guzmán, E. Luna, J. Miguel-Sánchez, E.Calleja and E. Muñoz. Infrared Physics & Technology 44 (2003) 377–382
- [4] R. Gargallo, J. Miguel-Sánchez, Á. Guzmán, U. Jahn, E. Muñoz, Microelectronics Journal 37 (2006) 1547–1551
- [5] R. Gargallo-Caballero, A. Guzmán and E. Muñoz, accepted as oral presentation in Congreso de Dispositivos Electrónicos (CDE07), El Escorial, Jan 31st to Feb 2nd 2007.

6.3 MBE growth of III-V-N quantum structures for optoelectronic devices. ³

The ISOM has a long tradition of research devoted to molecular beam epitaxy (MBE, Fig 1)

growth of traditional arsenide binary and ternary compunds (Al,Ga)(As) and nitrides (In,Al,Ga)(N) for their applications on optoelectronic devices (Detectors, emitters, etc.). In the recent years, a lot of effort have been done on a new kind of materials in which small amounts of nitrogen are incorporated to the arsenic sitesin the semiconductor structure. These materials are called 'dilute nitrides' and have a lot of interesting properties.



Figure 1 - (In,Al,Ga)(As,Sb,N) MBE at ISOM.

1.- Interest of III-V-N for telecom industry

Due to the high T_0 , high refraction index contrast with AlGaAs and the possibility of emission at 1550 nm using GaAs substrates, there is at the present a great interest in this field of diluted nitrides.

2.- (Ga,In)(N,As) on (100) and (111)B

Almost every publication in the literature up to date, devoted to the research on diluted nitrides, is based on (In)GaAsN grown on GaAs (100). In those references we can find that some problems still arise related to the growth of this material. We can cite some of them briefly. First, it is widely reported in the literature a strong reduction in the optical quality with the incorporation of nitrogen in the InGaAsN layers [2-5]. Another problem that is usually found, is the transition from the 2D to the 3D growth mode, due to the decomposition of the material [6-9]. For this reason, InGaAsN requires a low growth temperature (around 400 °C) to avoid the deterioration of these layers. In our case, we have chosen (111)B GaAs substrates for the development of dilute nitridesbased devices. This election is not arbitrary, and is due to the following reasons. First of all, our group and others demonstrated the growth of high quality InGaAs based devices on this orientation, as well as the development of low threshold (200 A/cm²) InGaAs laser diodes. [10,12-15]. Secondly, the intrinsic properties of the materials grown on this orientation, make the GaAs (111)B substrates interesting candidates for the development of InGaAsN based devices. The first of these properties is the presence of a piezoeletric field in the strained heterostructures grown on this orientation.[11,12] This piezoelectric field modifies the band structure of the devices, giving rise to the possibility for the development of non-linear devices and optical modulators. [13-15] Another interesting property is the absernce of the Stranski-Krastanov or 3D growth mode (layer + islands) in this kind of surfaces. [16] This is due to the fact that the misoriented substrates grow in the step-flow growth mode. This last property may avoid the decomposition of the material duing growth, obtaining thus flatter layers, with better optical properties. Additionally, for the InGaAs/GaAs system, the posibility of growing wider quantum wells (QWs) without relaxation on GaAs (111)B than on GaAs (100) was reported. [17,18] Thus, the emission wavelength from the QWs could be extended toward longer values. This may reduce the concentration of N of the QWs

³ Contact person: Alvaro de Guzmán Fernández: guzman@die.upm.es

(required to reach long wavelenghts). Thus, we could reduce the nitrogen induced damage previously described. The resarch in diluted nitrides grown on (111) is a new and interesting field, in which still only very few works have been published in the literature. [19-27]. First of all, the growth of high quality Bragg reflectors is quite complex, due to the small difference in the diffraction index of the materials suitable for their growth. The absence of these high quality Bragg reflectors based on the InP material system makes the VCSEL technology quite complicated. Secondly, the conduction band discontinuity between the barrier and the quantum well (QW) levels is small. This causes a poor confinement of the electrons. [1] Due to this last reason, the characteristic temperature (To) of the InP-based laser diodes is low. A convenient candidate to substitute these InP-based emitters is the so-called diluted nitride InGaAsN/GaAs system, proposed in 1996 by Kondow et al. [1]. This group demonstrated that the addition of small amounts of nitrogen to the InGaAs layers (less than 5%) causes a strong reduction in the bandgap. Thus, it's possible to achieve wavelengths long enough using GaAs technology, to be effectively integrated in the optical communications systems. [1]. The electron confinement in the conduction band of this system is much higher, implying a higher characteristic temperature (up to 150 K [1]) than that found for the InGaAsP/InP system. Additionally, it is possible to grow virtually lattice-matched high quality Bragg reflectors based on the Al(Ga)As/GaAs system. This allows the fabrication of vertical cavity surface emitting lasers (VCSELs) with a simple technology. Some of the advantages of these lasers are an easier alignment with the optical fiber in the final device, and the possibility of in-situ wafer testing, without cutting nor cliving the laser devices, saving time and money in industrial productions. For all these reasons, there is at the present a great interest in this field of diluted nitrides. Almost every publication in the literature up to date, devoted to the research on diluted nitrides, is based on (In)GaAsN grown on GaAs (100). In those references we can find that some problems still arise related to the growth of this material. We can cite some of them briefly. First, it is widely reported in the literature a strong reduction in the optical quality with the incorporation of nitrogen in the InGaAsN layers [2-5]. Another problem that is usually found, is the transition from the 2D to the 3D growth mode, due to the decomposition of the material [6-9]. For this reason, InGaAsN requires a low growth temperature (around 400 °C) to avoid the deterioration of these layers. In our case, we have chosen (111)B GaAs substrates for the development of diluted nitrides-based devices. This election is not arbitrary, and is due to the following reasons. First of all, our group and others demonstrated the growth of high quality InGaAs based devices on this orientation, as well as the development of low threshold (200 A/cm²) InGaAs laser diodes. [10,12-

15]. Secondly, the intrinsic properties of the materials grown on this orientation, make the GaAs (111)B substrates interesting candidates for the development of InGaAsN based devices. The first of these properties is the presence of a piezoeletric field in the strained heterostructures grown on this orientation.[11,12] This piezoelectric field modifies the band structure of the devices, giving rise to the possibility for the development of non-linear devices and optical modulators. [13-15] Another interesting property is the absence of the Stranski-Krastanov or 3D growth mode (layer + islands) in this kind of surfaces. [16] This is due to the fact that the misoriented substrates grow in the stepflow growth mode. This last property may avoid the decomposition of the material duing growth, obtaining thus flatter layers, with better optical properties. Additionally, for the InGaAs/GaAs system, the possibility of growing wider quantum

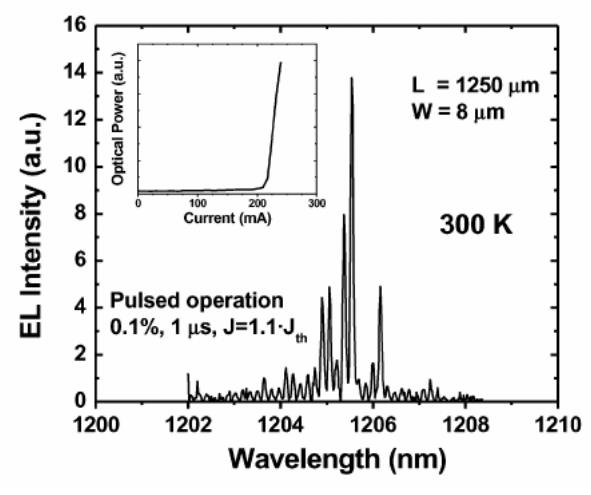


Figure 2.- Room-temperature lasing spectrum from an GaInNAs—GaAs LD under pulsed operation. The inset shows the light power versus current measurements (300 K) from the same GaInNAs—GaAs LD.

wells (QWs) without relaxation on GaAs (111)B than on GaAs (100) was reported. [17,18] Thus, the emission wavelength from the QWs could be extended toward longer values. This may reduce the concentration of N of the QWs (required to reach long wavelengths). Thus, we could reduce the nitrogen induced damage previously described. The research in diluted nitrides grown on (111) is a new and interesting field, in which still only very few works have been published in the literature. [19-27] and in which we demonstrated the first dilute nitride laser grown on a GaAs (111)B substrate. [28] (Fig. 2)

3.- The role of Nitrogen ionic species on MBE growth of III-V-N layers

The strong reduction of the optical quality of quantum wells, due to the formation of non-radiative defects, is mainly due to the creation of Ga vacancies [29], interstitial incorporation of nitrogen [4] and damage caused by the ionized nitrogen species from the plasma [5,26,27,30,31]. The formation of the first two types of defects is directly related to the growth dynamics and can be controlled by using the proper growth conditions. In our lab, we study the latter type of defects, i.e., those formed by ions generated in the nitrogen plasma, and their impact on the GaInNAs QWs grown on GaAs (111)B and (100) has been assessed. In order to incorporate nitrogen in the dilute nitride QW an atomic nitrogen source is needed. The most extended method to achieve this goal in

MBE systems is to create a plasma from ultra-pure nitrogen. In these plasmas, different species coexist simultaneously: electrons (ē), atomic nitrogen (N), diatomic nitrogen (N₂) and their excited species (N₂⁺, etc) [30,31]. The ratio of the ionized species to the atomic species is called ionization factor. The lower this ionization factor, the higher the quality of the plasma for epitaxial growth applications.

Since electron cyclotron resonance (ECR) plasma sources show high ionization factors [32,33], the most extended nitrogen sources for the growth of nitrides and diluted nitrides are radio frequency plasmas (rf) and direct-current (dc) plasmas. In our lab, we use an Oxford Applied rf source. To precisely control the amount of atomic nitrogen in the plasma, we used an Optical Emission Detector (OED) that detects the characteristic emission of atomic nitrogen. This device gives an in-situ and real-time value proportional to the amount of atomic nitrogen in the plasma. It consists of an optical detector, capped with a narrow band-pass optical filter tuned to the emission energy of the photons emitted from excited nitrogen atoms in the plasma. We have developed different ways for in-situ characterization of plasmas allowing to determine optimum working conditions for

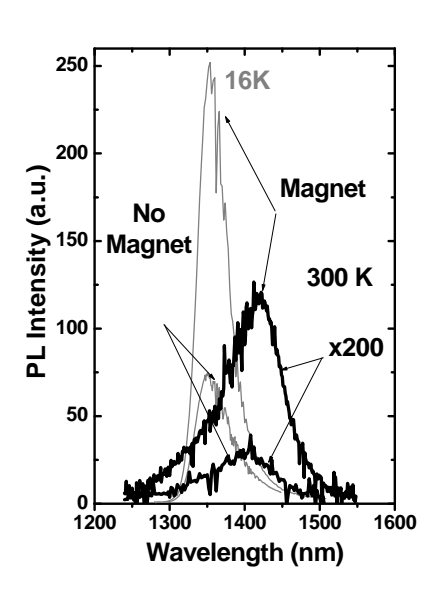


Figure 3: Low (16k, grey) and RT (black) spectra for two equivalent as-grown samples, with and without a magnetic field during the QW growth.

epitaxial growth are described. We additionally demonstrated how these ionic species are detrimental for the optical quality of dilute nitrides. (Fig 3)

4.- (AI,Ga)(As,N) growth and characterization

We additionally study the relatively less known AlGaAsN compound. AlGaAs is a direct bandgap semiconductor up to around 40 % Al, but to our knowledge, the type of transition for the AlGaAsN quaternary material is still unknown. Only very few works have been devoted to the study of the growth of this compound [34] and to its characterization [35-38]. A more intensive structural and optical study of AlGaAsN could provide better understanding of the way that the very electronegative N atom incorporates to the III-V host matrix. Additionally, the impact of N

and N₂ species on the properties of AlGaAs layers is of great interest due to the extensive use of this ternary as the cladding layers in (Ga,In)(N,As,Sb) long wavelength lasers on GaAs. The growth of these claddings under a residual N₂ overpressure, after the growth of the InGaAsN quantum well, can lead to the generation of structural defects that directly have an impact on lasing performance [39]. In our work, we use a radiofrequency nitrogen plasma source and a solid source molecular beam epitaxy system to grow AlGaAs(N) thick layers on GaAs (100), capped with GaAs layers to avoid AlGaAs(N) oxidation. Two different effects were analyzed: the impact of a N₂ overpressure on the growth of AlGaAs, and the incorporation of N in AlGaAs using the plasma source with a 0.3 sccm N flux and varying the substrate growth temperature. In the AlGaAs samples with a N overpressure, we find a broadening of the X-Ray diffraction peaks associated with poorer structural quality, but no N incorporation. In the samples grown with a N plasma, the X-Ray diffraction peaks associated to the strained AlGaAsN shifted apart from the GaAs substrate as the growth temperature was decreased. This indicates a stronger N incorporation for reduced substrate temperatures, as found for related materials, such as GaInNAs, but contrary to what was theoretically expected from delta lattice parameter and valence force field calculations.

- [1] M. Kondow et al., Jpn. J. Appl. Phys., Part 1 35, 1273 (1996).
- [2] H. P. Xin, K. L. Kavanagh and C. W. Tu, J. Cryst. Growth 208, 145 (2000).
- [3] W. Li, M. Pessa, T. Ahlgren and J. Decker, Appl. Phys. Lett. 79, 1094 (2001).
- [4] S. G. Spruytte, et al., J. Crys. Growth 227-228, 506 (2001).
- [5] Z. Pan, L. H. Li, W. Zhang, Y. W. Lin, R. H. Wu, and W. Ge, Appl. Phys. Lett. 77, 1280 (2000).
- [6] H. P. Xin, K. L. Kavanagh, Z. Q. Zhu, C. W. Tu, Appl. Phys. Lett. 74 (1999) 2337.
- [7] P.R. Chalker, et al., J. Crys. Growth 233, 1 (2001).
- [8] J.-M. Chauveau, A. Trampert, K.H. Ploog, M.-A. Pinault and E. Tournié, Appl. Phys. Lett. 82 3451 (2003).
- [9] J.-M. Chauveau, et al., J. Crys. Growth 251, 383 (2003).
- [10] J.J. Sanchez, et al., Journal of Crystal Growth 192 (1998) 363.
- [11] J.F. Nye, Physical Properties of Crystals Oxford University Press, Cuarta Edicion(1967)
- [12] I. Izpura, J.J. Sanchez, J. L. Sanchez-Rojas, E. Munoz, Microelectronics Journal 30 (1999) 439.
- [13] V. Ortiz y N.T. Pelekanos, Appl. Phys. Lett 77 (2000) 788.
- [14] E. A. Khoo, J. Woodhead, J.P.R. David, R. Grey y G.J. Rees, Elec. Lett. 35 (1999) 150.
- [15] E. A. Khoo, et al., IEE Proc.-Optotelectron. 145 no.1, (1999) 62.
- [16] M. Gutierrez, et al., Appl. Phys. Letters, 80 (2002) 1541.
- [17] A. Sacedon, et al., Appl. Phys. Lett. 65 (1994) 3212.
- [18] F. Calle, A. L. Alvarez, A. Sacedon, E. Calleja, Phys. Stat. Sol. (a) 152 (1995) 201.
- [19] A. Arnoult, F. González-Posada, S. Blanc, V. Bardinal, C. Fontaine, Physica E. 23, (2004) 352.
- [20] S. Blanc, A. Arnoult, H. Carrere, C. Fontaine, Sol. State Elect. 47 (2003) 47.
- [21] S. Blanc, A. Arnoult, H. Carrere, C. Fontaine, Physica E 17 (2003) 252.
- [22] S. Blanc, et al., IEEE Proc. Optoel. 150 (2003) 64.
- [23] J. Miguel-Sánchez, A. Guzmán, J.M. Ulloa, A. Hierro, E. Muñoz, Applied Physics Letters 84, (2004) 2524.
- [24] J. Miguel-Sánchez, A. Guzmán, J. M. Ulloa, A. Hierro and E. Muñoz, Physica E, 23 (3-4) 62 (2004).
- [25] J. Miguel-Sánchez, et al., J.Crys. Growth, 270 (1-2), 62 (2004).
- [26] J. Miguel-Sánchez, A. Guzmán and E. Muñoz, Appl. Phys. Letters, 85, 1940 (2004).
- [27] J. Miguel-Sánchez, A. Guzmán, J. M. Ulloa, A. Hierro and E. Muñoz J. Crys. Growth 278, 234
- [28] J. Miguel-Sánchez, A. Guzmán, J. M. Ulloa, M. Montes, A. Hierro, E. Muñoz, P. Tech. Lett. 17,2271,2005
- [29] Li, M. Pessa, T. Ahlgren and J. Decker, 2001, Appl. Phys. Lett. 79, 1094.
- [30] H. Carrère, A. Arnoult, A. Ricard, X. Marie, Th. Amand, E. Bedel-Pereira, 2003, Sol. State Elect. 47, 419.
- [31] H. Carrère, A. Arnoult, A. Ricard, E. Bedel-Pereira, 2002, J. Crys. Growth 243, 295.
- [32] Grill, 'Cold Plasma in Materials Fabrication: From Fundamentals to Applications', Wiley-IEEE Press, 94.
- [33] M. R. Wertheimer, M. Moisan, 1994, Pure and Appl. Chem. 66, 1343.
- [34] V.A. Odnoblyudov, et al., Techn. Phys. Lett. 28, 517 (2002).
- [35] K. Yamamoto, M. Uchida, A. Yamamoto, A. Masuda, A. Hashimoto, Phys. Stat. Sol. (b) 234, 915 (2002)
- [36] W. Shan, et al., Phys. Rev. B, 62, 4211 (2000)
- [37] J. Wagner, T. Geppert, K. Köhler, P. Ganser, M. Maier, Appl. Phys. Lett. 83, 2799 (2003).
- [38] T. Geppert, J. Wagner, K. Köhler, P. Ganser, M. Maier, Appl. Phys. Lett. 80, 2081 (2002).
- [39] J. M. Ulloa, A. Hierro, M. Montes, B. Damilano, M. Hugues, J. Barjon, J.Y. Duboz, J. Massies, Appl. Phys. Lett. 87, 251109 (2005).

6.4 III-Nitride Nanocolumnar heterostructures 4

During the last years, the ISOM has a very active research line focused on the growth and characterization of nitride based nanocolumns. In this field pioneering work on nanocolumns and nanocolumnar heterostructures has been conducted and published. After the demonstration of first nanocolumnar devices from detectors, Lasers, LEDs, HEMT, SAW [1-4], the next challenge for nitride nanocolumnar heterostructures is to prove that it is possible to integrate such nanoobjects into wide spread Si integrated circuit (IC) technology. For that purpose, the study on the growth of GaN nanocolumns on Si and their characterization were conducted. For that purpose, the Si(001) substrate is the preferred one because it is the most widely used in the mainstream IC technology.

GaN nanocolumns on Si(001) grown by Pambe: Optical and Structural study

Several groups have attempted in the past to grow III-N compact layers on Si(001), either seeking the metastable zinc-blend (cubic) phase [5] or using a complicated buffer [6] to obtain wurtzite GaN while avoiding cubic phase inclusions. In addition to the substrate integration difficulties, III-N compact layers grow on non-compliant substrates show high concentrations of threading dislocations due to the very high lattice and thermal mismatch.

In the last couple of years a lot of effort has being made to achieve and control the formation of III-N nanostructures like nanocolumns (or nanorods, whiskers, nanopillars...). These nanostructures offer a very high crystalline quality due to the strain free structure and the absence of dislocations and extended defects. In addition, these one dimensional semiconductor structures are known to be suitable for the studies of quantum effects and the realization of quantum devices. After the successful self assembled growth and control of size and density of nanocolumns (GaN, AlGaN, InN [7-9]) by Plasma Assisted Molecular Beam Epitaxy (PAMBE) on Si(111), it has been reported the consecutive growth of several types of heterostructures (quantum disks (QDs) [10,11], nanocavity [12]). Thus, this simple process (without any buffer) to grow GaN nano-devices will be a straightforward way for the direct integration of nitride nano-devices on Si(001). This letter shows that the GaN wurtzite nanocolumns can be grown directly on Si(001), having the same extraordinary properties as similar nanostructures grown on an hexagonal substrate like Si(111).

The samples were grown by PAMBE with a RF-plasma source to activate the nitrogen. The substrates used were on axis (± 0.5 -1°) Si(001) wafers. The growth temperature was that used to grow GaN nanocolumns on Si(111). Growth is initiated with GaN, without any buffer. In order to obtain columnar morphologies, the growth proceeded under excess nitrogen [7,8] (N-rich conditions: III/V ratio << 1). The growth rate was estimated from SEM measurements (Figure 1) to be of some $0.2\mu\text{m/h}$. Samples structural and optical properties were assessed by Scanning Electron Micrography (SEM), High Resolution Transmission Electronic Microscopy (HR-TEM) and low temperature photoluminescence (PL).

_

⁴ Contact person: Enrique Calleja: calleja@die.upm.es

Figure 1 shows GaN nanocolumns grown on Si(001) mainly vertically aligned with rather uniform heights, diameters and distribution density. The nanocolumns diameter ranged from 20 to 40 nm. The morphology of the GaN nanocolumns grown on Si(001) is identical to that of the GaN nanocolumns grown on Si(111).

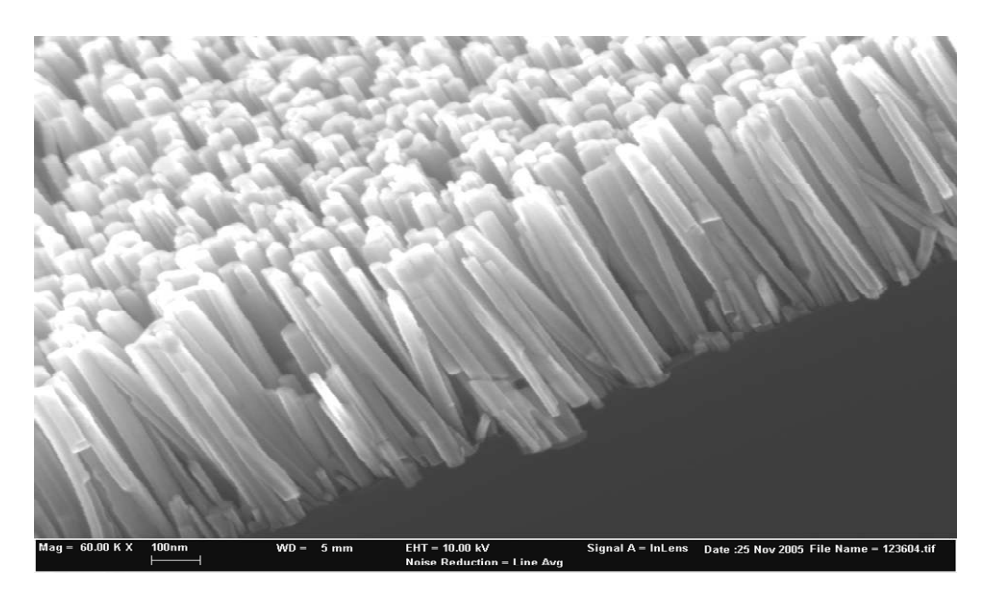


Figure 1: SEM micrograph of GaN nanocolumns grown by PAMBE on a Si(001) substrate

Optical properties of the GaN nanocolumns grown on the Si(001) substrate and on Si(111) (reference sample) have been studied at 10K by Continuous Wave (CW) PL with the 325-nm line of an He-Cd laser, dispersed by a Jobin-Yvon THR 1000 monochromator and detected with a UV-enhanced GaAs photomultiplier and a lock-in amplifier. Figure 2 shows the PL spectrum measured at 10 K of GaN nanocolumns grown on Si(001).

PL linewwidths are found to be identical in GaN nanocolumns grown either on Si(001) or Si(111) [13,14]. Near band-edge peaks observed at 3.470-3.478 eV are attributed to the exciton transitions. The inset in the fig. 2 shows that the near band edge emission consists of four distinct peaks at 3.448, 3.470, 3.474 and 3.478eV. that attributed to an undetermined contaminant or structural defect; a neutral-donor bound exciton D0X; and the free excitons A (FXA) and B (FXB) respectively [13,15,16]. Emission is dominated by the D0X with a full width half maximum (FWHM) of 2.3 meV. The FWHM value of excitonic peaks in GaN

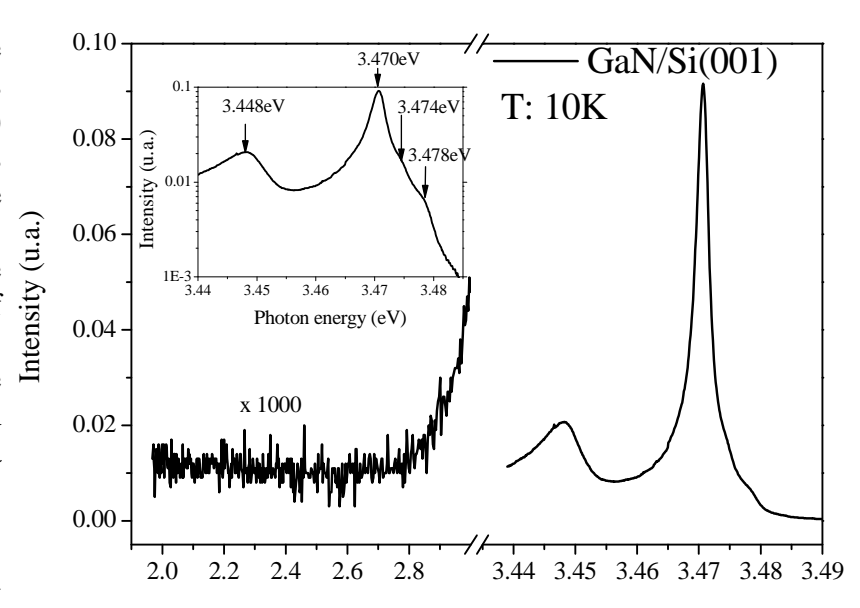
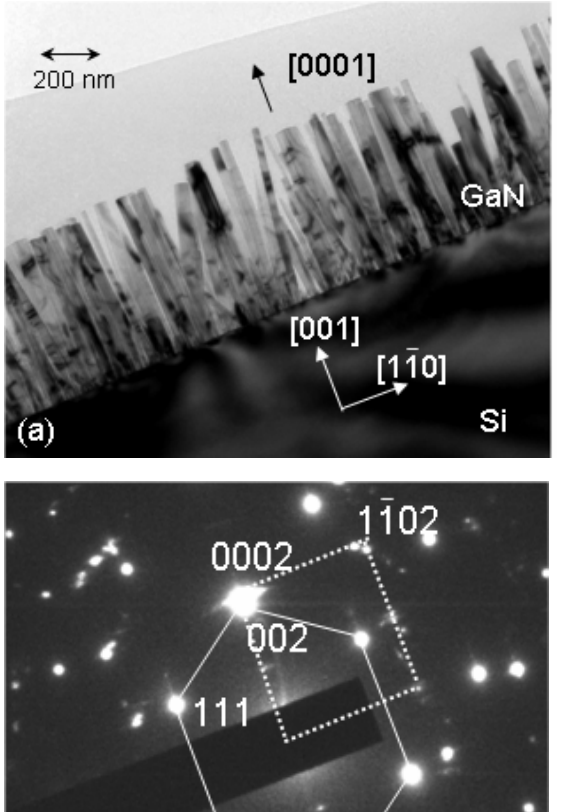


Figure 2.- PL spectrum of GaN nanocolumns measured at 10 K. No deep level emission is observed at 2.3 eV. The inset shows the dominant near band edge emission.

nanocolumns is narrower than those corresponding to compact layers [15,16]. Lower energy emissions attributed to deep level emissions, structural defects and impurities, like the so-called yellow band centred at 2.2eV, were not observed, as shown in figure 2 [17]. No cubic GaN-related PL signatures, typically observed around 3.3eV, were evidenced [18].

The excitonic emission energy position clearly proves that nanocolumns are fully relaxed and the absence of signatures around 3.2 eV shows that the film is hexagonal. This has been further assessed by electron diffraction and Raman experiments. The intensity and sharpness of the optical emissions indicate a very high crystal quality.



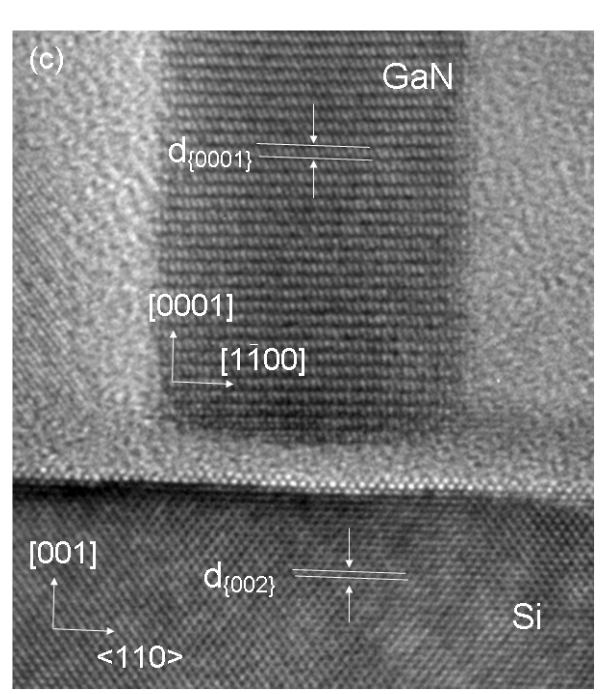


Figure 3. (a) Cross-sectional TEM image of GaN nanocolumns grown on Si(001).

- (b) The corresponding selected area diffraction pattern. The solid and the dashed lines indicate the Si[110] and GaN[11-20] zone axis orientation, respectively. All spots in the pattern belong to either Si or hexagonal GaN.
- (c) Cross-sectional TEM image of a GaN nanocolumn epitaxially aligned to the Si(001) substrate.

HR-TEM measurements, were carried out in a Jeol JEM 3010 microscope operating at 300kV, prove that the GaN nanocolumns grown on Si(001) are structurally uniform and single crystalline with the growth direction along the hexagonal [0001] axis (see Fig.3.a and b). The nanocolumns diameters vary between 20 and 40 nm and their density is rather high occasionally resulting in column coalescence. As in the case of (Ga,Al)N nanocolumns [19] grown on Si(111), no threading dislocations or other extended defects were detected (very few stacking faults were found, which are probably related to the coalescence process). Selected area diffraction patterns (SAD) in fig. 3(b) reflect a texture-like behavior of the columns, i.e., the GaN(0002) planes are parallel to the Si(002), however, the in-plane alignment is not well defined, although few columns show an epitaxial orientation with their [11-20] or [1-100] directions parallel to the Si<110> axis, respectively. An example is given in fig. 3(c) that shows a HR-TEM micrograph of a perfect epitaxially aligned hexagonal nanocolumn with GaN(0002)||Si(002) and GaN[11-20]||Si<110>.

The Si(001)/ GaN nanocolumn interface appears amorphous, most probably due to nitridation of the Si substrate prior to the growth, yielding a Si_xN_y layer of a few nanometers thick. The study of the degree of column twist with respect to the Si substrate surface is still in progress.

In conclusion, this work investigates the optical and structural properties of the GaN nanocolumns grown directly on Si(001). The sharp and narrow PL features evidences high crystalline quality as was the case in the (Al)GaN nanocolumns grown on Si(111). The nanocolumns are hexagonal and strain free. Moreover, the structural properties measured by TEM proved that the growth of the GaN is along the [0001] direction without any defects. We demonstrated for the first time the growth of GaN nanocolumns on Si(001) having the same extraordinary crystalline properties as GaN nanocolumns grown on Si(111). With these experiments, we open the possibility to integrate directly GaN nano-devices on the Silicon technology.

- [1] Z.C. Huang, J.C. Chen, D.B. Mott, and P.K. Shu, Electron. Lett. 32, 1324 (1996)
- [2] S. Nakamura, M. Senoh, S. Nagahama, N. Isawa, T. Yamada, T. Matsushita, H. Kiyoku, and Y. Sugimoto, Jpn. J. Appl. Phys. 35, L74 (1996)
- [3] S. Nakamura, T. Mukai, and M. Senoh, Jpn. J. Appl. Phys. 30, L1998 (1991)
- [4] M.A. Khan, A. Bhattarai, J.N. Kuznia, and D.T. Olson, Appl. Phys. Lett. 63, 1214 (1993)
- [5] B. Yang, O. Brandt, A. Trampert, B. Jenichen, and K.H. Ploog, Appl. Surf. Science 123, 1 (1998)
- [6] S. Joblot, F. Semond, Y. Cordier, P. Lorenzini, and J. Massies, Appl. Phys. Lett. 87, 133505 (2005)
- [7] M.A. Sanchez Garcia, E. Calleja, E. Monroy, F.J. Sanchez, F. Calle, E. Muñoz, and R. Beresford, J. Cryst. Growth 183, 23 (1998).
- [8] J. Ristic, M.A. Sanchez-Garcia, E. Calleja, J. Sanchez-Paramo, J.M. Calleja, U. Jahn, and K.H. Ploog, Phys. Stat. sol. (a) 192, 60 (2002)
- [9] J. Grandal and M.A. Sanchez-Garcia J. Cryst. Growth 278, 373 (2005).
- [10] J. Ristic, E. Calleja, M.A. Sanchez-Garcia, J.M. Ulloa, J. Sanchez-Paramo, J.M. Calleja, U. Jahn, A. Trampert, and K.H. Ploog, Phys. Rev. B 68, 125305 (2003)
- [11] A. Kikuchi, M. Kawai, M. Tada, and K. Kishino, Jpn. J. Appl. Phys. 43, L1524 (2004)
- [12] J. Ristic, E. Calleja, A. Trampert, S. Fernandez-Garrido, C. Rivera, U. Jahn, and K.H. Ploog, Phys. Rev. Lett. 94, 146102 (2005)
- [13] E. Calleja, M.A. Sanchez-Garcia, F.J. Sanchez, F. Calle, F.B. Naranjo, E. Muñoz, U. Jahn, and K.H. Ploog, Phys. Rev. B 62, 16826 (2000)
- [14] Y.S. Park, C.M. Park, D.J. Fu, T.W. Kang, and J.E. Oh, Appl. Phys. Lett. 85, 5718 (2004)
- [15] E. Calleja, M.A. Sanchez-Garcia, F.J. Sanchez, F. Calle, F.B. Naranjo, E. Muñoz, S.I. Molina, A.M. Sanchez, F.J. Pacheco, and R. Garcia, J. Cryst. Growth 201/202, 296 (1999).
- [16] F.Calle, F.J. Sanchez, J.M.G. Tijero, M.A. Sanchez-Garcia, E. Calleja, and R. Beresford, Semicond. Sci. Technol. 12, 1396 (1997)
- [17] M.A. Reshchhikov and H. Morkoc, J. Appl. Phys. 15, 061301 (2005)
- [18] M. Godlewski, J.P. Bergman, B. Monemar, U. Rossner, R. Langer, and A. Barski, Mat. Sci. Eng. B50, 113 (1997)
- [19] A.Trampert, J. Ristic, U. Jahn, E. Calleja and K.H. Ploog, 13th International Conference on Microscopy in Semiconductor Materials.

6.5 Lasing Characteristics of 1.3-1.52 µm GaInNAs/GaAs QW Laser Diodes: Degradation Mechanisms ⁵

Diluted nitride laser diodes (LD) have already demonstrated their potential for 1.30-1.31 μm emission, with excellent figures of merit already reported for these devices, including low threshold current densities (J_{th}), and high power emissions ^{1,2}. However, one of the challenges remaining is to extend the emission wavelength above 1.31 μm , with the final goal of reaching 1.55 μm with improved performances that could compete with the traditional InP family. This wavelength extension requires to increase the N content in the GaInNAs quantum well (QW), but is typically accompanied by a very large degradation of all laser characteristics, in particular a very large increase in J_{th} ^{3,4,5} However, the mechanisms responsible for this increase are still under debate, especially at long wavelengths. We analyze here the mechanisms causing the degradation of J_{th} and external differential quantum efficiency (η_d) in single quantum well LDs with 1.3 to 1.52 μ m lasing wavelengths.

Molecular beam epitaxy of the QW LDs was performed at the <u>Centre National de la Recherche Scientifique (France) by Benjamin Damilano and coworkers</u> with a RF-plasma source for N and solid sources for the other elements. Details on the optimization of the growth conditions are discussed elsewhere ⁶. The LD active regions were made by a 300-400 nm-thick GaAs waveguide, with a 70 or 100 Å-thick GaInNAs single QW in the centre. A series of samples were grown with different N compositions and an In concentration of 38-40 %. A reference InGaAs QW LD was also grown with the same layer structure as the GaInNAs LDs, and a 100 Å-thick 20 % In QW. The N content was extracted by using the nominal In and QW thickness as known parameters, and by applying the band-anti-crossing (BAC) model ⁷ to match the measured PL emission energy of each QW LD. All structures were processed as broad area LDs (see Ref. 5 for details). The Fabry-Perot resonant cavities were defined by cleavage of the LD stripes to lengths from 600 to

 $1500~\mu m$. The as-cleaved devices were then accessed with a fine probe and measured p-side up, sitting on a Cu heatsink, under pulsed conditions (1 μs , 0.1 %).

As shown in Figure 1, the set of GaInNAs LDs covered the spectral region from 1.29 to 1.52 μm , with J_{th} and η_d representing state of the art results for quaternary LDs emitting above 1.4-1.45 μm . ⁵ However, a strong tendency of J_{th} and η_d to degrade with increasing wavelength is observed. Such degradation has also been observed before, ^{3,4} and in particular, has been clearly correlated to a degraded PL intensity.³

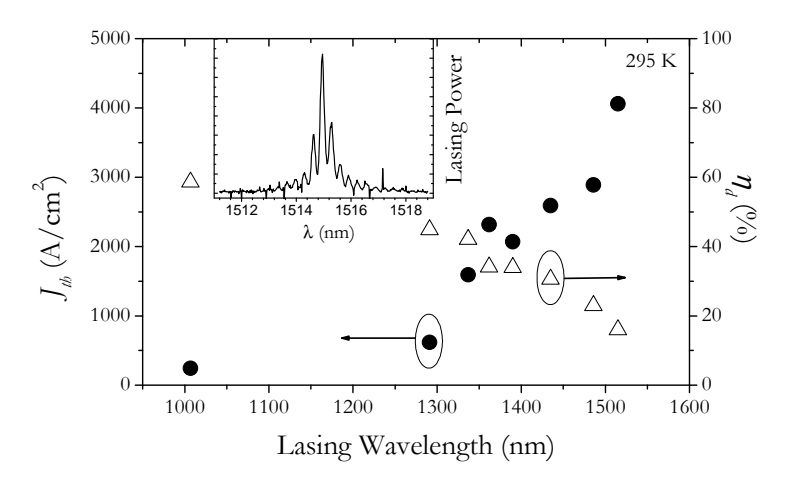


Figure 1: Dependence on the lasing wavelength of the threshold current density (J_{th}) and external differential quantum efficiency (η_{ext}) of GaInNAs/GaAs LDs. The inset shows the lasing spectra for the 1.515 μ m LD.

_

⁵ Contact person: Adrián Hierro: ahierro@die.upm.es

We first focus on the determination of the internal quantum efficiency (η_i) and internal optical losses (α_i) of the 1.29-1.52 μm series of LDs. For this analysis, η_d was measured in six to seven LDs from each bar with a given cavity length (L), and η_i and α_i were deduced from a linear

regression to the $1/\eta_d$ vs. L curve. ⁸ The resulting values are shown in Figure 2 as a function of N content in the GaInNAs QW. We see that η_i decreases when N is added to InGaAs, which has been observed before, ⁹ but remains constant with increasing N up to 2.0 %, contrary to what is reported in samples grown by metal-organic-chemical-vapor deposition with GaAsP in the barriers. ⁹ To understand this decrease, we will next analyze the mechanisms that affect η_i .

As reported by Smowton and Blood, 10 η_i is given by the product of three terms: the lateral current spreading efficiency (η_s) , the radiative efficiency of the QW (η_r) , and the current injection efficiency (η_{inj}) . The first term, η_s ,

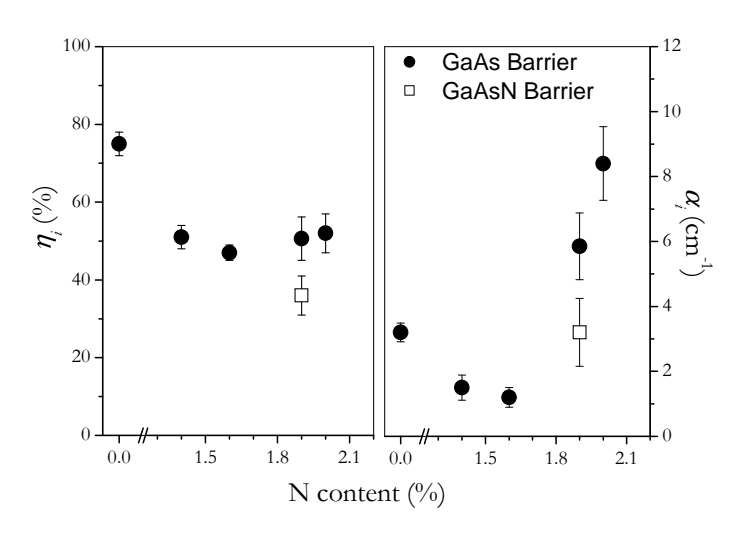


Figure 2: Dependence on N of the internal quantum efficiency (η_i) and optical losses (α_i) of GaInNAs/GaAs LDs.

should be close to unity in our structures, since the LD mesas are etched passed the waveguide region. ¹⁰ The second term, η_r , is also expected to be close to unity above threshold when the Fermi level is pinned in the QW. ¹⁰ Thus, η_i is limited by the current injection efficiency, η_{inj} , which is related to carriers lost in the barriers by recombination, or by drift or diffusion through the cladding layers, but is not related to recombination at the QW itself.

Looking at previous reports, the origin of this degraded η_i in GaInNAs LDs could be ascribed to higher hole leakage, as discussed in Ref. 9. Since η_i is in fact limited by the carrier injection efficiency, an increasing hole leakage would produce a decrease of η_i (as it is the case in Ref. 10), opposite to the approximately constant value it shows in Figure 1 for N contents from 1.4 to 2 %. Moreover, the InGaAs LD reference contains 20 % In, while all the GaInNAs LDs contain 38-40 % In. Since the valence band offset (ΔE_v) in GaInNAs/GaAs remains almost unchanged as a result of adding N, as shown in Ref. 6, ΔE_v should be larger (~20-25 meV) in the GaInNAs LDs than in the InGaAs reference LD. Thus, hole leakage cannot satisfactorily explain the behavior of η_i . Recalling again that η_i is limited by the carrier injection efficiency and that the LD layer structure is the same for the InGaAs and GaInNAs LDs, the decrease of η_i from InGaAs to GaInNAs can be explained to result from a higher loss of carriers through recombination in the barriers or claddings. This loss mechanism would then remain constant with increasing N content in the QW (Fig. 2), strongly suggesting that it is the presence of residual N in the MBE chamber during the growth of the barriers that is responsible for the generation of defects in these layers. These defects in turn cause higher carrier losses and give rise to an increased Jth and a decreased \(\eta_d \). In order to verify this picture, a 1390 nm GaInNAs LD with an unoptimized 3-nm thick GaNAs barrier was analyzed $(J_{th}=3.28 \text{ kA/cm}^2 \text{ for a } 1000 \text{ }\mu\text{m}\text{-long cavity})$. The resulting η_i is shown in Fig. 2, and is indeed smaller than in the LDs not containing intentional N in the barrier, supporting the picture that N incorporation in the QW barrier can be the origin of a higher carrier loss.

The next loss mechanism that can partially explain the increase of J_{th} with λ is the loss of photons by optical reabsorption, given by α_i (Fig. 2). In the GaInNAs LDs this parameter tends to increase with increasing N content, and thus directly degrades both J_{th} and η_d . The origin of the larger α_i at higher N contents could be related to the higher intra-valence band absorption, which is expected at longer wavelengths. As it will be shown below, the carrier transparency density does not vary with the N content in GaInNAs QWs, and thus it could not contribute to the increase in α_i .

The internal transparency current density (J_{tr}) was also obtained (note that this parameter is only related to the carrier recombination mechanisms in the QW). ⁸ Assuming that the gain has a logarithmic dependence on the current density, J_{tr} can be deduced from a plot of $ln(\eta_i \cdot J_{th})$ vs. 1/L. ⁸ The resulting values are shown in Fig. 3. We note that adding 1.4 % N to the InGaAs reference has

a small impact on J_{tr} , from 135 to 196 A/cm², but further increasing the N content leads to a monotonic increase of J_{tr} , which reaches 906 A/cm² at 2 % N. This strong increase in J_{tr} above 1.4% N is the third and dominant mechanism leading to the degradation of J_{th} at long lasing wavelengths.

To analyze this increase with N content, we note that, assuming Boltzman statistics, J_{tr} is directly given by $J_{tr}=qV(Cn_{tr}+Bn_{tr}^{2}+An_{tr}^{3})$, where V is the volume, n_{tr} is the transparency carrier density, and C, B and A are the

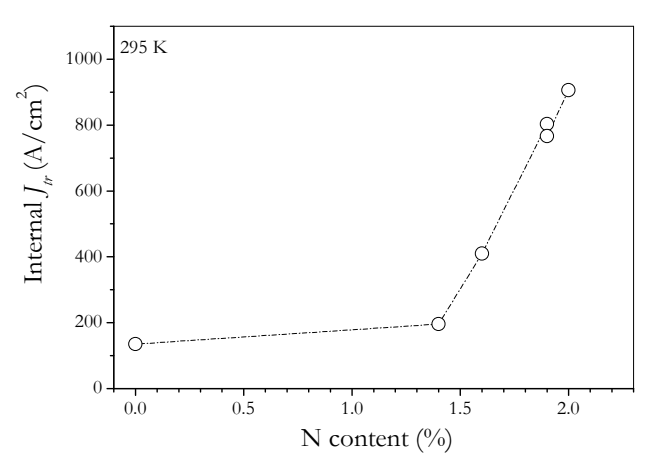


Figure 3: Impact of N on the internal transparency current density of GaInNAs/GaAs LDs

monomolecular defect-related (non-radiative), bimolecular (radiative), and Auger (non-radiative) recombination coefficients, respectively. 8 One possible explanation for the increase of J_{tr} with N content (Fig. 3) could be an increase of n_{tr} . This possibility was examined by calculating the dependence of n_{tr} on N content using the BAC model, and following the approach from Ref. 12 to calculate the material gain. The results are shown in Fig. 4, where two effects can be observed. First, n_{tr} increases when N is added to InGaAs (maintaining the In content constant at 39%), but remains approximately constant with N content, contrary to what it is obtained experimentally for J_{tr} (Fig. 3). Second, n_{tr} decreases from the 20 % In InGaAs reference LD to the 39 % In GaInNAs LDs, also contrary to the measured increase of J_{tr} . Consequently, n_{tr} has to be ruled out as the origin of the increase of J_{tr} with N content.

The contribution to J_{tr} from the bimolecular radiative component, $J_{tr}^{rad} = B \cdot n_{tr}^{2}$, was also calculated as a function of N content (Fig. 4). We note that, in fact, J_{tr}^{rad} decreases with increasing N content (in agreement with what is reported in Ref. 13 or pairs of In-N contents leading 1.3 μ m emission) and neither can explain the overall increase of J_{tr} with N. Thus, only a large increase in the monomolecular (defect-related) or Auger coefficients could account for such effect. Fhese et al have measured these coefficients in a MBE-grown GaInNAs/GaAs single QW LD, with 36% In and 1.7% N, and emitting at 1.3 μ m with $J_{th}\sim600$ A/cm². They found that the radiative and Auger components are only ~20 and ~25 % of the total current, respectively, whereas the defect-related component was ~55 %. Using these results for our 1.29 μ m LD (1.4 % N, with a similar structure and J_{th}), we estimate that the Auger coefficient would need to increase by a factor of ~15 to entirely account for the increase in J_{tr} from 1.4 to 2 % N. Such increase is extremely unlikely

and, indeed, in InGaAsP the factor is between two and four when shifting from 1.30 to 1.55 μ m. ⁸ Thus, the monomolecular (defect-related) recombination coefficient, C, is the coefficient that likely

accounts for most of the large increase in J_{tr} , and therefore in J_{th} (Fig. 1), with increasing N content. This is strongly supported by the characteristic reduction in photoluminescence efficiency observed when the N content is increased in the GaInNAs QW.

In this work the mechanisms causing the degradation of J_{th} and η_d in GaInNAs/GaAs LDs from 1.29 to 1.52 µm have been analyzed. The first mechanism is the decreased carrier injection efficiency when N is present in

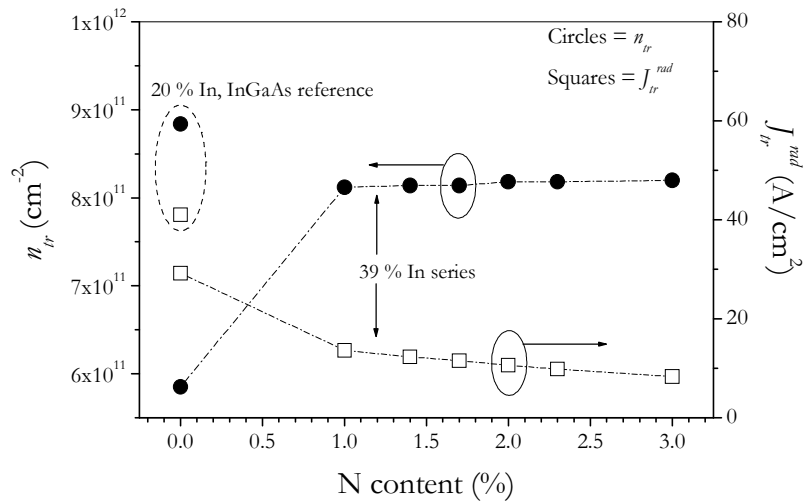


Figure 4: Dependence on N of the transparency carrier density (n_{tr}) and radiative current density (J^{rad}_{tr}) .

the chamber, which is related to carrier recombination at defects in the barriers. The second one is an increased internal optical loss for larger N contents. And the third and dominant factor for J_{th} , is the large increase of J_{tr} with increasing N, which can be directly linked to an increase in the defect-related recombination coefficient in GaInNAs QWs at larger N contents.

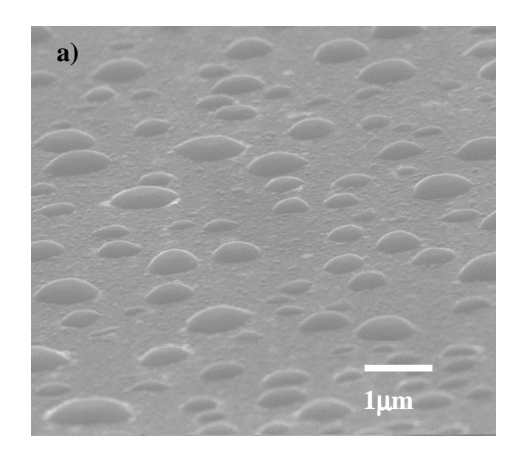
- 1.- D.A Livshits, A.Yeov, H. Riechert, Electron. Lett. 36,1381 (2000).
- 2.- N. Tansu, A. Quandt, M. Kanskar, W. Mulhearn, L.J. Mawst, Appl. Phys. Lett. 83, 18 (2003).
- 3.- G. Jaschke, R. Averbeck, L. Geelhaar, H. Riechert, J. Cryst. Growth 278, 224 (2005).
- 4.- J. S. Harris, J. Cryst. Growth 278, 3 (2005).
- 5.- A. Hierro, J.M. Ulloa, E. Calleja, B. Damilano, J. Barjon, J.-Y. Duboz, J. Massies, IEEE Photon. Tech. Lett. 17, 1142 (2005).
- 6.- B. Damilano, J. Barjon, J.Y.-Duboz, J. Massies, A. Hierro, J.-M. Ulloa, E. Calleja, Appl. Phys. Lett. 86, 071105, (2005).
- 7.- W. Shan, W. Walukiewicz, J.W. Ager III, E.E. Haller, J.F. Geisz, D.J. Friedman, J.M. Olson, and S.R. Kurtz, Phys. Rev. Lett. 82, 1221 (1999).
- 8.- L. A. Coldren, S. W. Corzine, "Diode Lasers and photonic integrated circuits", Wiley and Sons, (1995).
- 9.- J-Y. Yeh, N. Tansu, L. Mawst, IEEE Photon. Tech. Lett. 16, 741 (2004).
- 10.- P. M. Smowton, P. Blood, IEEE J. Sel. Topics Quant. Electron. 3, 491 (1997).
- 11.- M. Galluppi, L. Geelhaar, H. Riechert, Appl. Phys. Lett. 86, 131925 (2005)
- 12.- J.M. Ulloa, J. L. Sánchez-Rojas, A. Hierro, J. M. G. Tijero, and E. Tournié, IEEE J. Sel. Topics Quant. Electron. 9, 1 (2003).
- 13.- S. Tomić, E. P. O'Reilly, IEEE Photon. Tech. Lett. 15, 6, (2003).
- 14.- R. Fhese, S. Tomić, A.R. Adams, S.J. Sweeney, E.P. O'Reilly, A. Andreev, H. Riechert, , IEEE J. Select. Topics Quantum Electron. 8, 801(2002).

6.6 Characterization of InN layers and nanocolumns grown on Silicon (111) by Plasma-Assisted Molecular Beam Epitaxy ⁶

In recent years III-nitrides and their alloys have attracted much attention mainly due to their potential application in optoelectronic and electronic devices [1]. Main efforts have been focused on the development of GaN and Ga-rich InGaN and AlGaN alloys. With these two alloys the electromagnetic spectrum ranging from ultraviolet up to the visible zone is covered. The InN binary has received much less attention in the past as compared with GaN and AlN; however the recent determination of the band gap energy, as low as 0.7 eV [2], has extended the range of application of III-nitrides into the near infrared part of the electromagnetic spectrum and a great deal of renewed interest has arised.

One of the main problems to obtain high crystal quality films of this material, as for all the nitrides, is the lack of a suitable substrate. The lattice mismatch between InN and the typical used substrates in Nitrides is about 25% with sapphire, 15% with 6H-SiC and 8% with Si(111). Nevertheless good quality films have been obtained on all these substrates [3-5].

The most critical parameter to grow high quality InN films is the substrate temperature [6], due to the low dissociation temperature of InN (550°C) and the extremely high equilibrium vapor pressure of nitrogen in this compound. An excess of temperature during the growth may dissociate the InN, leaving the substrate covered with In droplets, since dissociation takes place at a much lower temperature than the desorption of metallic In.



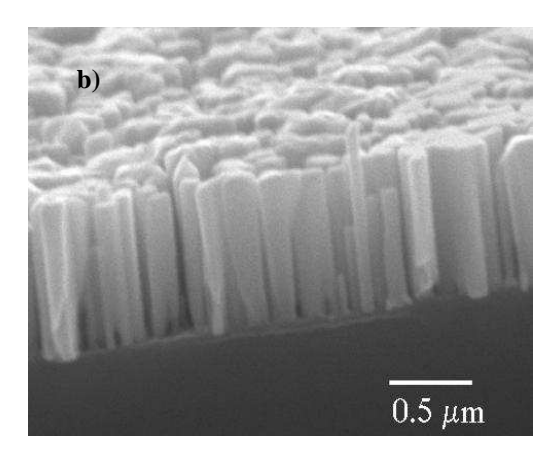


Figure 1. Scanning electron microscope photographs of InN layers described in Table 1: a) Sample A, b) Sample B.

A first series of InN samples were grown on Si(111) at different substrate temperatures to establish the influence of this parameter in the morphology of the layers (Table 1). All these InN layers were grown on top of a 50 nm thick AlN buffer layer. Growths performed at substrate temperatures above 500 °C show dissociation of the InN layer and the formation of metallic In droplets on the surface (Figure 1a) while reducing the temperature down to 475° C leads to the formation of columnar material (figure 1b). When growing at 500° C, too close to the dissociation limit (550° C), samples under stoichiometry conditions exhibit some degree of decomposition at the surface as shown in figure 2a (sample C); while samples grown with an excess of nitrogen shows

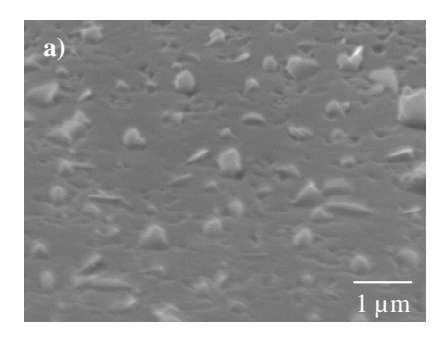
_

⁶ Contact person: Miguel Angel Sánchez: sanchez@die.upm.es

pyramidal shape due to the segregation of the metallic indium and dissociation of the InN, figure 2b (sample D). This effect indicates that the dissociation temperature of InN is lower than the temperature needed to desorb the excess indium, as it has previously been reported by other researchers [7]. In order to avoid this phenomenon, the substrate temperature is pointed out as the first critical parameter to be selected.

Table 1. Selected samples to study the effect of substrate temperature.

Sample	Subs. Temp. (°C)	RF Nitrogen Plasma Power (W)	Indium Beam Equivalent Pressure (Torr)
A	550	220	2.5 x 10 ⁻⁷
В	475	220	2.5×10^{-7}
C	500	200	5.5×10^{-7}
D	500	315	2.5×10^{-7}



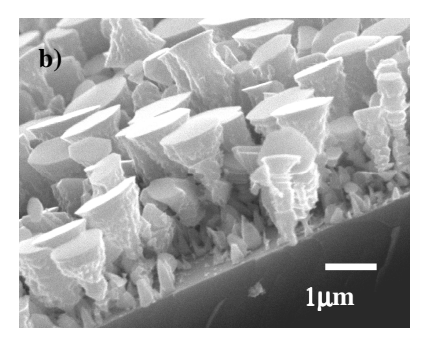


Figure 2. Scanning electron microscope images of InN layers grown at 500°C. a) Close to stoichiometry, b) under Nitrogen rich conditions.

A new series of samples were grown to determine the influence of the III/V ratio on the morphology of the samples, by varying only the indium molecular flux and keeping the rest of the growth parameters fixed, as described in Table 2. The ratio between the molecular indium flux and the active nitrogen (i.e. III/V ratio) is the fundamental parameter controlling the morphology of the films. N-rich conditions lead to columnar InN samples (Figure 1b) with very intense lowtemperature photoluminescence emission at 0.74 eV, while compact layers are obtained when using growth conditions towards In-rich (Figure 1c). It is worthy to note that the effective III/V ratio is also strongly affected by the substrate temperature. Therefore, a slight change in the growth temperature has a direct effect on the morphology of the layers. The In molecular flux was varied from sample D to sample F (see Table 2) corresponding to III/V ratios with N-rich conditions for sample D, low indium flux, and close to stoichiometry for sample F. The morphologies of these samples are shown in the SEM cross-sectional photographs of Figure 3. Sample D, grown with Nrich conditions, consists in an array of columnar nanocrystals (Figure 3a), with morphology very similar to the one obtained in GaN layers grown under N-rich conditions [8]. As the In molecular flux is increased towards In-rich conditions (samples E and F), the structure of the layers evolves to a more coalesced morphology (Figures 3b and 3c, respectively). For these three samples (D, E and F) the growth rate measured by SEM, was between 0.77 and 0.93 µm/hour. This high growth rate, together with the III-V ratio, can be considered an additional factor for a non-optimal nucleation process at the beginning of the InN growth, by preventing the total coalescence of the InN columns or grains (sample F). The growth rate can be lowered, while maintaining close to stoichiometry conditions, by re-adjusting the plasma power and indium flux as in sample G of Table 2 (growth rate of $0.4 \,\mu\text{m/h}$). The morphology of this sample (Figure 3d) exhibits a better coalescence.

Table 2. Selected samples to study the effect of increasing the indium molecular flux

Sample	Subs. Temp. (°C)	RF Nitrogen Plasma Power (W)	Indium Beam Equivalent Pressure (Torr)
D	475	300	2.5 x 10 ⁻⁷
Е	475	300	3.5×10^{-7}
F	475	300	6.5×10^{-7}
G	475	185	4.0×10^{-7}

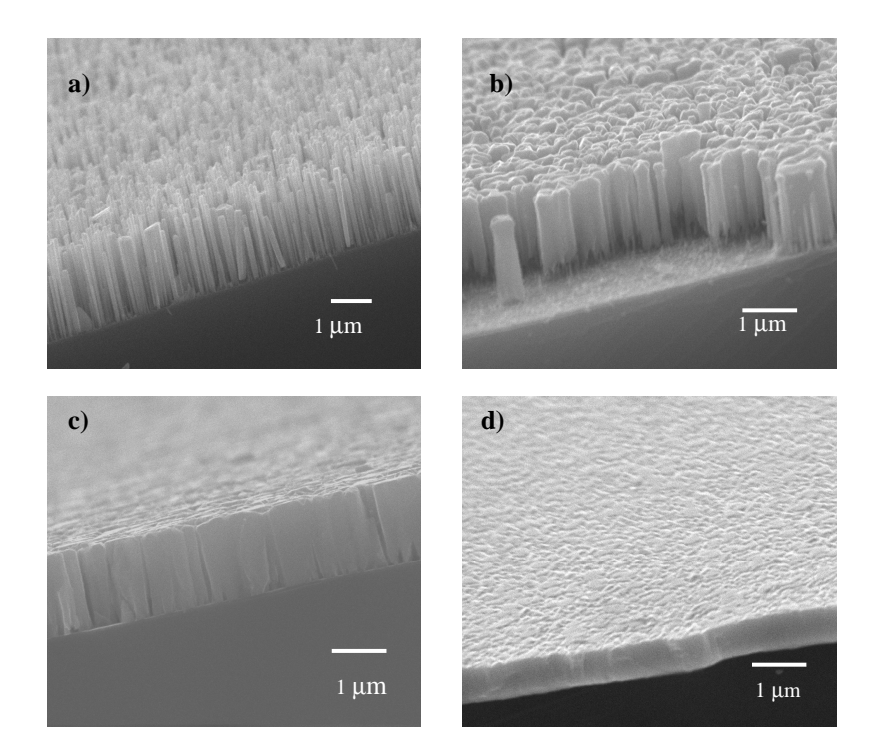


Figure 3. Scanning electron microscope photographs of InN selected samples increasing the indium molecular flux: a) Sample D, b) Sample E, c) Sample F and d) Sample G.

Low temperature PL was performed on the series of samples described in Table 2. The N-rich layer (sample D) exhibits an emission at 0.75 eV while the intensity of the PL signal for the other two samples is two orders of magnitude lower. In all cases, the emission is observed in the range 0.74-0.76 eV with no other emission present at higher energies.

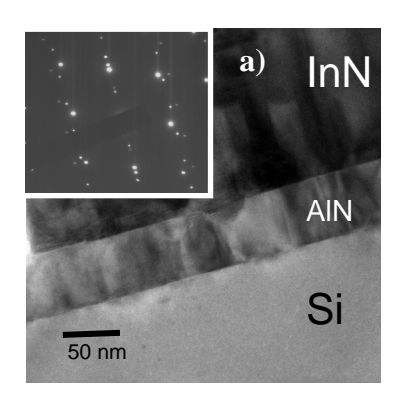
The decrease in the PL intensity as the material becomes more compact has also been observed in GaN layers with similar morphologies as the ones described in this work [8]. During the coalescence of the nanocolumns, grain boundaries and extended defects are generated, acting as non-radiative centers and being the main factors responsible for this phenomenon.

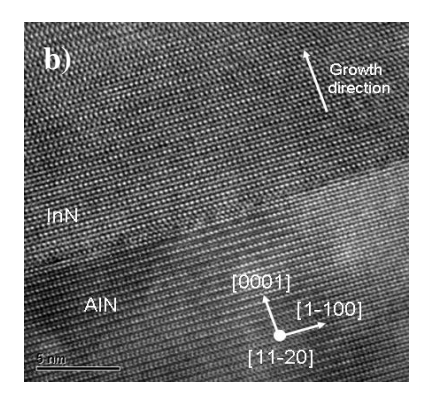
Excitation power dependence has been also investigated at 16 K, observing no variation on the position of the emission energy and a linear increase of the integrated intensity with the excitation power over two orders of magnitude.

It is also confirmed by high resolution transmission electron microscopy that the columnar material exhibits a morphology free of defect, similar to the case of GaN nanocolumns [9], and without segregation of metallic indium (Figure 4c). All these findings suggest that the PL emission corresponds to a band-edge recombination, obtaining band gap values of 0.75 eV and 0.72 eV, at low and room temperature respectively.

Compact material exhibits also a PL emission at low temperature at 0.75 eV as is the case for the InN nanocolumns, but with an intensity two orders of magnitude lower. It should be noted that there are no other emissions at higher energies.

In order to verify the crystal quality, InN compact material was characterized by X-ray diffraction showing a rocking curve of the (0002) reflection with a full width at half maximum (FWHM) value down to 682 arcsec. Figure 4a shows transmission electron microscopy images of the InN-AlN and AlN-Si(111) interfaces. A perfect epitaxial alignment is observed via the selected area electron diffraction (SAED) pattern of the inset. Figure 4b is a high resolution TEM image of the abrupt interface between the InN and the AlN buffer layer.





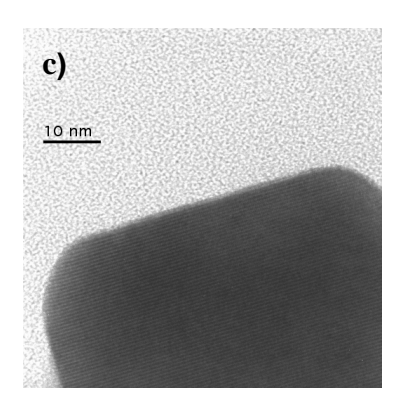


Figure 4. a) TEM analysis of InN / AlN / Si (111) interfaces. The inset shows the perfect epitaxial alignment. b) HRTEM image of the abrupt interface between the InN and the AlN buffer layer. c) HRTEM of a InN defect- free nanocolum (top part); no metallic Indium inclusions are observed.

- [1] S. Nakamura, 1995, J. Vac. Sci. Technol. A13 705.
- [2] V V. Yu. Davydov, A. A. Klochikhin, R. P. Seisyan, V.V. Emtsev, S.V. Ivanov, F. Bechstedt, J. Furthmüller, H. Harima, A. V. Mudryi, J. Aderhold, O. Semchinova, J. Graul, 2002, Phys. Status Solidi **B 229**, R1.
- [3] Y. Nanishi, Y. Saito, T. Yamaguchi, F. Matsuda, T. Araki, H. Naoi, A. Suzuki, H. Harina, T Miyajima, 2004, Mater. Res. Soc. Symp. 798.
- [4] T. Ive, O. Brandt, M. Ramsteiner, M. Giehler, H. Kostial, K.H. Ploog, 2004, Appl. Phys. Lett. 84, 1671.
- [5] J. Grandal, M.A. Sánchez-García, F. Calle, E. Calleja, 2005, Phys.Stat. Sol. (c) 2 No. 7. 2289-2292.
- [6] J. Grandal, M.A. Sánchez-García, 2005, J. Crys. Growth, 278, 373-377.
- [7] C.S. Gallinat, G. Koblmüller, J.S. Brown, S. Bernardis, J.S. Speck, G.D. Chern, E.D. Readinger, H. Shen, M. Wraback, 2006, Appl.Phys. Lett. **89**, 032109.
- [8] M. A. Sanchez-Garcia, E Calleja, E. Monroy, F. J. Sanchez, F Calle, E Muñoz, R. Beresford, 1998, J. Crys.Growth **183**, 23.
- [9] J. Ristic, M. A. Sánchez-García, J.M.Ulloa, E. Calleja, J. Sánchez-Páramo, J.M. Calleja, U. Jahn, A. Trampertand, K.H. Ploog, 2002, Phys. Status Solidi (b), **234**, No. 3, 717.

6.7 AlGaN/GaN High Electron Mobility Transistors ⁷

Despite the significant advances made in GaN technology, new progresses and basic understanding are still needed in materials quality, device processing and reliability issues. In the case of GaN HEMT, it has been long recognized that the AlGaN/GaN surface plays a key role in controlling the channel two dimensional electron density (2DEG), in current collapse problems, behaviour of passivation layers, breakdown voltage optimization, etc. A series of related problems ranging from wafer cleaning procedures and surface treatments, to finding the optimum passivation layer in relation to device performance and reliability, still needs further research efforts. Improvements in the AlGaN/GaN heterostructure (HS), like introduction of channel In alloys, thin AlN spacer layer, use of quaternary barrier alloys, etc., pose some materials issues like interface quality control, more accurate strain and composition assessment procedures, reproducibility problems, origin of residual traps, reliability of new designs, etc. Besides, the final goal for high temperature high power devices keeps alive a whole range of processing and fundamental questions in relation to a better understanding of HEMT operation at high temperatures, optimized ohmic contacts, reliability issues, etc.

At ISOM we have been working on AlGaN/GaN transistors for about a decade, first under partial support from ESA and later with the financial support of the Ministry of Defense-CIDA and the Spanish Ministry of Education. Along this period the whole spectrum, from AlGaN/GaN HS growth by MBE to full device processing and power amplifier prototyping has been covered. The recent participation of ISOM in project Korrigan, financed trough the EDA, has allowed us to use this past experience to now address some questions related to nitrides surface physical and chemical properties, passivation issues, high temperature characterization and modelling, traps and parasitics, and aiming to get knowledge and understanding for physical mechanisms that may be below device degradation and reliability problems. Thanks to the cooperation with U. Autónoma de Madrid, very powerful tools for AlGaN/GaN surface and structural characterization are now being used [RBS, ERDA, at CMAM, Prof.A.Climent, and X-ray photoelectron spectroscopy (XPS), AES, at the Surface Phys. Lab., Prof. C. Palacio].

a) Surface cleaning and treatments.

Aiming to study AlGaN/GaN HEMT electrical characteristics vs. some technological processing steps and AlGaN surface treatments, three steps have been studied in detail: cleaning recipes, exposure to plasma atmospheres and annealing treatments. We selected a set of representative cleaning procedures and surface treatments that HEMT wafers suffer during the various device fabrication steps. After one or several of these steps, AlGaN surfaces are studied by XPS. Samples were grown by metal-organic chemical vapour deposition (MOCVD) on a sapphire substrate. Three wafers were grown with a 1.25 µm GaN and a 28 nm AlGaN layer, labelled KQ20, KQ21 and KQ23. The aluminium content in the AlGaN barrier was 33, 35 and 33 %, respectively. As-grown, heterostructures cleaned in organic solvents were measured by a Hg-profiler. The capacitance-voltage (CV) measurements were undertaken from 0 to -10 V obtaining the 2-DEG carrier concentration (n_s), pinch off voltage (V_{th}) and 2-DEG distance to the surface (W_B). Then, two different surface heterostructures were exposed to: a) PE-CVD N₂-Plasma and b) rapid thermal annealing (RTA): 30 s at 845 °C.

⁷ Contact person: Elías Muñoz: elias@die.upm.es

In sample KQ21, taking the organics treated surface as a reference, pinch off voltage, V_{th} , is reduced, $\Delta V th = -1.8 \text{ V}$, for the N_2 -plasma treated sample and is almost maintained, for the RTA

step, $\Delta V_{th} = 0.3$ V. Similarly, the N₂-plasma treated sample shows less 2-DEG charge density, $\Delta n_s = -2.8 \ 10^{12} \ cm^{-2}$, and increases after RTA, $\Delta n_s = 1.4 \ 10^{12} \ cm^{-2}$.

Similarly, the N_2 -plasma treated sample shows less 2-DEG charge density, $\Delta n_s = -2.8 \ 10^{12} \ cm^{-2}$, and increases after RTA, $\Delta n_s = 1.4 \ 10^{12} \ cm^{-2}$ In contrast, the mean position of the electrons from the surface, W_B , diminishes either for the RTA and the N_2 -plasma treatments: ΔW_B -5.6 and -2.1 nm, respectively.

Carbon and oxygen contamination for the three samples were measured by XPS. Carbon concentration is reduced with both the RTA and N₂-Plasma. However, we found more coherent results on the three samples for the N₂-plasma cleaning than for the RTA step. This one reduces carbon concentration in a percentage of (40 \pm 20), while N₂-Plasma does by (70 \pm other On the hand, concentration variation is lower, thus the standard deviation from the mean value is less than 3, on each surface for the different treatments. Despite of this fact, it is not coherent over the three samples, due to a higher concentration of oxygen in sample KQ23 for the N₂-plasma treatment. Finally, regarding other contaminants,

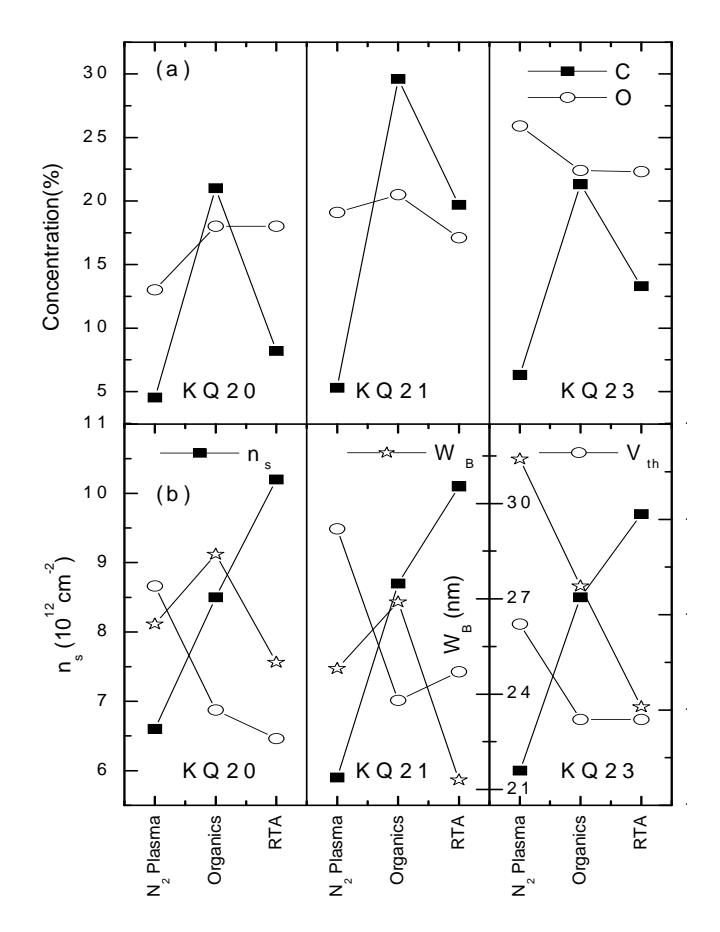


Figure. 1. (a) Oxygen and carbon contamination (b) 2-DEG, V_{th} and W_{B} , for samples KQ20, KQ21 and KQ23, after organics, RTA and N_2 -plasma.

fluorine contamination was found on the surface samples on a range between 3.5-4.7 %, not included in fig 2 (a), only after the N₂-plasma treatment. The electrical characteristics of the 2-DEG are summarized in fig.1. The pinch off voltage is increased with N₂-plasma treatment, $\Delta V th = (1.3 \pm 0.4) \text{ V}$, but showing no effect with RTA, $\Delta V th = (0.2 \pm 0.2) \text{ V}$. The 2-DEG carrier density is reduced, $\Delta ns = (-2.4 \pm 0.3) \text{ cm}^{-2}$, with the N2-plasma, and increased, $\Delta ns = (1.4 \pm 0.3) \text{ cm}^{-2}$, with the RTA. Moreover, the mean distance of the electrons to the surface is increased, $\Delta WB = (5 \pm 2) \text{ nm}$, after RTA, but no clear tendency is observed for the N₂-Plasma treatment $\Delta WB = (0.1 \pm 3.6) \text{ nm}$.

Summarizing, RTA reduces WB, increasing n_s with almost the same V_{th} on the three samples. In addition, AlGaN surface composition showed a similar oxidation but almost half of the carbon compared to the organics treatment. On the other hand, N_2 -plasma treatment, reduces both n_s and V_{th} , while there is no clear change on WB. Moreover, XPS on the N2-plasma treated samples reveals a less carbon contaminated surface and a slight difference oxidation degree than the organics treated ones.

b) Surface Passivation of AlGaN/GaN HEMT

We are studying some optimization steps in the deposition of Silicon Nitride (Si_xN_y) , the most widely used layer to mitigate collapse effects. Our efforts have been focused to investigate the effect of surface pre-treatments before SiN layer deposition. Both Metal-Insulator-Semiconductor (M-I-S) structures on GaN templates and AlGaN/GaN HEMTs have been used as test vehicles. From the electrical characterization of the M-I-S devices we have obtained a reduction around 60% of the density of the interface traps (D_{it}) between the SiN and GaN as the N_2 plasma pre-treatment is used. This is in agreement with the results obtained for HEMTs, where the output characteristics of the devices with that plasma pre-treatment were better than those without it. Figure 2 shows the increase of the DC maximum drain-source current (I_{ds^-max}) and the maximum transconductance ($g_{m max}$) in the case of using the N_2 pre-treatment respect to the case without it.

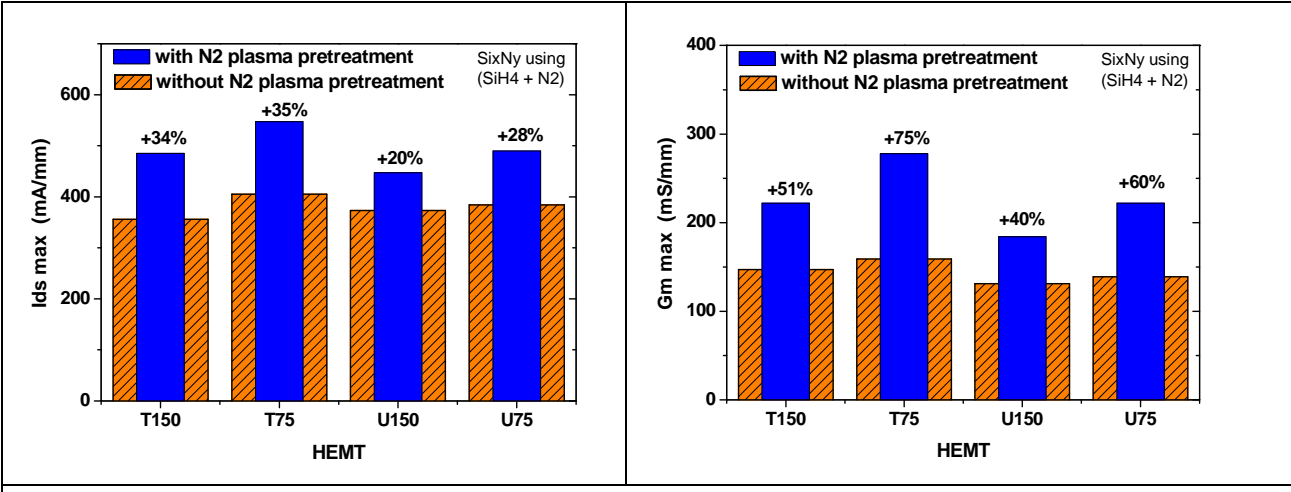


Figure.2.- Maximun values of drain-source current density (left) and trasconductance (right) of several HEMTs passivated with SiN using (SiH4+N2) with and without N_2 plasma pre-treatment.

We have also studied the use of different precursor gases to form the Si_xN_y film. The main effect on the M-I-S structures, when N_2 is used instead of NH_3 , was the high reduction of the hysteresis in the C-V characteristics, probably due to the 30% lower concentration of the Hydrogen in the film. In addition, it was proved that the effect of the N_2 plasma pre-treatment in the reduction of the Dit was independent of the precursor gases used to form the Si_xN_y . Nevertheless, Ids max and gm max in HEMT were even higher in the case of using $(SiH_4 + N_2)$. These results may suggest that the reduction of hydrogen in the film is not a main point to reduce the trap density at the insulator/semiconductor interface, and a surface pre-treatment based on a N_2 plasma before the Si_xN_y deposition seems to be beneficial in this sense.

c) Analysis of HEMTs at high temperature

The performance and modelling of HEMT transistors at high temperature (HT) is an important issue regarding applications. In order to gain a deep insight, we have performed DC measurements in HEMTs grown on several substrates, in the temperature range from room temperature (RT) up to 350°C (HT). Both I_{DS} and g_m of a HEMT decrease significantly as temperature increases, mainly due to the reduction of the electron mobility at HT. Differences in this thermal evolution have been observed between HEMT on SiC and on sapphire. It is well known that HEMTs on SiC substrates show a better performance at RT than those on sapphire, although in our samples their I_{DS} and g_m worsen faster at HT, as shown in Fig. 3a. Furthermore, HEMTs on SiC show an irreversible degradation above 300°C (Fig. 3b), whereas those on sapphire present a quite reversible behaviour along the thermal cycle. These findings require extra verification and understanding.

Measurements in TLM test structures, through the above same thermal cycling conditions, have been carried out to assess ohmic contact resistance and electron mobility variation with temperature. Ohmic resistance increases linearly with temperature, following some expected behaviour with T of the metal layer components, whereas the electron mobility decreases, being the scattering due to polar optical phonons the dominant mechanism at HT. The reversible behaviour of both parameters in such structures after the thermal cycle suggests that other specific parts of the HEMT device, such as the Schottky gate contact, passivation layer, layer relaxation, trap generation, etc., should be responsible for the experimentally observed HEMT degradation.

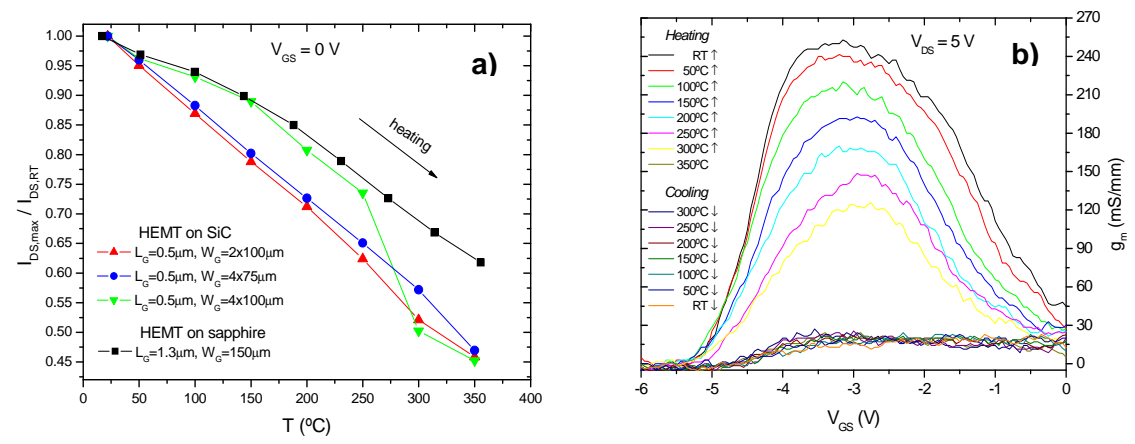


Figure 3. a) Normalized maximum drain current, $I_{DS,max}/I_{DS,RT}$, at $V_{GS}=0$ V, for several HEMTs on SiC and sapphire as temperature increases/decreases. b) g_m temperature evolution in a HEMT transistor on SiC with a gate length of 0.5 μ m and a gate width of 200 μ m.

d) Parasitics and traps

The detection of traps in the various regions of a HEMT device is being studied by transient I-V responses and capacitance techniques, both in the dark and under illumination with photons of selected energies. Slow transient I-V recordings (from ms to seconds) have been detected, and linked to surface traps and passivation quality. Dispersion analysis by C-V-f techniques is being used to compare HEMT devices made by Molecular Beam Epitaxy (MBE) and MOVPE, using Si, SiC and sapphire substrates, and being processed by several foundries. It is intended to develop a kind of screening procedures to compare the final traps shown in the devices studied in the final comparison. Those devices, with their C-V-f fingerprints, will be thus tracked as they suffer thermal storage tests, RF stress cycles and operation life tests. As an example, Figure 4 shows the dispersion characteristics in two wafers, grown by MOVPE, on SiC (left) and on sapphire (right). Such procedure and results need further efforts to be completed.

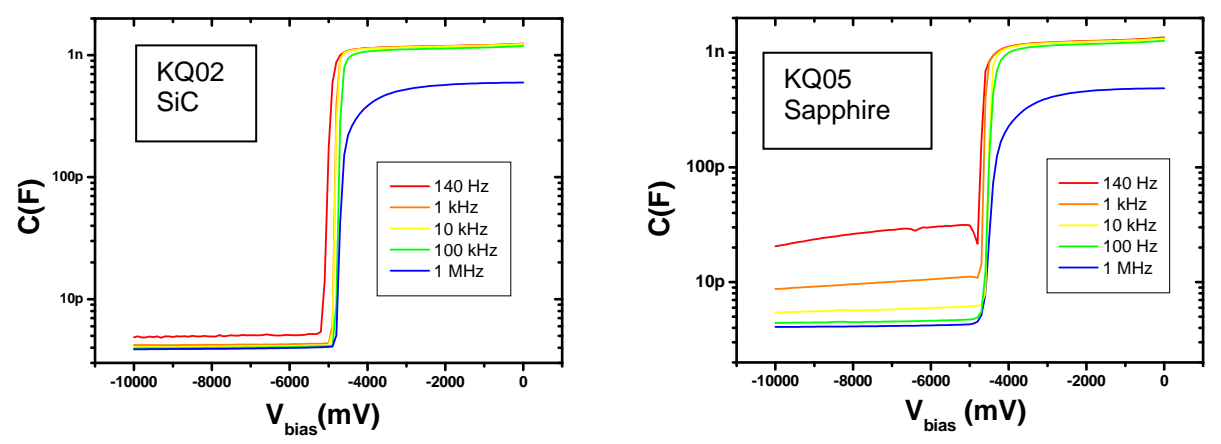


Figure 4.- C-V characteristics from KQ02 (left, on SiC) and KQ05 (right, on Sapphire) wafers at 140 Hz (red), 1, 10, 100 and 1000 kHz (orange, yellow, green and blue solid lines, respectively).

6.8 SAW and PSAW Devices in Nitride Heterostructures: Characteristics and Novel Applications 8

Surface acoustic wave (SAW) devices have undergone a great development in the last three decades in the field of fast analog signal processing due to their compactness and reliability. Nowadays, they are key components in wireless communications and systems, both in the IF and RF ranges, as well as in tag and sensor applications. Most of the outstanding characteristics of SAW devices rely on the correct choice of the piezoelectric substrate material used for their fabrication.

(Al,Ga)N layers combine a high sound velocity, a considerable electromechanical coupling, and an outstanding thermal and chemical stability [1-3]. However, the required heteroepitaxial growth of nitrides imposes the study of the acoustic propagation properties and the dispersion of the particular layered system. In addition, wave confinement may arise on these systems depending on the layer(s)-substrate combination. Thus, the first section of this paper will be devoted to the dispersion characteristics of the different SAWs and pseudo-SAWs (PSAW) propagating in (Al,Ga)N layers on sapphire(0001). The polarization mixture induced by the acoustic anisotropy of the substrate will be described.

On the other hand, the semiconductor character and direct bandgap of nitrides enables the combination of SAW devices with electronics and optoelectronics [4]. Therefore, the interaction of SAWs and PSAWs with carriers will be addressed in sections 2 and 3. In particular, section 2 is devoted to the performance of SAW devices on AlGaN/GaN heterostructures, which present a two dimensional electron gas (2DEG) at the heterojunction produced by the bandgap discontinuity of the system. Finally, section 3 is dedicated to the integration of SAW devices with UV photodetectors in GaN layers, based on the transport of the photogenerated carriers by the SAWs and PSAWs.

1.- Anisotropy-induced polarization mixture in (Al,Ga)N/sapphire(0001) systems

Figure 1(a) and (b) shows the transmission characteristics of two SAW filters along the $[1\bar{1}00]$ and $[11\bar{2}0]$ directions of sapphire, in a GaN film and in an AlGaN/GaN bilayer on sapphire(0001), respectively. The anisotropy is produced by the trigonal symmetry of sapphire (crystal class 3m), since wurtzite nitrides (crystal class 6mm) present isotropic elastic and piezoelectric properties in the c-plane [5]. The higher sound velocity in the substrate than in the layer allows the propagation of guided modes on the overlayer. Thus, in addition to the Rayleigh (R) mode, guides Sezawa (S_i) and Love (L_i) modes arise in the heterostructure. It has to be pointed out the unusual excitation of shear horizontal or L_i modes, since conventional interdigital transducers (IDT) are expected to excite only sagittal waves. This novel behaviour is produced by the polarization mixture induced the sapphire anisotropy [6]. The GaN and AlGaN/GaN on sapphire systems also support PSAWs above certain velocity threshold related to the longitudinal bulk wave velocity, as indicated in the dispersion curves of the GaN/sapphire(0001) heterostructure along the $[1\bar{1}00]$ and $[11\bar{2}0]$ directions shown in Figs. 2(a) and (b), repectively.

_

⁸ Contact person: Fernando Calle: calle@die.upm.es

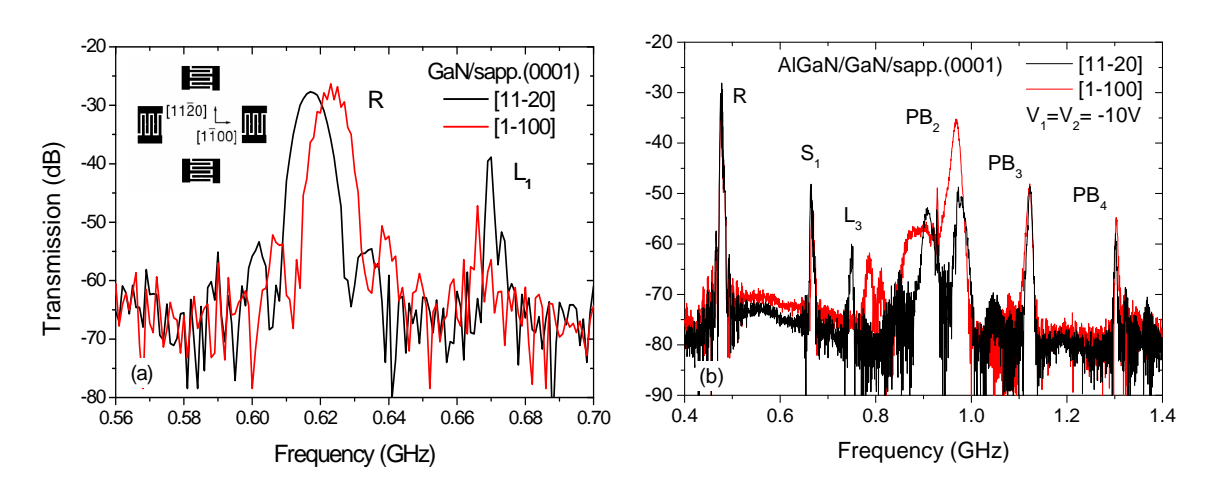


Figure 1. Transmission characteristics of two SAW filters on a (a) GaN film (H=1.2 μ m) and an (b) AlGaN/GaN structure (H=0.02/7.6 μ m) on sapphire(0001) along the [1100] and [1120] directions of the substrate, as shown in the inset of (a).

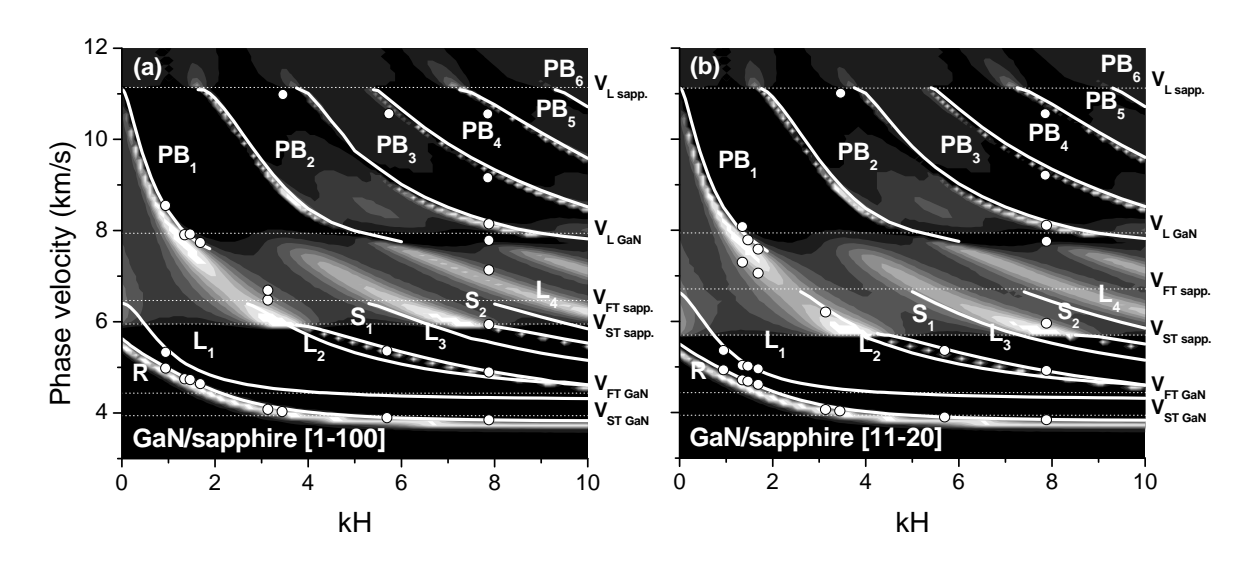


Figure 2. Phase velocity dispersion of the SAWs (R, S_i and L_i modes) and PSAWs (PB_i modes) propagating in the GaN/sapphire(0001) heterostructure along the (a) [1100] and (b) [1120] directions of the substrate.

2. Field-effect-modulated SAW devices in AlGaN/GaN heterostructures

Figure 3(a) shows the transmission of the Rayleigh mode for a SAW filter on a 2DEG AlGaN/GaN heterostructure for different symmetric input- and output-IDT-bias conditions ($V_1=V_2$). In the non-biased case, the SAW transduction is impeded since the piezoelectric fields are screened by the 2DEG. However, the application of a bias larger than the threshold voltage of the heterostructure allows to fully deplete the 2DEG under the IDTs, as indicated by the capacitance-voltage curve and the associated sheet density of charge shown in Fig. 3(b) [7-8]. This charge depletion is accompanied by a reduction of 25 dB in the insertion loss of the filter, Fig. 3(a). In addition to the 2DEG depletion, the filter response is also governed by the band diagram

modulation and the electromagnetic feedthrough induced by the particular DC polarization scheme [9]. The field-effect modulation of the insertion loss of the 2DEG AlGaN/GaN filters offers new synergies and capabilities. Thus, this voltage controlled filter can be integrated into GTC (Gain Time Control) circuits for radar applications, which require a time dependent control of the amplitude response of the system. Other applications, such the integration of the SAW technology with microwave electronics based on AlGaN/GaN HEMTs, as well as acousto-electric modulators and sensors are foreseen.

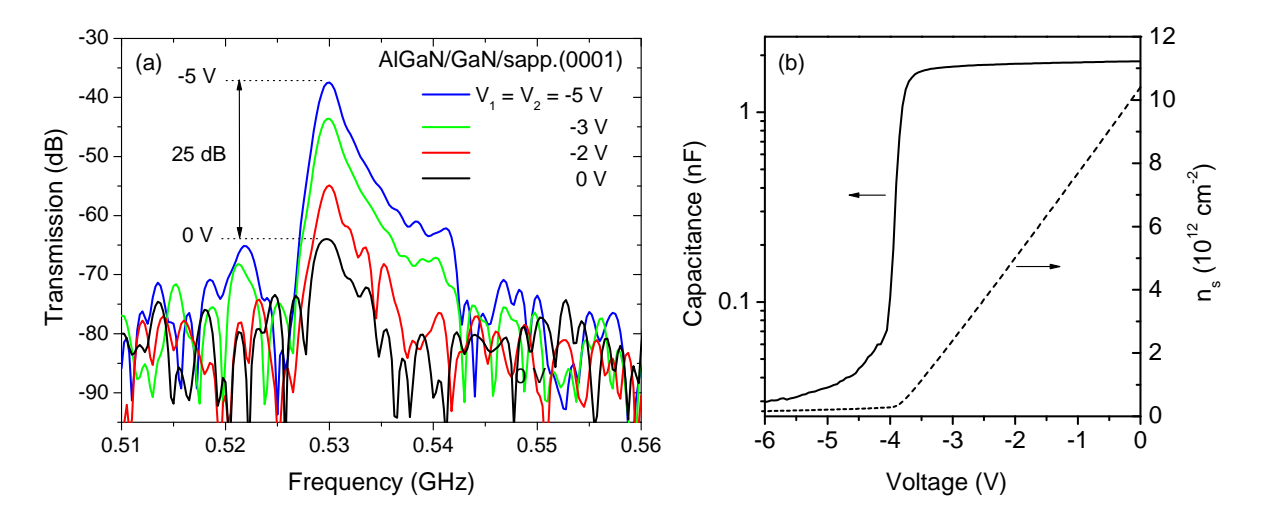


Figure 3. (a) Transmission spectra of the Rayleigh mode (time gated) for a SAW filter on a 2DEG AlGaN/GaN heterostructure on sapphire(0001) under different bias; (b) Capacitance-voltage characteristic and associated sheet carrier density, n_s , of the heterostructure.

3. SAW-assisted UV MSM photodetectors in GaN

Figure 4(a) shows a SAW delay line, in which the input IDT acts as a SAW generator and the output IDT as a metal-semiconductor-metal (MSM) photodetector [10]. The GaN film region between both IDTs is illuminated with an UV laser, indicated by the spot in the figure, whereas the MSM illumination is prevented.

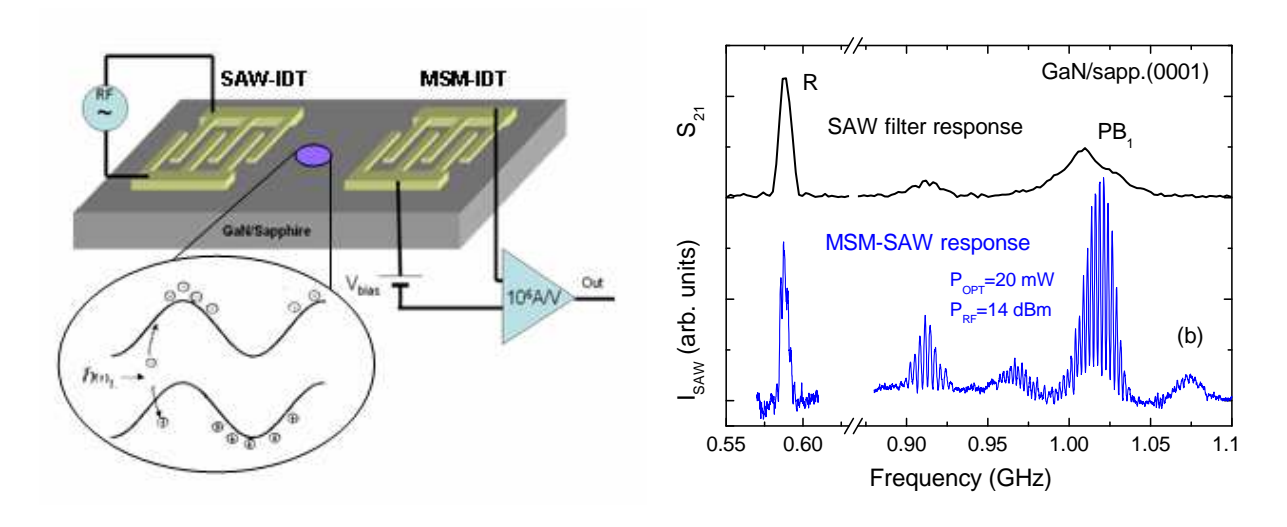


Figure 4. (a) MSM photodetector assisted by SAWs; (b) Responsivity of the MSM-SAW detector compared to the transmission characteristic of the SAW filter.

The SAW filter transmission and the responsivity of the MSM detector assisted by SAWs are compared in Figure 4(b). The responsivity is increased when the resonance frequencies of the IDT, corresponding either to SAWs or to PSAWs, are tuned. The photogenerated carriers, spatially separated by the piezoelectric fields accompanying the acoustic waves and confined in their moving potential wells, are swept to the MSM, which collects them. The responsivity of the system is linear with the optical irradiance, but non-linear with the RF power [11]. The latter saturates for high RF powers in the low optical power regime where all the photogenerated carriers are expected to be swept by the acoustic wave. The remote collection of the e-h pairs assisted by SAWs increases the active optical area of the photodetector, which is restricted to the depletion region around the Schottky contacts in a conventional MSM detector. In addition, it allows to take the detector out of the sensing region in the case of harsh environments. Moreover, further applications such as single or 2D-array multicolor detectors, acousto-optical modulators, and opto-chemical sensors are envisaged.

In summary, the propagation characteristics of SAWs and PSAWs in various nitride heterostructures are described. The field-effect modulation of the SAW device response in a 2DEG AlGaN/GaN heterostructure is presented. The advantages of the integration of a SAW device with a MSM photodetector and the performance of this new device are addressed. In addition to SAW devices, thin-film bulk acoustic resonators (TFBAR) and Microelectromechanical Systems (MEMS) based on nitride heterostructures are planned as future research lines.

- [1] T. Palacios, F. Calle, J. Grajal, E. Monroy, M. Eickhoff, O. Ambacher, and F. Omnès, Proc. 2002 IEEE Ultrason. Symp. 1, 57 (2002).
- [2] T. Palacios, F. Calle, E. Monroy, J. Grajal, M. Eickhoff, O. Ambacher, and C.Prieto, Mat. Sci. Eng. B 93, 154 (2002).
- [3] R. J. Jiménez Riobóo, E. Rodríguez-Cañas, M. Vila, C. Prieto, F. Calle, T. Palacios, M. A. Sánchez, F. Omnès, O. Ambacher, B. Assouar, and O. Elmazria, J. Appl. Phys. 92, 6868 (2002).
- [4] F. Calle, J. Pedrós, T. Palacios, and J. Grajal, Phys. Stat. Sol. c 2, 976 (2005).
- [5] J. Pedrós, F. Calle, J. Grajal, R. J. Rioboó, C. Prieto, J. L. Pau, J. Pereiro, M. Hermann, M. Eickhoff, and Z. Bougrioua, Superlattices and Microstruct. 36, 815 (2004).
- [6] J. Pedrós, F. Calle, J. Grajal, R. J. Jiménez Riobóo, Y. Takagaki, K. H. Ploog, and Z. Bougrioua, Phys. Rev. B 72, 075306 (2005).
- [7] F. Calle, J. Grajal, and J. Pedrós, Electron. Lett. 40, 1384 (2004).
- [8] J. Grajal, F. Calle, J. Pedrós, and T. Palacios, 2004 IEEE MTT-S Int. Microwave Symp. Digest 1, 387 (2004).
- [9] J. Pedrós, R. Cuerdo, F. Calle, J. L. Martínez-Chacón, and Z. Bougrioua, Proc. 2006 IEEE Ultrason. Symp. (in press).
- [10] T. Palacios, F. Calle, and J. Grajal, Appl. Phys. Lett. 16, 3166 (2004).
- [11] F. Calle, T. Palacios, J. Pedrós, and J. Grajal, Proc. SPIE vol 5502, 435 (2004).

6.9 Photonic devices based on slot-waveguides 9

The Institute for Systems based on Optoelectronics and Microtecnology (ISOM) has started a new research line focused on the development of novel photonic devices based on a recently demonstrated waveguide structure named slot-waveguide. By using the electric (E)-field discontinuity at the interface between high-index-contrast materials, this structure enables to guide and to confine light inside a nanometer-size area of low-index material, with high E-field amplitude and optical intensity in that region. This property allows highly efficient interaction between fields and active materials, which may lead to all-optical switching and parametric amplification on integrated photonics. Since, a strong E-field confinement is localized to a nanometer-sized low-index region; therefore the slot waveguide can be used to greatly increase the sensitivity of compact optical sensing devices or to enhance the efficiency of near-field optical probes. Besides, the use of a high index-contrast system enables the implementation of compact devices based on this new type of waveguide.

1.- Electrically-driven silicon resonant light emitting device based on slot-waveguide

ISOM, in collaboration with Cornell University (USA), is involved in the development of light emitting resonant devices on silicon based on slot-waveguides. Recent breakthroughs have boosted the interest in Si microphotonics as a technology for integrating optical and electronic components on a single Si chip. In particular, the demonstration of a continuous-wave optically-pumped Si laser has been of special relevance. However, such a device is optically-pumped and emits at 1.686 µm wavelength, limiting its practical applications. An electrically-driven Si light emitting device (LED) is desirable since it can be considered as the natural interface between photonics and electronics. In addition, emission at 1.55-µm-wavelength is also required for applications in the telecommunication field.

Among the different approaches for achieving an electrically-pumped Si-based light emitting material at $1.55~\mu m$ compatible with the CMOS technology, Erbium (Er)-doped SiO₂ has been shown to be a promising option. Si LEDs based on metal-oxide-semiconductor (MOS) structures with Er implanted in the thin gate oxide have shown external quantum efficiencies as high as 10%, which is comparable to that of standard III-V semiconductors LEDs. By current injection through the MOS structure, energetic (hot) electrons can excite Er ions by impact ionization and generate electroluminescence at $1.54~\mu m$.

An optical cavity can enhance the external quantum efficiency of LEDs and it is an essential element for a laser. In order to be employed with the aforementioned Er-doped SiO₂ active material for on-chip applications, an optical cavity should: 1) permit electrical injection, 2) present a high optical mode-active material overlap, 3) be made of CMOS-compatible materials, 4) be micron-size, and 5) exhibit a high quality-factor Q. A planar waveguide-based cavity, such as a ring or disk resonator, is a good choice for this purpose since it can provide a long light-matter interaction path. However, Er-doped SiO₂ has low refractive index and, therefore, a conventional strip waveguide using this material as the core would present two important drawbacks: a) waveguides would require a large cross-section area, which makes difficult current injection through the thick oxide, and b) the low-index-contrast system SiO₂/air does not facilitate miniaturization.

_

⁹ Contact person: Carlos Angulo: cbarrios@die.upm.es

Slot-waveguides overcome the aforementioned drawbacks. This waveguide enables to concentrate a large fraction of the guided mode into a thin low-index layer (slot) sandwiched between two high-index strips. Thus, if the slot-waveguide geometry consists of two doped Si strips (electrodes), sandwiching a thin Er-doped-SiO₂ slot layer (gate oxide), current injection through the gate oxide can be achieved, generating light in the oxide-slot region where the guided-mode is strongly confined. Thus, the aforementioned requisites 1, 2 and 3 are fulfilled. The feasibility of requisites 4 and 5 has been demonstrated, reporting 50-µm-diameter high-Q (~20,000) optical resonators in silicon-on-insulator based on slot-waveguides with losses as low as 10 dB/cm. In this work, we show how by using these advantageous characteristics of the slot-waveguide geometry, compact electrically-driven resonant cavity light-emitting devices (RCLED) for Si microphotonics can be obtained.

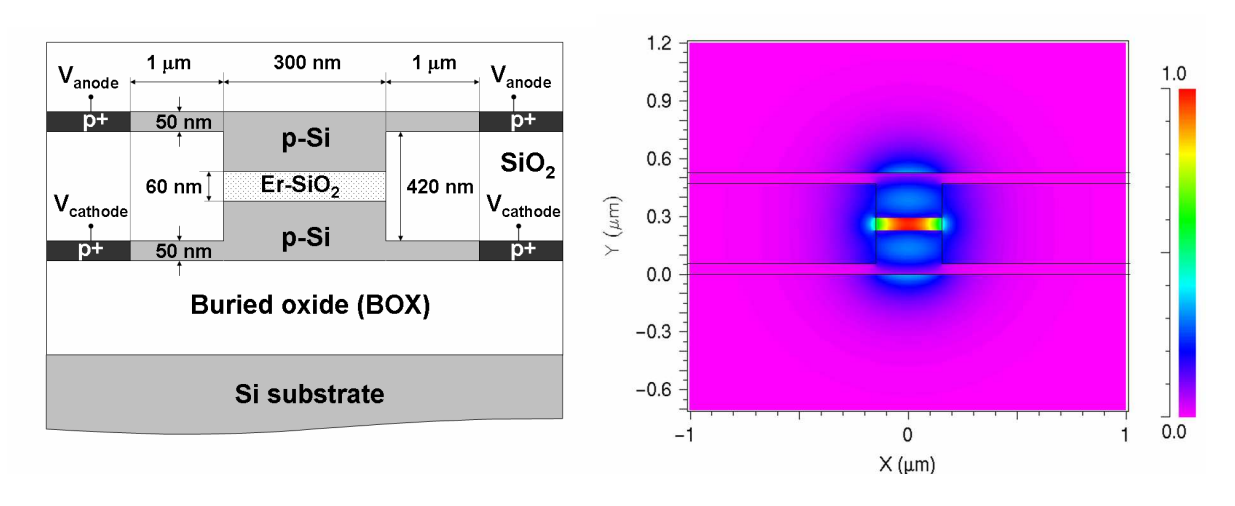


Figure 1. a) Schematic cross-sectional view of a horizontal MOS slot-waveguide. b) Transverse E-field amplitude (contour) of the quasi-TM optical mode.

We have recently demonstrated disk resonators based on horizontal slot-waveguides on both Si/SiO₂/Si and Si₃N₄/SiO₂/Si configurations, with quality factors as high as 45,000 and optical losses as low as 1.5 cm⁻¹, which makes them very promising for implementing electrically-pumped light emitting devices (laser or LED) in Si.

2.- Ultrasensitive nanomechanical photonic sensor based on horizontal slot-waveguide resonator

ISOM is also involved in the development of another photonic device based on a slot-waveguide for sensing applications: a novel nano-opto-mechanical deflection sensor.

Micro-opto-electro-mechanical (MOEM) devices based on the principles of integrated optics and micromachining technology on silicon have immense potential for sensor applications. In particular, microcantilevers represent ultrasensitive nanomechanical sensors for the detection of chemical and biochemical reactions in both gas-phase and liquid environments. In these devices, either a laser beam reflected off the cantilever surface is monitored with a position-sensitive photodetector or the coupling efficiency between two optical waveguides is measured. Subangstromg and subnanometer resolutions have been exhibited by these devices.

Integrated optical microresonators have been also shown to be efficient devices for biochemical sensing. Optical enhancement produced in disk and ring resonators makes the response of these photonic structures very sensitive to small variations of its optical length (refractive index, physical length or both) originated by biochemical reactions.

Thus, a sensor combining the advantages of both of the aforementioned devices (microcantilever and optical microresonator), would benefit from the high sensitivity of both structures leading to an overall enhanced sensitivity. In this work, I show how by using a recently invented photonic structure called slot-waveguide, such a device can be achieved. A slot-waveguide consists of two stripes or slabs of a high index material separated by a thin low-index region (slot). In such a structure, the electric (E)-field discontinuity at the interface between high-index-contrast materials enables to guide and to confine light inside a nanometer-size area of low-index material, making it very sensitive to small variations of the slot distance.

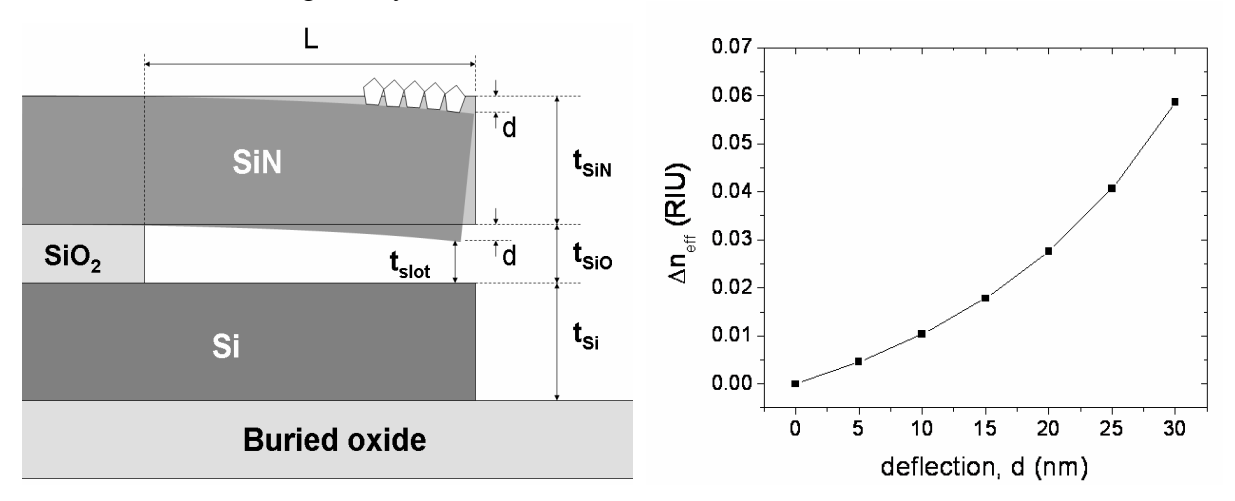


Figure 2. A) Sensor device operation. Surface stress on the upper surface of the cantilever produced by the adsorption or recognition of molecules results in a static bending of the cantilever. B) Variation of the effective refractive index of the disk mode as a function of the deflection d.

Ultrahigh sensitivity results from the combination of the high sensitivity of the slot-waveguide to slot distance variations and the high sensitivity of a disk resonator to effective index variations. A deflection sensitivity of 33 nm⁻¹ is predicted, representing an enhancement of 4 orders of magnitude as compared to state-of-the-art microcantilever sensors.

3.- Ultrahigh sensitivity slot-waveguide biosensor on a highly integrated chip for simultanous diagnosis of multiple diseases

ISOM is a partner of the European Project entitled "Ultrahigh sensitivity Slot-wAveguide BIOsensor on a highly integrated chip for simultanous diagnosis of multiple diseases" (SABIO). This is a multidisciplinary project involving the emerging fields of micro-nano technology, photonics, fluidics and bio-chemistry, targeting to contribute to the development of intelligent diagnostic equipment for the healthcare of the future. SABIO will address this objective through the demonstration of a compact polymer-based and silicon-based CMOS-compatible micro-nano system. It integrates optical biosensors for label-free biomolecular recognition based on a novel photonic structure named slot-waveguide with immobilised biomolecular receptors on its surface. This structure offers the possibility of confinement and guidance of light in a nanometer-size void

channel enhancing the interaction between an optical probe and biomolecular complexes (antibodyantigen). A slot-waveguide interferometric biosensor is predicted to exhibit a surface concentration detection-limit lower than 1 pg/mm², that is the state-of-the-art in label-free integrated optical biosensors, with additional advantages such as the possibility of multiplexed assay, which, together with reduced reaction volumes, leads to the ability to perform rapid multianalyte sensing and comprehensive tests. This offers the further advantageous possibility of assaying several parameters simultaneously (e.g. several cancer-associated antigens in one sample or several diseases antigens, such as those originating from several infectious pathogens). Consequently, statistical analysis of these results can potentially increase the reliability and reduce the measurement uncertainty of a diagnostic over single-parameter assays. In addition, the SABIO micro-nano system device applied to its novel protein-based diagnostic technology has the potential to be fast and easy to use, making routine screening or monitoring of diseases more costeffective. The ultimate target of SABIO is demonstrating the feasibility of diagnostics 'outside' of laboratory settings (e.g. at 'point of care', in such as General Practitioner's surgery, in the field or in urgent situations). A final prototype consisting of a packaged biochip will be used on clinical samples in order to detect important virus diseases such as viral hepatitis, liver cancer and cytomegalovirus (CMV).

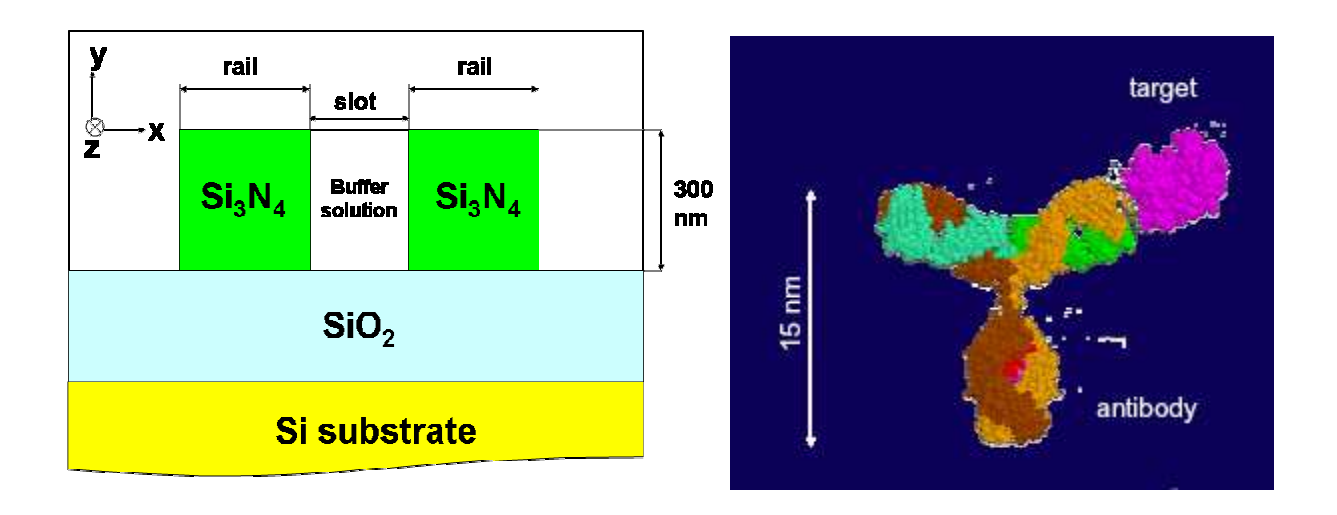


Figure 3. A) Schematic cross section of a silicon nitride slot-waveguide for the detection of biomolecules (antibodies, antigens). B) Schematics of a typical antibody and target biomolecules.

- 1.- B. Schmidt, C. A. Barrios, and M. Lipson, "Si₃N₄-SiO₂-Si slot-waveguide disk resonators in a silicon photonic platform" Materials Research Society (MRS) Fall meeting, paper L2.8, Boston, Massachussets, USA, 2006.
- 2.- C. A. Barrios, Q. Xu, J. Shakya, C. Manolatou, and M. Lipson "Compact Silicon Slot-Waveguide Disk Resonator," Conference on Lasers and Electro-Optics (CLEO) 2006, paper CTuCC3, Long Beach, California, USA, 2006.
- 3.- C. A. Barrios, "Ultrasensitive Nanomechanical Photonic Sensor based on Horizontal Slot-Waveguide Resonator," IEEE Photonics Technology Letters, vol. 18, no. 22, pp. 2419-2421, 2006.

6.10 An approach to an integrated magnetic sensor 10

This work represents a joint effort from different groups within Europe to create a new technology of integrated magnetic sensors. Magnetic sensors based on magnetostrictive materials have been used in the past [1-3], showing very promising characteristics. Nevertheless, this family of sensors has never been successfully integrated due to many different problems.

We have developed the technology to integrate this type of sensors. The sensor head is a free-standing structure covering a total area of $200\times360~\mu\text{m}^2$ and less than $3~\mu\text{m}$ thick. This structure has a frame of Si/SiO_2 attached by four legs to the bulk (Figure 1). All the elements within the sensor head are connected to the contact pads through those four legs that also help to dissipate heat. The piezoresistive bridge (doped Si) is buried in the thin free-standing structure. Figure 1 right shows a picture of the device illuminated with back light were the bridge is visible.

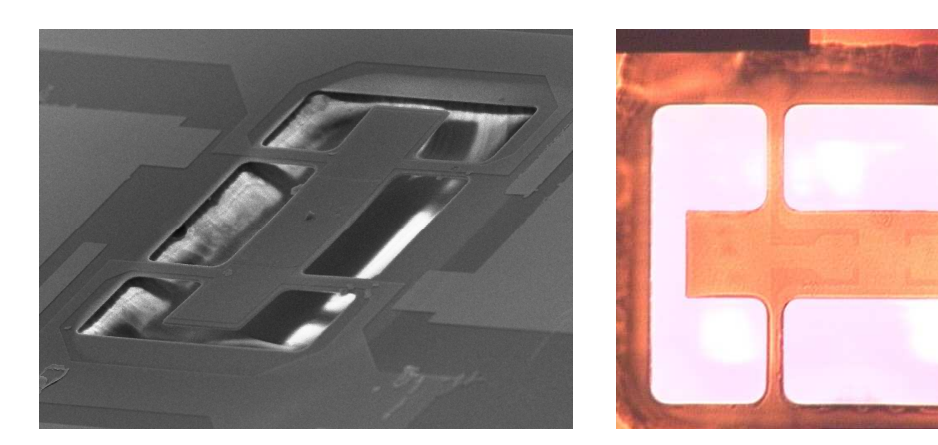


Figure 1. Left is a SEM picture of a device with all the layers visible. Right is a back light picture showing the embedded piezoresistive bridge.

The magnetic material is a 150 nm thick layer of $(Fe_{80}Co_{20})_{80}B_{20}$ ($\lambda_s\sim25$ ppm in our films), deposited by DC magnetron sputtering both below and on top of a 300 nm thick Cu layer acting as a current line. We call this configuration 'closed-flux': the pulsated current flowing through the Cu current line generates a field, which is antiparallel in the top and bottom magnetic layers. This antiparallel configuration helps the magnetization process of the magnetic elements, otherwise

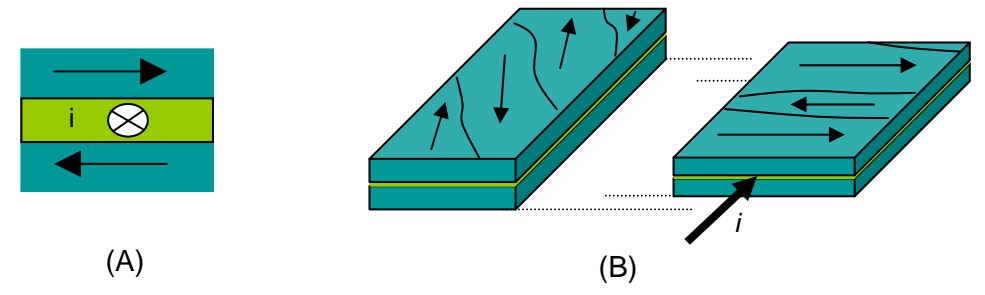


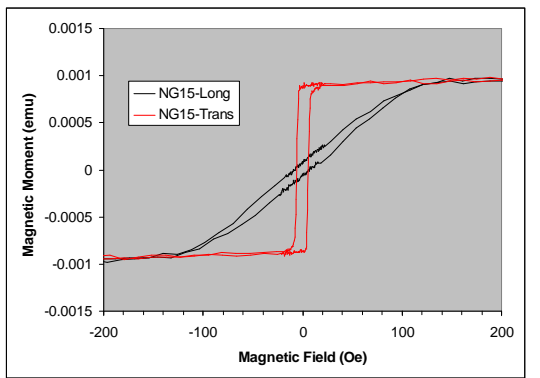
Figure 2. (A) Closed loop configuration. (B) Magnetization process of the magnetic material due to the current, showing the change in size.

_

¹⁰ Contact person: Jose Luis Prieto: joseluis.prieto@upm.es

difficult due to the demagnetizing field (Figure 2). This same figure shows how the current magnetizes the magnetic material and changes its size. The operation mode of the device drives the device to the mechanical resonance of the free standing structure, which depends on the dimensions and design, ranging from 10 kHz in simple cantilevers to 80 kHz in the 'crocodrile' structure shown in Figure 1.

Obviously, the coercivity of the magnetic material is crucial for the operation of the device. If the coercive field is high, the current required to magnetized the device would be too high and the dissipation of heat would be impossible. It is being known for decades that compositions giving softer magnetic properties are those with zero magnetostriction [4] (for instance Permalloy Ni₈₀Fe₂₀ or the amorphous Fe_{80-x}Ni_xB₂₀, with the softest properties for low content of Fe, which gives close to zero magnetostriction) and it is commonly believed that magnetostriction and large coercivity are inseparable. During this project, we have developed a method where both the coercive and the anisotropy field (Hc and Hk) in a magnetostrictive material can be reduced only by playing with the anisotropy direction and with the stress induced by the deposition technique (sputtering). The key is to play with the magnetoelastic energy during the sputtering deposition of the film. Dividing the sample in multilayers with perpendicular anisotropies, we have been able to have, on average, a clear reduction of the coercive field. Additionally, by having orthogonal anisotropies we are able to reduce the total anisotropy of the sample and therefore the anisotropy field. This is a very important control from the point of view of a magnetic sensor, as low anisotropy field implies lower dynamic range but larger sensitivity. Figure 3 shows the comparison between two samples, one single layer and one multilayer with orthogonal anisotropies. The improvement of the material is quite substantial.



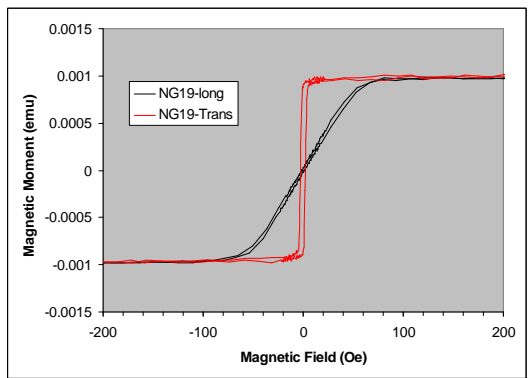
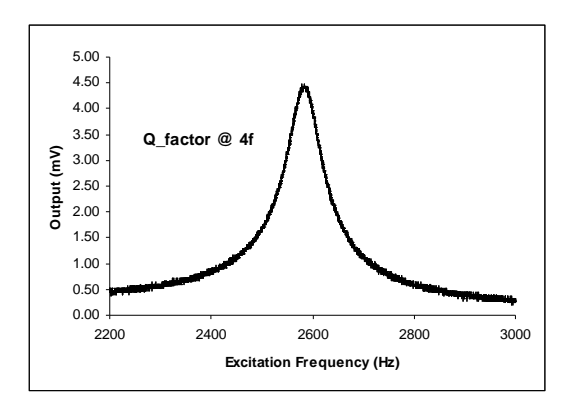


Figure 3. Comparison between the hysteresis loops in two samples, a single layer (left) and a multilayers with orthogonal anisotropies (right).

The device operates as follows: the electrical current flowing through the current line magnetizes the magnetic material at a frequency that is a harmonic of the mechanical resonance of the structure which, depending on the device is around 80 kHz. We have found that the output signal is quite large even at higher than the 2nd harmonic, which helps to avoid the noise created by the mechanical beat thermally induced by the exciting current, which is a 2nd harmonic. The sensing element is a piezoresistive Wheatstone bridge embedded in the Si frame. All the metal depositions are made before the sensor structure is released. The releasing technique will be briefly explained further below. The project is now through the optimization of the first devices, which are showing a moderate sensitivity or around 1 mV/Oe. This sensitivity should increase by a factor 100 when the devices are encapsulated in vacuum, as the Q factor of the devices increases dramatically

in those conditions. One interesting fact, as mentioned before is that the device does not loose much performance when working with the forth harmonic of the resonance. This has two advantages: it avoids the 2nd harmonic of the thermal drift of the current pulses and it allows operation at lower frequencies. Figure 4 shows the comparison between the response of a cantilever structure at second and fourth harmonic. Although the sensitivity drops slightly working at the fourth harmonic the Q factor is even better than at the second harmonic.



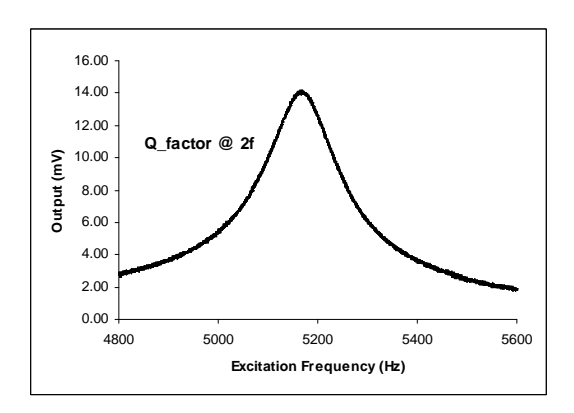


Figure 4. Response of a prototype device at the second and fourth harmonic of the mechanical resonance of the device.

Although the fabrication route is industry friendly and based on Si, it is complicated. Firstly, the piezoresistive elements are buried on a Si wafer. The wafer is aligned with a glass substrate with pre-etched cavities were the devices will be situated. The Si wafer is wet etched away, until its thickness is about three microns. At this stage, the Si and the embedded piezoresistive bridges are held by the glass with cavities. The Au contacts are deposited but a pulsated large current is required to make the contact with the piezoresistor ohmic. The chip as it is can be used for the deposition in the sputtering of the metallic layers, the closed flux trilayer. The last step is RIE etching with SF6 in order to define the structure.

Next page shows some data and pictures of finished devices.

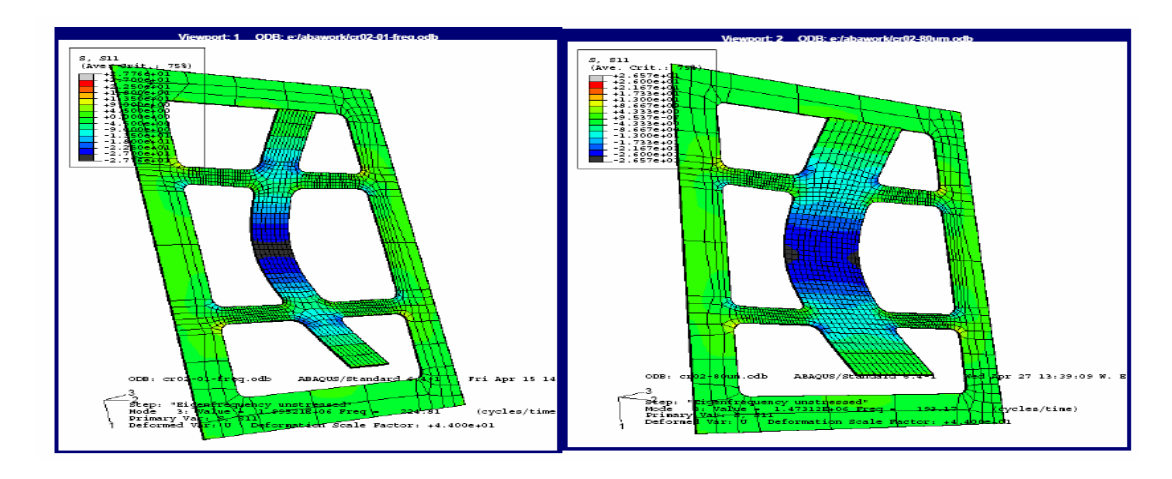
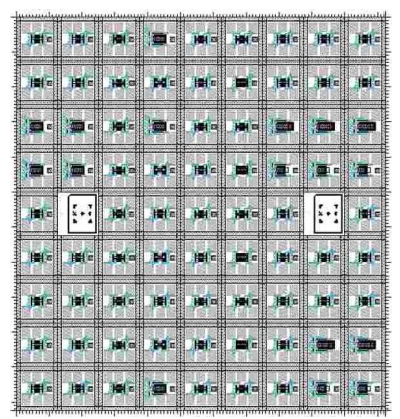


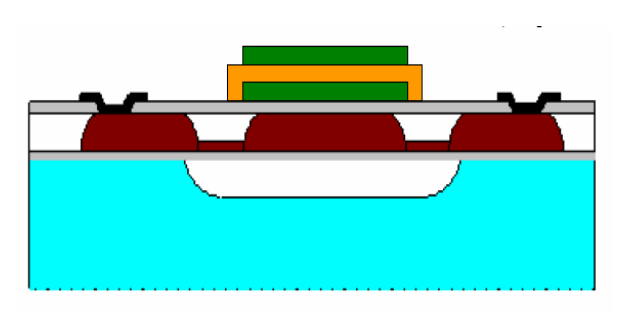
Figure 5.- Simulations of the mechanical behaviour of different configurations



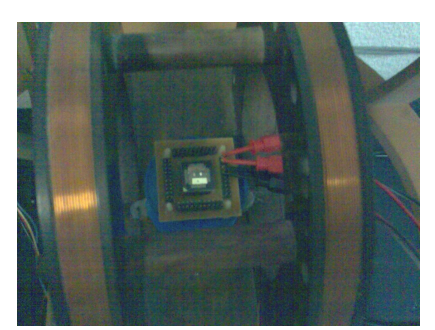
Chip Layout



SEM overview of the chip



Lateral view of the device



Top view of the measuring rig with chip

Eigenfrequencies of the interesting modes

Structure	Crocodile with 50µm width	Crocodile with 80µm width	Crocodile with 80µm width - H	Crocodile with 80µ m width – 1/3	Simple cantilever Main version	Simple cantilever Long version	Simple cantilever short version
E. frequency of the 1st mode	-		79 kHz	-	8.6 kHz	4.7 kHz	20 kHz
E. frequency of the 3 rd mode	212 kHz	194 kHz	240 kHz	201 kHz			

References

- [1] SS. Guo et al. Appl. Phys. Lett. 88, 182906 (2006)
- [2] J.L. Prieto et al. J. Mag. Mag. Mat. 215, 756 (2000)
- [3] M.D. Mermelstein, *IEEE Trans. Magn.* 28, 36 (1992)
- [4] Robert O'Handley, Modern Magnetic Materials. Principles and Applications, Wiley-Interscience, p.226 (2000)

6.11 New RFID system of low frequency that avoids screening magnetic problems ¹¹

1. Introduction.

The term RFID is the short of Radio Frequency IDentification and comprises all different technologies that uses radio frequency signals to transmit information from a movil element (tag) and a fixed station (excitation and reader). These technologies have lots of different application like object track, control access, real time location, manufacturing processing, medicine, agriculture, automatical identification, logistics, etc. Its comercial use is growing exponentically. During the last year, about 600 million tags have been sold and the value of this market is expected to be multiplied by ten during the next decade¹.

Basically, there are tree different RFID technologies attending to the physical way of comunication: inductive coupling, electromagnetic backscattering and electrical coupling. The two first groups can be classified according to its work frequency band: low frequency (LF- 125 and 134.2 kHz), high frequency (UF- 13.56 MHz), ultra high frequency (UHF- ~900 MHz) and microwave (ISM- 2.4 GHz). All this technologies have screening problems when working with metals in the surruondings. For example, a layer of 27 µm of aluminium completely shields a typical passive tag². Tags are called active if they have a battery and passive if they have not. The last type of tag are the most important from a comercial point of view. The screening problems can be avoided by reducing the work frequency. However, the previous mentioned technologies work by using resonant circuits that became ineficient below 100 kHz. The system developed at ISOM avoids such a problem and make possible work at very low frequencies down to 1 kHz.

2. Description.

The new RFID system is based on the measurement of the changes of magnetization of a magnetic core inside the card (that are produced by a circuit integrated in the card by opening and closing a winding around the magnetic core). To produce the magnetization of the magnetic core, power the circuit of the card and produce the current in the winding, it is employed an alternating magnetic field (emitter modulus). The changes of magnetization are detected (reception modulus) by a magnetic field sensor. The card is magnetized due to the magnetic field and so, the magnetization has the same frequency than the applied magnetic field. The higher magnetization of the magnetic core of the card, the higher amplitude of the signal at the reception modulus. Thus, by opening and short-circuiting the winding of the card (with a minor frequency than the magnetic field) and so by changing the magnetization of the magnetic core, information can be sent to the reception modulus.

Let us now to sum up the characteristics of the three modulus. Figure 1 represents a block diagram of the system.

74

¹¹ Contact person: Claudio Aroca: caroca@fis.upm.es

Emitter Modulus.

It consists in a source of an alternating magnetic field with a frequency minor to 100 kHz but with a region without magnetic field where the reception modulus can be set avoiding its saturation. The alternating magnetic field magnetizes the magnetic core of the contactless smart card and it powers the integrated circuit of the card too.

Reception Modulus.

It is used a tunable magnetic sensor of magnetic field (fluxgate) that detects the changes of the magnetization of the magnetic core of the card. To avoid the saturation of the sensor, it is placed in the region without magnetic field given by the excitation modulus. So, the sensor can measure the presence of a magnetic material magnetized by the magnetic field produced by the emitter modulus but not this magnetic field itself. It is made a double in phase demodulation³: the first one to obtain a signal proportional to the magnetic field and the second one to select only the magnetic fields that change with the same frequency than the magnetic field employed as excitation (that is the frequency of the magnetization of the card).

Tag.

It has a magnetic core and a short-circuitable winding around it. The magnetic field produced by the winding (due to the induced current by the alternating magnetic field of the emitter modulus) can produce a change of the magnetization of the magnetic core without employing a resonant circuit. The induced electromotive force in the winding is also used to power the integrated circuit of the card. This circuit opens and closes the same winding changing the magnetization of the magnetic core. Information can be send in this way.

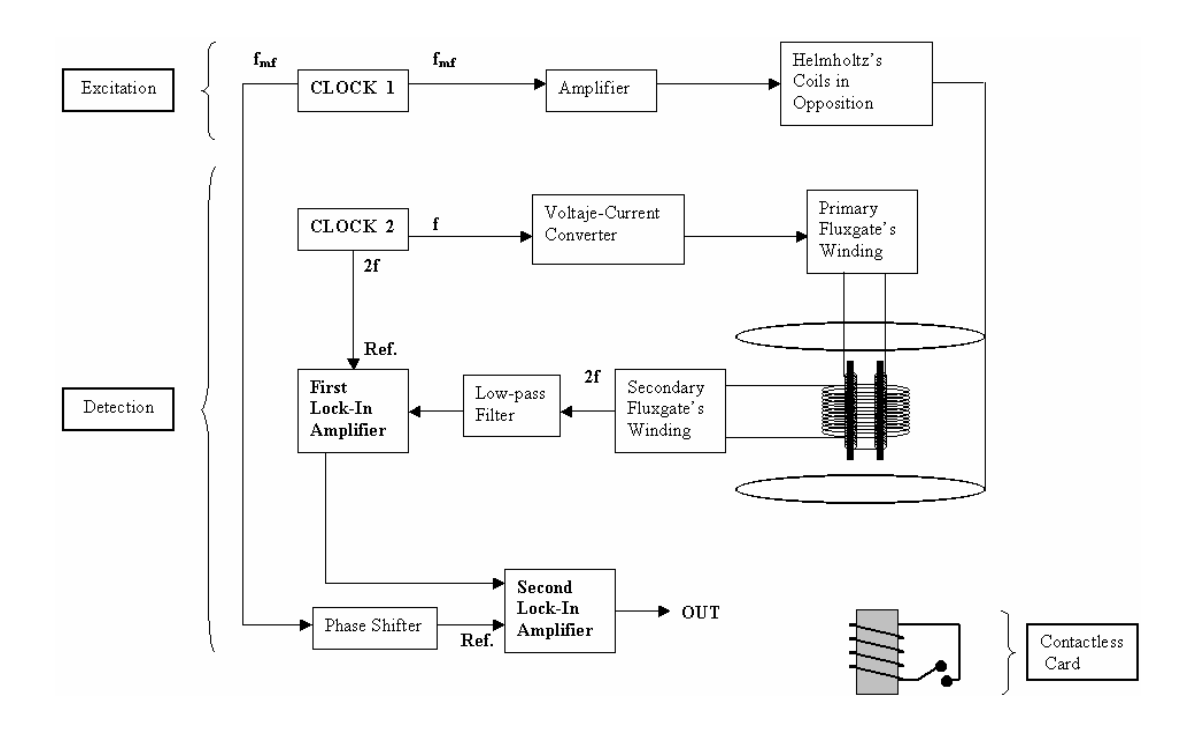


Figure 1. Block diagram of the system. The frequency of the excitation frequency of the primary winding of the fluxgate is used at the detection module (first lock-in amplifier) to select the second harmonic of the signal at the secondary winding. The second lock-in amplifier demodulates the signal produced by the firs lock-in. The modulation is due to the magnetization of a magnetic material in the contactless card or tag.

3.- Experimental Setup.

As it has been previously shown, the system used for the excitation of the card has to produce an alternating magnetic field, except in a region in which the magnetic field should be negligible to place there the reception system avoiding its saturation. Different geometries are possible. For example, a pair of Helmholtz coils connected in opposition and driven by a 1.9 kHz current has been used and the detection system is placed in the middle point of the two coils, where the field is almost zero. Some other interesting possibilities have been proven including planar geometries.

A card with the shape and dimensions of a credit card has been fabricated using two printed circuit boards with the tracks of the winding in the outer part and a soft magnetic thin film in the inner part. To fabricate the card both boards have been joined and the tracks have been welded. It forms 55 coils around the core with a total resistance of 4 Ω . The magnetic core is an electrodeposited CoP amorphous alloys with a thickness of 40 μ m.

The integrated circuitry in the tag must be done by using low powering components. In particular, we have used the PIC16F84 from MicroChip ($\epsilon = 2$ V; I = 15 μ A at 32 kHz). Other possibilities could be the Fairchild ECL logic (1V; 0.2 mA) or the Texas Instruments AUP family (V = 0.8 V; I = 0.5 μ A).

To detect the magnetic signal from the card, a tuneable sensor, placed in the region in which the alternating field is negligible, should be used. We have used two different kinds of fluxgates (the traditional bulk and a planar one) with a double demodulation similar to the one reported by Aroca and collaborators³. The amplitude of the second harmonic induced in the secondary winding of the fluxgate is proportional to the applied magnetic field. A first demodulation made with a lockin amplifier using 2f as the reference frequency, gives the second harmonic rectified. A second demodulation is made to detect a field with the same frequency that the alternating magnetic field (f_{mf}) produced by the excitation system. This allows the measurement of the variation of the field produced by the magnetization of the card. The fluxgate has been driven by a sinusoidal current signal of 12 kHz (f) supplied by a PIC by using a current-voltage converter.

All the signals are obtained from a Programmable Integrated Circuit (PIC 16F84A) using a Digital-to-Analog Converter (DAC 0808). The used lock-in amplifiers have been made ad-hoc using the components CD 4016, inverters and LM 387 operational amplifiers.

4.- Experimental Results and Conclusions.

The system works properly with magnetic fields of low frequency and amplitude. As an example, results are shown in figure 2 using the Helholtz coils set-up in opposition and being 1.9 kHz the excitation frequency and only just 1 oe its maximum amplitude (next to the coils). The card can be fed even through an aluminium foil of 200 μ m without any problems. The change of voltage level at the output of the reader module is shown in figure 2.B.

This system could substitute RFID systems in applications in which screening problems due to induced currents are a problem, like contruction. This technology has proven its efficiency sending and receiving information even when the card has been introduced in aluminum envelops of different thickness, as can be seen in the figures. It is important to note that, despite de low applied magnetic field (in the order of the earth magnetic field), it has been detected the card at about 10 cm using at the same time an aluminum envelop with a thickness of 0.2 mm.

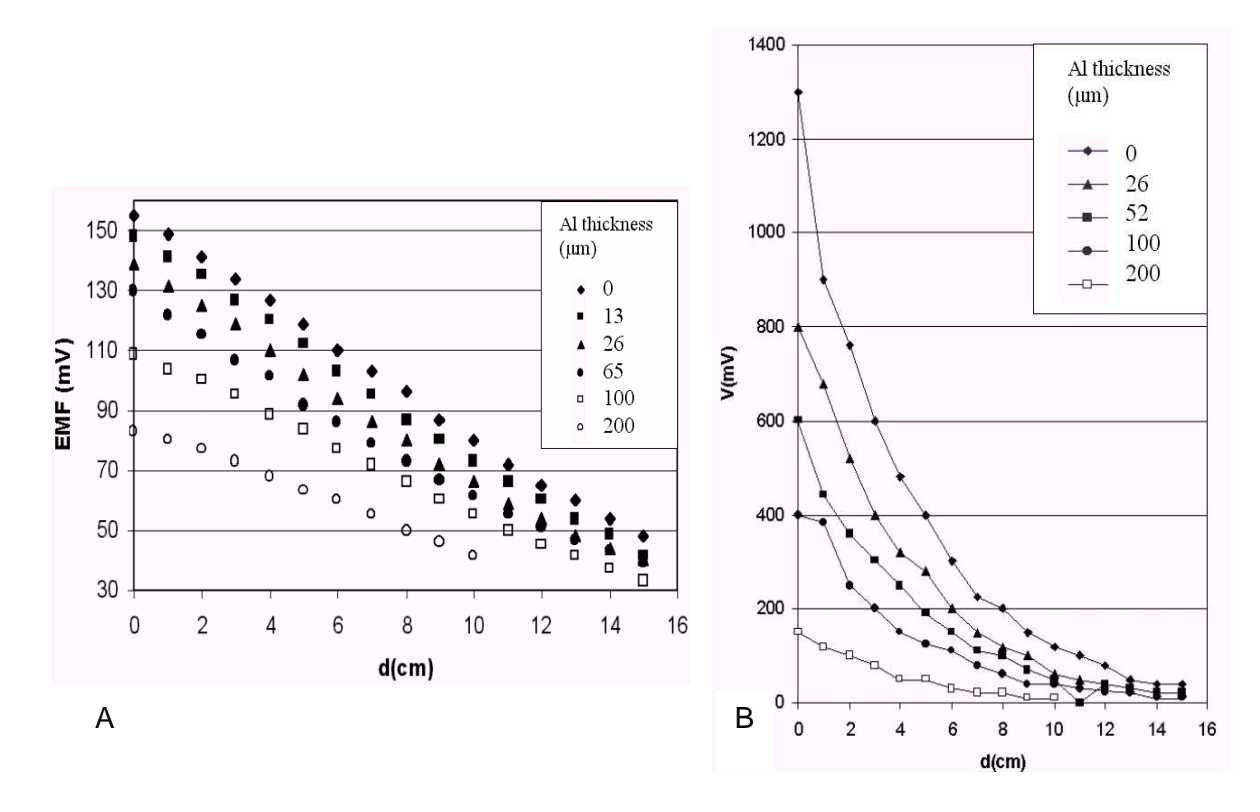


Figure 2. It is represented the electromotrive force (EMF) at the winding of the tag (Figure 2.A) and the change of the voltage at the output of the reader when opening and shortcircuiting this winding (Figure 2.B) versus the distance to the Helmholtz coils as a function of the thickness of the aluminium shielding. The excitation frequency is 1.9 kHz and the maximum amplitude (near the Helmholtz coils) of 1 Oe

By increasing the applied magnetic field the distance would increase the same rate as the magnetization depends linearly on this magnetic field. Other configuration could be proven as introducing the card (with the person) in a Helmholtz coil avoiding the dependence on the distance. The real limits on the distance (for a fixed applied magnetic field) will be given by the minimum electromotive force needed to power the integrated circuit on the card. Of course, if the card is powered by an external battery (by its integration in a mobile phone, for example) this distance will be highly increased.

References

- 1.- http://europa.eu.int/information_society/policy/rfid/index_en.htm
- 2.- S. Garfinkel, B. Rosenberg. RFID: Applications, Security and Privacy. Addison-Wesley Professional, 2005.
- 3.- C. Aroca, J.L. Prieto, P.Sánchez, E. López, M.C. Sánchez, Rev. Sci. Instrum. 66, p. 5355-5359, 1995.

6.12 Domain walls and exchange-interaction in Permalloy/Gd films 12

One of the research lines at the ISOM is focused on magnetic multilayer thin films obtained by dc-magnetron sputtering. In particular we are interested in multilayers of Transition Magnetic Metals (TMM) and Heavy Rare Earths like Fe/Gd or Co/Gd. These multilayers exhibit an antiferromagnetic coupling between Gd and TMM which results in twisted magnetic structures at the interfaces [1-6]. In these samples the magnetization process is mainly due to coherent magnetization rotation. However, for thicker layers and low exchange coupling, the magnetization process can be also due to nucleation and propagation of domain walls. In particular in the case of multilayers of hard/soft magnetic materials the magnetization inversion in the soft magnetic layers will be mainly due to domain wall (DW) displacements. This DW displacements could influence the exchange-bias field and it could even produce an apparent positive exchange coupling in antiferromagnetic coupled multilayers [7]. The explanation proposed shows that magnetization process in soft layers are not only dependent on the exchange-bias field and the applied magnetic field but are also dependent on the propagation and nucleation field.

In this report we describe the results obtained for a system based on two antiferromagnetic exchange coupled thin films, $(Ni_{80}Fe_{20})/Gd$, with a hard magnetic layer that produces the bias field (Gd) and a soft magnetic layer in which we study the magnetization process $(Ni_{80}Fe_{20})$. The Curie temperature of the hard magnetic film (290 K) is much lower than the soft one (853 K) and so the strength of the exchange coupling can be controlled by changing the system temperature. For a weak exchange coupling the magnetization process of the soft magnetic film takes place by DW displacements, whereas for a stronger exchange coupling, twisted magnetic structure will appear at the interface and magnetization rotation can be expected.

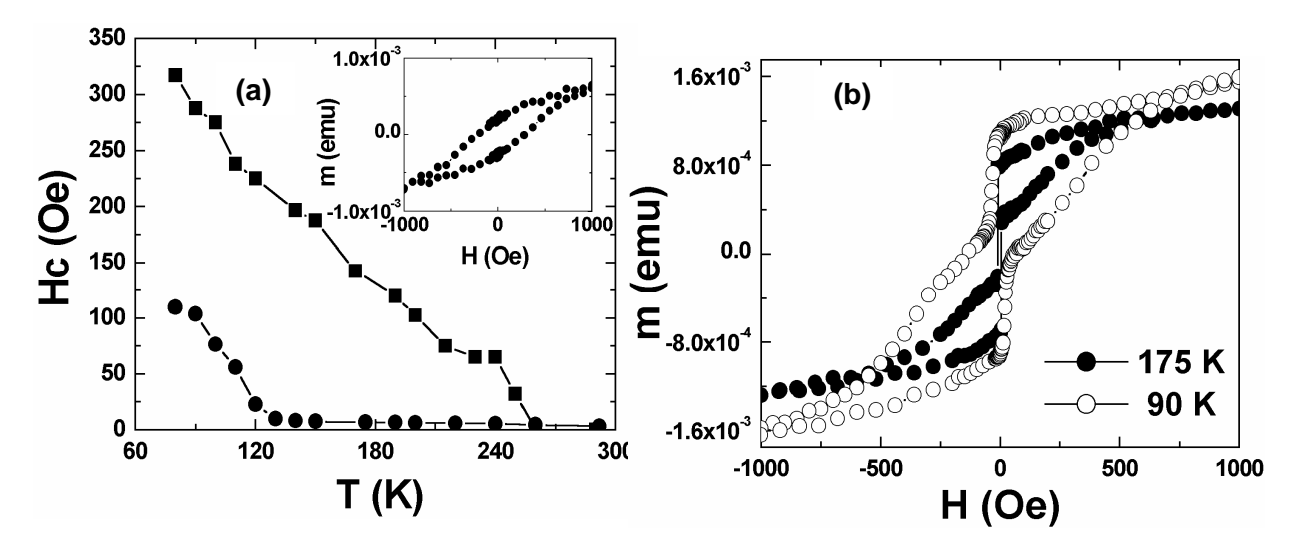


Figure 1. a) Coercive field as a function of the temperature for the bilayer Py(100 nm)/Gd(50 nm) (•) and a Gd layer of 50 nm (■). Inset: (•) Magnetic hysteresis loop of a 75 nm Gd single layer at 80 K. b) VSM hysteresis loop of the bilayer Py(100 nm)/Gd(50 nm) at (•) 175 K and (○) 90 K

Samples were grown in a dc-magnetron sputtering system on corning-glass substrates. The residual pressure in the growth chamber was under 4×10^{-7} mbar. Depositions were done at room

_

¹² Contact person: Marco Maicas: maicas@fis.upm.es

temperature being the Ar pressure 2×10^{-3} mbar and the deposition power 30 W in all cases. A 40 Oe magnetic field was applied during the growth to induce a magnetic anisotropy axis in the Py layer. In order to reduce the Ni diffusion into adjacent layers [8] we have grown Py as the bottom layer and then Gd on it [9]. In all samples Mo layers of 10 nm and 60 nm were used as buffer and capping layers. Samples were characterized in a Vibrating Sample Magnetometer (VSM). Two Py/Gd bilayers were required in thin samples with low magnetic signal. To that effect, Py/Gd bilayers separated by 20 nm Mo spacer layers, Mo(buffer)/[Py/Gd/Mo]2/Mo(capping) were grown.

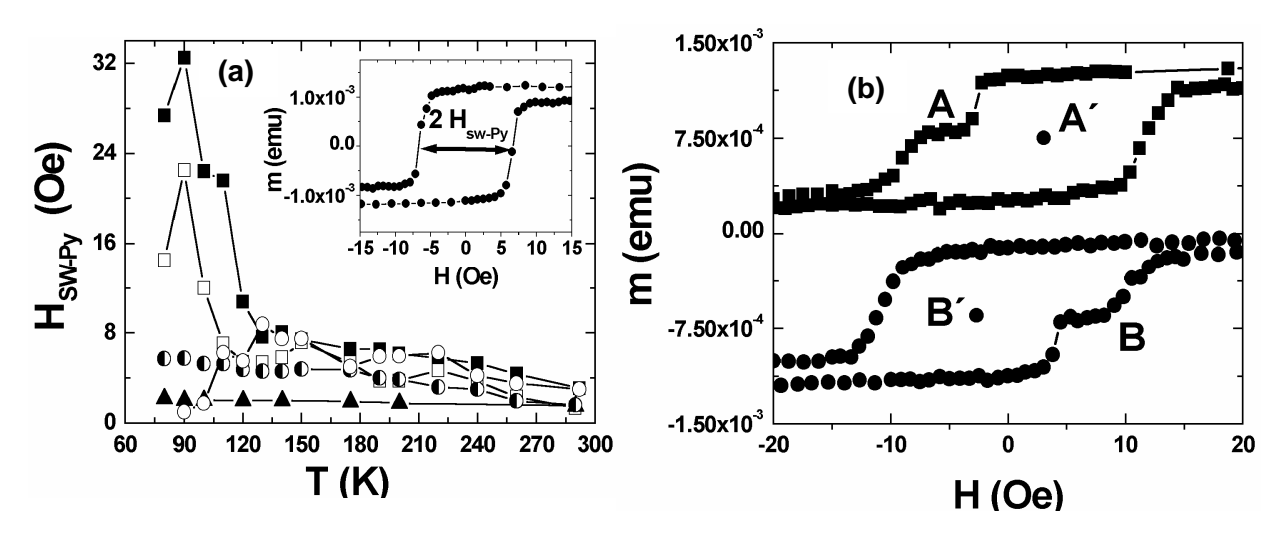


Figure 2. a) H_{sw} as a function of the temperature for the samples (■) Py(100 nm)/Gd(50 nm), (□) $[Py(50 \text{ nm})/Gd(50 \text{ nm})/Mo(20 \text{ nm})]_2$, (⋄) $[Py(25 \text{ nm})/Gd(50 \text{ nm})/Mo(20 \text{ nm})]_2$, (⋄) $[Py(50 \text{ nm})/Mo(20 \text{ nm})]_2$, (o) $[Py(50 \text{ nm})/Mo(20 \text{ nm})]_$

The coercive field of the Py/Gd bilayer, lower than the Gd one, increases as temperature decreases (Figure 1a) showing an unexpected temperature behavior for antiferromagnetically coupled bilayers. The Py/Gd bilayer hysteresis loops are approximately the superposition of a soft and a hard magnetic loop (Py and Gd loops) (Figure 1b). The coercive field is directly related to the two large Barkhausen jumps corresponding to the magnetization inversion of the Py layer. As temperature decreases the Gd remanent magnetization increases and the Barkhausen jumps are vertically shifted, so the coercive field increases widely by this effect (Figure 1b). This shift is not directly related to the magnetic coupling between Py and Gd layers. A more directly parameter related with the magnetic coupling is the switching field (H_{sw}). H_{sw} is the magnetic field necessary to switch the magnetization of the Py layer. Taking into account that the Gd layer is at remanence, the switching field is the Py coercive field plus the effective exchange bias field. It is measured as half the distance in the field axis between the middle points of the Barkhausen jumps (Figure 2a. Inset).

The Gd coercive field is much higher than the Py one. So if there would be a negative exchange coupling between layers the magnetic field necessary to switch the magnetization of the Py layer (H_{sw}) would decrease as temperature decreases and it would even become negative. H_{sw} increases almost linearly from room temperature (RT) up to 120 K (figure 2a). Below this temperature the H_{sw} behavior strongly depends on the Py thickness. For 50 nm and 100 nm Py samples there is a large increase of the switching field which, in principle, could be explained by a positive coupling at this temperature range. For 25 nm Py sample H_{sw} indicates a negative coupling.

To understand this behavior we have measured the exchange decoupled samples Py(x nm)/Mo(20 nm)/Gd(50 nm) (Figure 2a), observing that H_{sw} increases almost linearly for all temperature range, being its behavior similar to the exchange coupled samples in the RT to 120 K range. As in decoupled samples the magnetization processes are due to Py DWs displacements, it can be inferred that for the RT to 120 K range all other samples have similar magnetization processes and the DWs pinning mechanism is also similar. When the temperature decreases the linear increase of the decoupled sample H_{sw} , as opposed to the single Py layer (Figure 2a), only can be due to magnetostatic interaction between Permalloy DWs and the Gadolinium. The Py DWs stray field produces local changes in the Gd magnetization inducing a quasi-DW in Gd [12] that pins Py DW. This pinning could be produced by the interaction between the Gd quasi-DW and the Gd magnetoelastic energy fluctuations [13].

Below 120 K the H_{sw} behavior is strongly dependent on Py thicknesses. For 25 nm Py thickness all Py layer is exchange coupled to Gd layer and so H_{sw} decreases. In thicker Py layers H_{sw} increases. Therefore, we can assume that DW displacement magnetization processes still exist and that another stronger pinning mechanism associated to the exchange coupling appears. To confirm this DW pinning effect we measured minor hysteresis loops (Py 50nm/Gd50nm, at 100K) after saturating the bilayer first in one direction (a) and then in the opposite direction (b) (Figure 2b). The switching field is half the distance in field axis between A and B and the bias field is half the distance in the field axis between the centers of minor hysteresis loops A' and B'. H_{sw} would be reduced by the bias field effect but as the pinning effect is even higher, H_{sw} increases. As this effect is not observed in the exchange decoupled samples, the large coercive field increase in minor hysteresis loops must be due to DWs pinning caused by the exchange coupling.

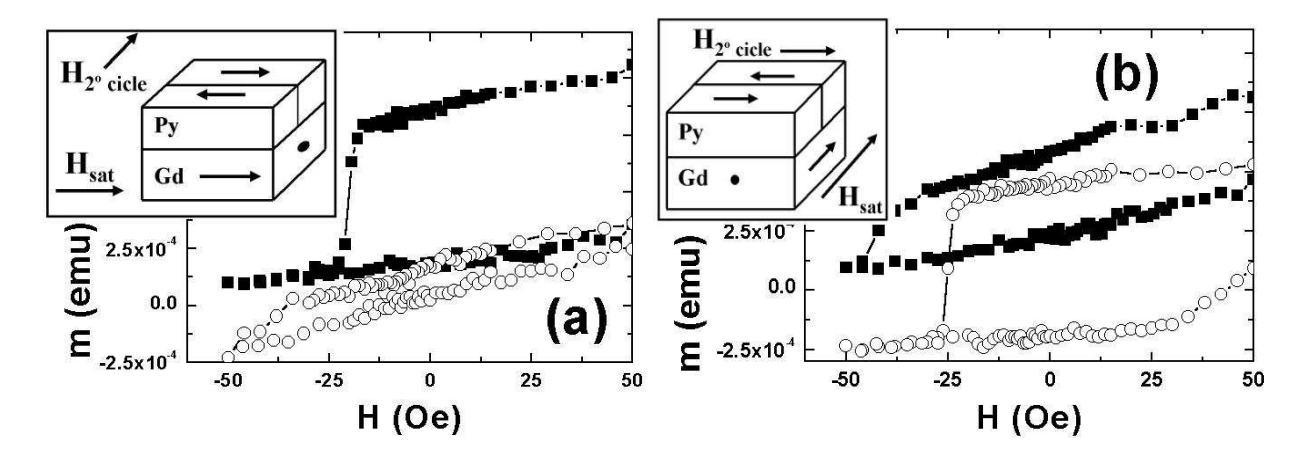


Figure 3. A bilayer a of Py(100 nm)/Gd(50 nm) has been measured at 80 K. (a) A first minor hysteresis loop has been measured after an applied magnetic field of 10^4 Oe has been applied in the Py easy axis direction (\blacksquare). Then, the sample is rotated $\pi/2$ and a second hysteresis loop is recorded with the applied magnetic field in the hard axis direction (\circ). Inset: Schematic representation of the measurement configuration. (b) In this case, a first minor hysteresis loop has been measured after a magnetic field of 10^4 Oe has been applied in the Py hard axis direction (\blacksquare). Then, the sample is rotated $\pi/2$ and a second hysteresis loop is recorded with the applied magnetic field in the easy axis direction (\circ). Inset: Schematic representation of the measurement configuration.

To verify these assumptions we have measured minor hysteresis loops, at 80 K, in the thicker (100nm) Py/Gd bilayers with the Py domain magnetization parallel (Figure 3a) and perpendicular (Figure 3b) to Gd magnetization, in such a way that the bias field is first parallel and then perpendicular to the magnetizing field. Figure 3a shows the low field zone of the magnetization curve obtained after saturating the sample at 10^4 Oe in the Py easy axis, then reducing the field up to -50 Oe to observe the Py magnetization inversion. Being the Gd coercive

higher than |-50| Oe, we can suppose that the Gd magnetization is almost at remanence. Then another minor hysteresis loop is measured applying the magnetizing field perpendicular to Gd magnetization and so to Py easy axis. The magnetization process will be mainly due to 90° magnetization rotation. As the negative exchange coupling takes place in the easy axis direction the bias field reduces the hysteresis loop slope and increases the apparent anisotropy field (in the Py single layer the anisotropy field is about 15 Oe). In the same way, Figure 3b shows the low field zone of the magnetization curve obtained after saturating the sample at 10⁴ Oe in the Py hard axis, then reducing the field up to –50 Oe. Afterwards, a minor hysteresis loop is measured applying the magnetizing field in direction perpendicular to Gd magnetization and so parallel to Py easy axis. In this case the magnetization process is mainly due to DW displacements and as the negative exchange coupling effect on domain energy is not dependent on magnetization direction, the bias field is perpendicular to DWs. The unique pressure on DW is produced by the applied field. The coercive field is in the same order than the H_{sw} measured in figure 2a. This confirms that the large increase of H_{sw} below120 K is due to the DW pinning produced by exchange coupling.

In summary, in Py-Gd bilayers the interface exchange interaction is weak over temperature of 120 K and the magnetostatic interaction between Py DW and Gd magnetization can explain the switching field behavior. Below this temperature the magnetization process is due to an in-plane magnetization rotation. The exchange interaction produces a negative bias field that reduces the switching field. However, in samples with thicker Py layer the magnetization process seems to be mainly due to DW displacements. The exchange interaction results in two effects: 1) an exchange coupling between Py DWs and Gd magnetization and 2) a negative exchange coupling of Gd with the Py domain magnetizations that can be considered like a bias field. The first one produces a strong pinning in DW displacements due to the high Gd magnetostriction and to the local Gd anisotropy fluctuations, a pinning that increases the switching field. The second one reduces the switching field. In spite of the negative exchange coupling between Py and Gd layers, for certain temperatures and Py thickness the first effect is greater than the second one and apparent positive exchange interaction appears between Py and Gd. In principle these effects are not restricted to multilayers with antiferromagnetic coupling and they could also appear in systems with ferromagnetic coupling

References.

- [1] D. Haskel, G. Srajer, J. C. Lang, J. Pollmann, C. S. Nelson, J. S. Jiang, S. D. Bader, Phys. Rev. Lett. 87, 207201 (2001).
- [2] J.P. Andres, L. Chico, J. Colino, J.M. Riveiro, Phys. Rev. B 66, 094424 (2002).
- [3] R.E. Camley, D.R. Tilley, Phys. Rev. B **37**, 3413 (1988).
- [4] R.E. Camley, Phys. Rev. B **39**, 12316 (1989).
- [5] J.L. Prieto, B.B. van Aken, G. Burnell, C. Bell, J.E. Evetts, N. Mathur, M.G. Blamire, Phys. Rev. B 69, 054436 (2004).
- [6] J. Colino, J.P. Andrés, J.M. Riveiro, J.L. Martínez, C. Prieto, J.L. Sacedón, Phys. Rev. B 60, 6678 (1999).
- [7] B. Altuncevahir, A. R. Koymen, J. Magn. Magn. Mater. **261**, 424 (2003).
- [8] J.A. González, J.P. Andres, M.A. Arranz, M.A.L. de la Torre, J.M. Riveiro, J. Appl. Phys. 92, 914 (2002).
- [9] R. Ranchal, C. Aroca, M.C. Sánchez, P. Sánchez, E. López, Appl. Phys. A 82, 697 (2006).
- [10] R. Ranchal, C. Aroca, M.C. Sánchez, P. Sánchez, E. López, phys. stat. sol (a) 203, 1415 (2006).
- [11] J.L. Prieto, M.G. Blamire, J.E. Evetts, Phys. Rev. Lett. 90, 027201 (2003).
- [12] M. Maicas, M. A. Rivero, E. López, M. C. Sánchez, C. Aroca, P. Sánchez, J. Magn. Magn. Mater. 203, 289 (1999).
- [13] M. Kersten, Phys. Z. **39**, 860 (1938).

6.13 Nanocavity oscillation and collapse in viscoelastic fluids 13

Overview of the Methodology

The goal of this research line is to formulate and solve the field equations and conservation laws in a micro-macro framwork, which will include as a micro part the stochastic equations. Towards this direction, an appropriate continuum discretization scheme is being developed and later on will be coupled with the stochastic models. This scheme is able to handle the numerical solution of the problem in total, thus provide solution under flow conditions for the *macro fields* (velocity, pressure, stress fields) and the *micro fields* as well.

At the same time information for biological molecules (proteins, toxins) absorption is included by applying appropriate BC's and in addition surface tension effects will be taken into account. The system to be considered consists of a droplet containing a nematic liquid crystal that forms an interface with an isotropic fluid (e.g. water) where proteins are dissolved, leading to the absorption of nanoscopic particles (proteins) in the LC/aqueous interface. Generally, in addition to the coupling between micro and macro unknowns, these types of problems which incorporate free surfaces and complex geometries possess additional difficulties due to continuous change of the flow domain. Therefore, the choice of the discretization scheme for the macroscopic numerical solution is very crucial for solving accurately the flow problem.

To handle this problem some recent developed methods to tackle free surfaces, variable topology and three dimensional problems using stochastic molecular constitutive laws [1-5] will be coupled with a quasi-elliptic mesh generation scheme which is capable to adjust to the geometry of the flow domain [6-7].

Nanocavity response under oscillatory ambient pressure

A nanocavity is assumed to be surrounded by an infinite liquid either Newtonian or viscoelastic. Flow is induced by varying the ambient pressure periodically with time: $P=P_0+Pasin(\omega t)$, where $P_0=1$ atm, Pa the amplitude of the oscillations. This phenomenon may appear in cases of medical ultrasound diagnosis so the determination of the conditions at which nanocavity collapse can be observed is very important to avoid undesired effects in medical applications [8,9]. The discretization scheme, is able to conform to these oscillations, avoiding remeshing, and gives accurate predictions for the nanocavity radius and the flow kinematics. We describe mathematically the problem in spherical coordinates, with the centre of the coordinate system placed in the centre of the nanocavity. This problem has been extensively been studied, in its 1D simplification [8, 10-12]. In this case by taking into account the symmetry of the problem in respect to angle θ the problem degenerates in the solution of one differential equation for the nanocavity radius, R_b with time. We validated our results with the 1D solution and the agreement is excellent.

The governing flow equations consist of the momentum and mass conservation equations and the constitutive equation for the extra stress tensor:

_

¹³ Contact person: Manuel Laso: laso@diquima.upm.es

$$\rho \left(\frac{\partial \mathbf{u}}{\partial t} + \mathbf{u} \cdot \nabla \mathbf{u} \right) = -\nabla \mathbf{P} + \nabla \cdot \boldsymbol{\tau}$$
 (1)

$$\nabla \cdot \mathbf{u} = 0 \tag{2}$$

$$\nabla \cdot \mathbf{u} = 0 \tag{2}$$

$$\tau = \eta \left(\nabla \mathbf{u} + (\nabla \mathbf{u})^{\mathrm{T}} \right) \tag{3}$$

where τ denotes the deviatoric part (extra stress) of the total stress tensor σ ($\sigma = -PI + \tau$) and ρ , η are the liquid density and viscosity respectively. The shape of the nanocavity-liquid interface, $R_b(\theta,t)$, is determined by the kinematic condition:

$$\frac{\partial \mathbf{R}_{\mathbf{b}}}{\partial \mathbf{t}} + \mathbf{u} \cdot \nabla \mathbf{R}_{\mathbf{b}} = \mathbf{u} \tag{4}$$

$$P_{gas} V^{\gamma} = constant$$
 (5)

where P_{gas} and V denote the instantaneous gas pressure and volume of the nanocavity and $\gamma = 1.4$. Additionally, at the nanocavity-liquid interface, a normal force balance condition is applied which is actually imposed as a natural condition in momentum equation (1).

$$\mathbf{n} \cdot (\mathbf{\tau}_{G} - \mathbf{\tau}_{L}) = (2\Re\sigma)\mathbf{n} + (P_{G} - P_{L})\mathbf{n}$$
 (6)

where, **n** is the unit vector normal to the interface pointing always outwards from the centre of the coordinate system and $2\Re$ is the curvature of the interface calculated at each point defined through $2\Re = \nabla \cdot \mathbf{n}$. The imposed oscillatory pressure in the outer boundary:

$$P_{\text{out}} = P_0 + \text{Pa sin}(\omega t) \tag{7}$$

is applied also as a natural boundary condition in the momentum equation (eq. 1), by replacing the value of pressure with eq. (8) in the boundary integral arising by integrating by parts the weak form of eq. 1. [13]. The method chosen, which produces the mesh adjusted to the new position of the boundaries at every time step and belongs to the methods of Arbitrary Lagrangian Eulerian methods. At each time step the mesh in the physical, flow domain which evolves with time is mapped into a constant, computational domain and the transformation is achieved by solving a Laplace like equation. [6,7]. In particular for this geometry the physical domain which is described by the coordinates (r,θ) , $R_b(\theta,t) \le r \le R_{out}(t)$, $0 \le \theta \le \pi$ is mapped into a constant computational domain (η,χ) , defined by the initial geometry at t=0, $R_{b0} \le \eta \le R_{out0}$, $0 \le \chi \le \pi$. This mapping is achieved by solving the following Laplace equation for the r-coordinate:

$$\nabla \cdot \nabla \eta = 0 \tag{8}$$

The lines with constant η values are parallel to the deforming nanocavity. The solution of equation (8) gives the r –position in the mesh of each nodal point. For this specific problem we do not solve any other equation for the remaining coordinate θ since the mesh produced by simply setting $\theta = \chi$, was proven to be sufficient. Equation (8) is solved together with appropriate boundary conditions that take into account the movement of the boundaries (i.e. eq. 4 for the nanocavityliquid interface).

The input parameters for these validation runs were taken from the literature and correspond to conditions encountered in ultrasonic medical applications [8]. In more details the density and the viscosity of the surrounding liquid are $\rho = 10^3 \text{kgr/m}^3$ and $\eta = 3 \times 10^{-2} \text{ Ns/m}^2$ respectively and the surface tension, $\sigma = 0.072 \text{N/m}$. The initial nanocavity radius is of the order of 1µm. Typical values for the imposed frequency and the amplitude of the imposed pressure oscillations are: f =3 MHz

and Pa = 2 bar. These values result in a Reynolds number $Re = \frac{\rho \omega R_{b0}^2}{\eta} = 0.62$, and a Weber

number We = $\frac{\sigma}{\rho R_{b0}^3 \omega^2}$ = 0.2. Deviations from spherical shape were quantified by computing a

nanocavity deformation parameter (which is defined by the ratio of the difference of the two nanocavity axis over their sum) which was found to be smaller than 10^{-6} . The surrounding liquid in the problem description is regarded to be infinite. In practice we develop a mesh with a much larger outer radius than the nanocavity radius. The initial nanocavity shape is described by an expression of the form:

$$R_{b0}(\theta) = a_0 + \varepsilon a_0 P_{n}(\theta) \tag{10}$$

where $0 < \varepsilon < 1$ and P_n a Legendre polynomial of order $n \ge 1$.

We impose the same periodic external pressure (eq. 7) and we are focusing in the case with large pressure amplitude, Pa = 30 bar. During flow, we analyze the shape of the nanocavity at each time step to check if the imposed initial perturbation in nanocavity shape remains in time. The shape of the nanocavity is decomposed in Legendre polynomials to examine if the imposed initial perturbation remains in the nanocavity shape or if a spherical symmetric shape is preferred:

$$R_{b}(\theta,t) = \sum_{k=0}^{N} a_{k}(t) P_{k}(\cos \theta)$$
 (11)

The coefficients a_n are calculated through the equation:

$$a_{k}(t) = \frac{(2k+1)}{2} \int_{0}^{\pi} R_{b}(\theta, t) P_{k} \sin \theta d\theta$$
 (12)

No mode coupling is observed in this calculations.

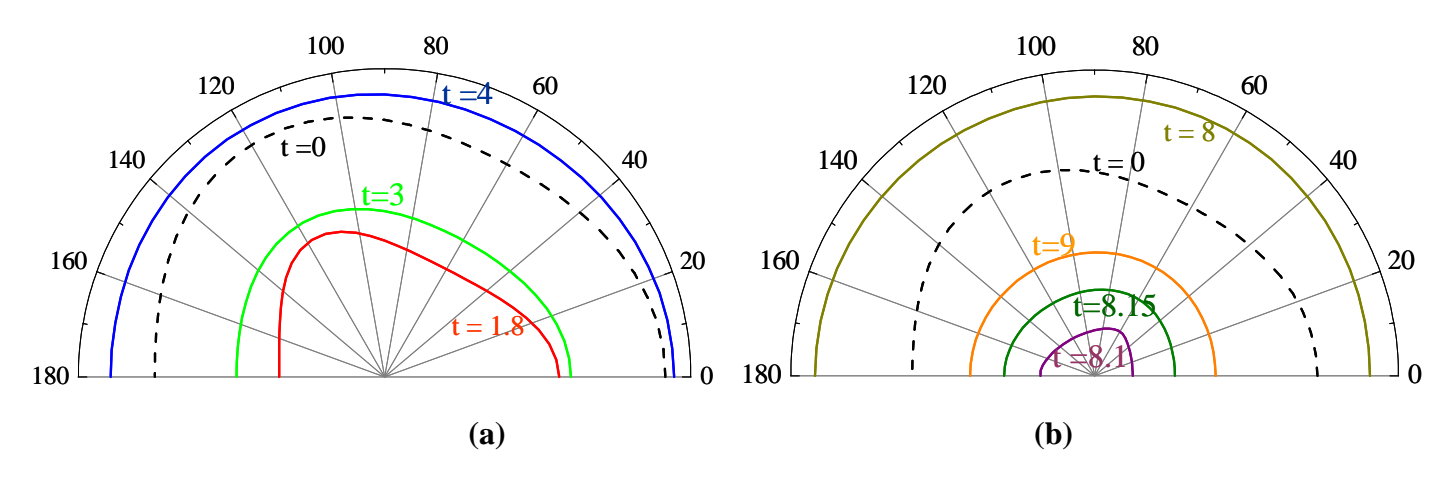


Figure 1.- Snapshots of nanocavity shape during the oscillation when the initial shape is described by Rb0 = 1 + 0.1 P3:

a) during the I^{st} period

b) during 2^{nd} period

In Figure 1 snapshots of the nanocavity interface are shown during 1^{st} and 2^{nd} period of applied oscillation when a perturbation of a 3^{rd} order Legendre polynomial is added in the initial nanocavity shape. The initial nanocavity radius dependence on angle θ is described by:

$$R_{b0}(\theta) = 1 + 0.1 P_3 = 1 + 0.1(5 \cos 3\theta - 3 \cos \theta)/2$$
).

In these snapshots it is also shown that the perturbation is present in the 1st period (it is mostly evident when the nanocavity reaches its minimum) and is less important in 2nd period. For the parameters used in these cases, the surface tension effect is important which tends to smoothen out the perturbations. We have indeed observed that in the limit of negligible surface tension the initial perturbation is present at longer times.

References

- [1] J. Comenzana, A.Ledda, M. Laso, B. Debbaut, J. of Rheol. 2001, 45, 237.
- [2] E. Grande, M. Laso, M. Picasso, J. Non-Newt. Fluid Mech. 2003, 113, 127.
- [3] J. Ramirez, M. Laso, Model. and Simul. in Materials Sci. and Engin. 2004, 12, 1.
- [4] M. Laso, J. Ramirez Journal of Non-Newt. Fluid Mech. 2005, 127, 41, M. Laso, J. Ramirez, M. Picasso, Journal of Non-Newt. Fluid Mech. 2004, 122, 215.
- [5] A. Bonito, M. Picasso, M. Laso, Journal of Comp. phys. 2006, 215, 691.
- [6] Y. Dimakopoulos, J. Tsamopoulos, Journal of Comp. Phys. 2003, 192, 494.
- [7] K. Foteinopoulou, V.G. Mavrantzas, Y. Dimakopoulos, Tsamopoulos, J. Phys. of Fluids 2006, 18, 042106.
- [8] J. Jimenez-Fernandez, A. Crespo, Ultrasonics 2005, 43, 643.
- [9] C.X. Deng, F.L. Lizzi, Ultrasound Med. Biol. 2002, 28, 277.
- [10] C.E. Brennen, Cavitation and Nanocavity Dynamics, Oxford University Press: Oxford, 1995.
- [11] Z.C Feng, L. G. Leal, Annu. Rev. Fluid Mech. 1997, 29, 201.
- [12] E.A. Brujan, T. Ikeda, Y. Matsumoto Phys. of Fluids 2004, 16, 2402.
- [13] X. Xie, M. Pasquali, Journal of Non-Newt. Fluid Mech. 2004, 122, 159.

6.14 Bijective-mapping min-map Monte Carlo for chain molecules 14

We have developed a novel Monte Carlo (MC) simulation scheme based on Theodorou's bijective mapping strategy (D. N. Theodorou, Journal of Chemical Physics 124 034109 (2006)). This Min-Map Bias Monte Carlo acts in combination with any other proper, bare MC. It carries over the bare MC move from the original configuration space $\Omega^{(0)}$, where trial move acceptance may be low, to a different configuration space, $\Omega^{(1)}$, where acceptance is higher. The bare MC move is then performed in $\Omega^{(1)}$ and the resulting configuration is finally mapped back to $\Omega^{(0)}$. Mappings between $\Omega^{(0)}$ and $\Omega^{(1)}$ entail weighted selection of trial configurations, the bias of which is subsequently removed in the overall acceptance criterion. The new method is applied, in conjunction with Continuum Configurational Bias as bare MC scheme, to the simulation of explicit-hydrogen linear alkanes in the canonical ensemble. Min-Map Bias MC is found to alleviate the pervasive problem of very low acceptance rates encountered when using an explicit molecular description.

Computation of excess chemical potential is based on the evaluation of ensemble averages of the type:

$$\left\langle \min \left[1, \frac{\int_{\Gamma^{(0)}(\mathbf{r}^{(0)})} \exp[-\beta U_1(\mathbf{r})] d\mathbf{r}}{\int_{\Gamma^{(0)}(\mathbf{r}^{(0)})} \exp[-\beta U_0(\mathbf{r})] d\mathbf{r}} \right] S^{(0)}(\mathbf{r}^{(0)}) \right\rangle$$
(1)

where $\beta = (k_B T)^{-1}$ and $\langle \ \rangle_i$ denotes an ensemble average over all points $\mathbf{r}^{(I)}$ in $\Omega_i^{(I)}$, I = 0,1 sampled according to the canonical probability density, i.e. proportional to $\exp \left[-\beta U_I \left(\mathbf{r}^{(I)} \right) \right]$. In Theodorou's min-map chemical potential method the ratio of configurational integrals can be interpreted as Boltzmann factors of the excess Helmholtz free energy difference between system 1 confined in subset $\Gamma^{(1)}$ and system 0 confined in subset $\Gamma^{(0)}$. However, the idea of establishing a bijective relationship between domains in the configuration spaces $\Omega^{(0)}$ and $\Omega^{(1)}$ can be applied as the basis of a generating scheme for trial MC moves. The overall trial generation method is schematically depicted in the following figure:

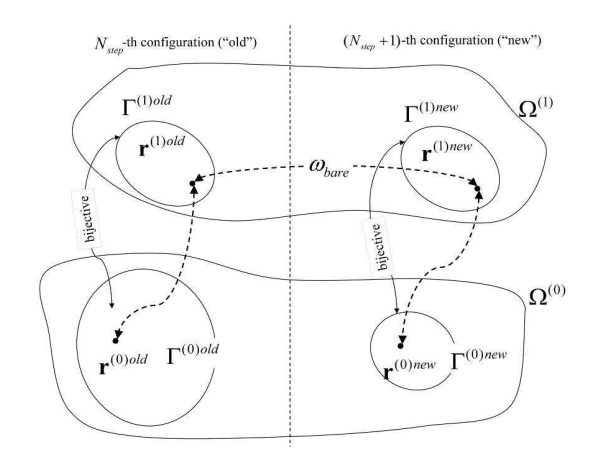


Figure 1. Schematic representation of the bijective mapping and of the correspondence between configurations in spaces $\Omega^{(0)}$ and $\Omega^{(1)}$. Transition between the N_{step} -th ("old") configuration and the $(N_{\text{step}}+1)$ -th ("new") configuration is attempted, through a "bare" MC move, in space $\Omega^{(1)}$.

¹⁴ Contact person: Manuel Laso: laso@diquima.upm.es

Application to continuum configurational bias Monte Carlo

It may happen that the efficiency of the bare MC acting on configurations that belong to $\Omega^{(0)}$ is so poor as to render it useless, while the same bare scheme acting on configurations that belong to $\Omega^{(1)}$ is efficient. The situation just described is far from being exceptional, as will be discussed below. Hence, the effect of the factors pre- and post multiplying ω_{bare} in the acceptance/rejection criterion can be such that an increase in overall efficiency is achieved while strictly preserving the properness of the combined MC scheme. To achieve this end, instead of performing the bare move in configuration space $\Omega^{(0)}$, where the bare scheme is assumed to be correct, but inefficient, individual configurations are projected from $\Omega^{(0)}$ to $\Omega^{(1)}$ where the bare move is performed, in the hope that its efficiency may be higher and that the acceptance criterion may yield greater overall acceptance. Obviously, the success of this strategy depends entirely on the specifics of the molecular system under investigation and on the way of selecting corresponding configurations in $\Omega^{(0)}$ and $\Omega^{(1)}$. Hence, ω_{bare} is the ratio of the products of Boltzmann weights for the old and the new (trial) configurations:

$$\omega_{bare}^{(1)} = \frac{W_{old}^{(1)}}{W_{new}^{(1)}} = \prod_{k=1}^{m} W_{k,old}^{(1)}$$

$$\prod_{k=1}^{m} W_{k,new}^{(1)}$$
(2)

The probabilities of the old and new configurations in the canonical ensemble in the acceptance criterion lead to:

$$P = \min \left[1, \frac{\int\limits_{\Gamma^{(0)old}\left(\mathbf{r}^{(0)old}\right)}^{\mathbf{r}^{(0)old}\left(\mathbf{r}^{(0)old}\right)} \exp\left[-\beta U_{0}\left(\mathbf{r}'\right)\right] d\mathbf{r}'}{\int\limits_{\Gamma^{(1)old}\left(\mathbf{r}^{(0)old}\right)}^{\mathbf{r}^{(0)old}\left(\mathbf{r}^{(0)old}\right)}^{\mathbf{r}^{(0)old}\left(\mathbf{r}^{(0)old}\right)} \exp\left[-\beta U_{1}\left(\mathbf{r}'\right)\right] d\mathbf{r}'} \frac{\exp\left[-\beta U_{1}\left(\mathbf{r}^{(1)old}\right)\right]}{\exp\left[-\beta U_{1}\left(\mathbf{r}'\right)\right] d\mathbf{r}'} \frac{\partial_{bare}^{(1)}}{\int\limits_{\Gamma^{(0)old}\left(\mathbf{r}^{(0)old}\right)}^{\mathbf{r}^{(0)new}\left(\mathbf{r}^{(0)new}\right)}^{\mathbf{r}^{(0)new}\left(\mathbf{r}^{(0)new}\right)} \exp\left[-\beta U_{0}\left(\mathbf{r}'\right)\right] d\mathbf{r}'} \\ \min \left[1, \frac{\int\limits_{\Gamma^{(0)old}\left(\mathbf{r}^{(0)old}\right)}^{\mathbf{r}^{(0)new}\left(\mathbf{r}^{(0)new}\right)}^{\mathbf{r}^{(0)new}\left(\mathbf{r}^{(0)new}\right)} \exp\left[-\beta U_{0}\left(\mathbf{r}'\right)\right] d\mathbf{r}'} \frac{\exp\left[-\beta U_{1}\left(\mathbf{r}^{(1)new}\right)\right]}{\exp\left[-\beta U_{1}\left(\mathbf{r}^{(1)old}\right)\right]} \omega_{bare}^{(1)} \frac{\int\limits_{\Gamma^{(0)new}\left(\mathbf{r}^{(0)new}\right)}^{\mathbf{r}^{(0)new}\left(\mathbf{r}^{(0)new}\right)} \exp\left[-\beta U_{1}\left(\mathbf{r}'\right)\right] d\mathbf{r}'} \frac{\exp\left[-\beta U_{1}\left(\mathbf{r}^{(1)old}\right)\right]}{\exp\left[-\beta U_{1}\left(\mathbf{r}^{(1)old}\right)\right]} \omega_{bare}^{(1)} \frac{\int\limits_{\Gamma^{(0)new}\left(\mathbf{r}^{(0)new}\right)}^{\mathbf{r}^{(0)new}\left(\mathbf{r}^{(0)new}\right)} \exp\left[-\beta U_{1}\left(\mathbf{r}^{(1)old}\right)\right]} \omega_{bare}^{(1)} \frac{\int\limits_{\Gamma^{(0)new}\left(\mathbf{r}^{(0)new}\right)}^{\mathbf{r}^{(0)new}\left(\mathbf{r}^{(0)new}\right)} \exp\left[-\beta U_{1}\left(\mathbf{r}^{(1)old}\right)\right]} \omega_{bare}^{(1)} \frac{\int\limits_{\Gamma^{(0)new}\left(\mathbf{r}^{(0)new}\right)}^{\mathbf{r}^{(0)new}\left(\mathbf{r}^{(0)new}\right)} \exp\left[-\beta U_{1}\left(\mathbf{r}^{(1)old}\right)\right]} \omega_{bare}^{(1)} \frac{\int\limits_{\Gamma^{(0)new}\left(\mathbf{r}^{(0)new}\right)}^{\mathbf{r}^{(0)new}\left(\mathbf{r}^{(0)new}\right)} \exp\left[-\beta U_{1}\left(\mathbf{r}^{(1)old}\right)\right]} \frac{\int\limits_{\Gamma^{(0)new}\left(\mathbf{r}^{(0)new}\right)}^{\mathbf{r}^{(0)new}\left(\mathbf{r}^{(0)new}\right)} \exp\left[-\beta U_{1}\left(\mathbf{r}^{(0)new}\right)\right]} \frac{\int\limits_{\Gamma^{(0)new}\left(\mathbf{r}^{(0)new}\right)}^{\mathbf{r}^{$$

This equation has a very simple structure which also suggests why the min-map biased MC move may be advantageous over the bare MC scheme.

For a two-bond deep cut, the last two torsional degrees of freedom of a chain in the united atom representation, φ_{N-1} and φ_N , drive sites (N-1) and (N) respectively. In the course of a CCB chain regrowth, the total potential energy function associated with site (N-1) is a function of φ_{N-1} only: $U_{N-1}(\varphi_{N-1})$. Once a particular value $\varphi_{N-1} = \varphi_{N-1}^*$ has been selected in the regrowth process, the total potential energy function associated with site (N) is a function of φ_N and parametrically of φ_{N-1}^* : $U_N(\varphi_N; \varphi_{N-1}^*)$. CCB approximates the restricted configurational partition function associated with these two bonds

$$Q = \iint d\varphi_{N} d\varphi_{N-1} \exp\left[-\beta \left(U_{N-1}(\varphi_{N-1}) + U_{N}(\varphi_{N}; \varphi_{N-1}^{*})\right)\right]$$
 by
$$Q = \iint d\varphi_{N} d\varphi_{N-1} \exp\left[-\beta \left(U_{N-1}(\varphi_{N-1}) + U_{N}(\varphi_{N}; \varphi_{N-1}^{*})\right)\right] = \left\{\int d\varphi_{N-1} \exp\left[-\beta U_{N-1}(\varphi_{N-1})\right]\right\} \left\{\int d\varphi_{N} \exp\left[-\beta U_{N}(\varphi_{N}; \varphi_{N-1}^{*})\right]\right\}$$
(3)

where in the second factor of the right hand side, φ_{N-1} takes on the constant value $\varphi_{N-1} = \varphi_{N-1}^*$ corresponding to the torsion angle chosen in the regrowth process. In a united atom representation, \overline{Q} and Q are sufficiently close for the acceptance ratio to be appreciable. In the explicit hydrogen representation, \overline{Q} is a poor approximation to Q and acceptance drops steeply. The reason for \overline{Q} and Q to differ markedly is that the energy landscape for the explicit hydrogen representation is more "rugged" than for the united-atom representation. Differences in level of detail in energy landscapes are more pronounced the closer individual atoms come to each other, i.e. the higher the density. The presence of additional explicit atoms makes the energy landscape more intricate and \overline{Q} becomes an increasingly poor approximation to Q. This is illustrated quantitatively in Figure 2 which shows the contour levels of the total energy associated with the last two torsional angles φ_{N-1} and φ_N as a function of these for a particular alkane chain in a dense system

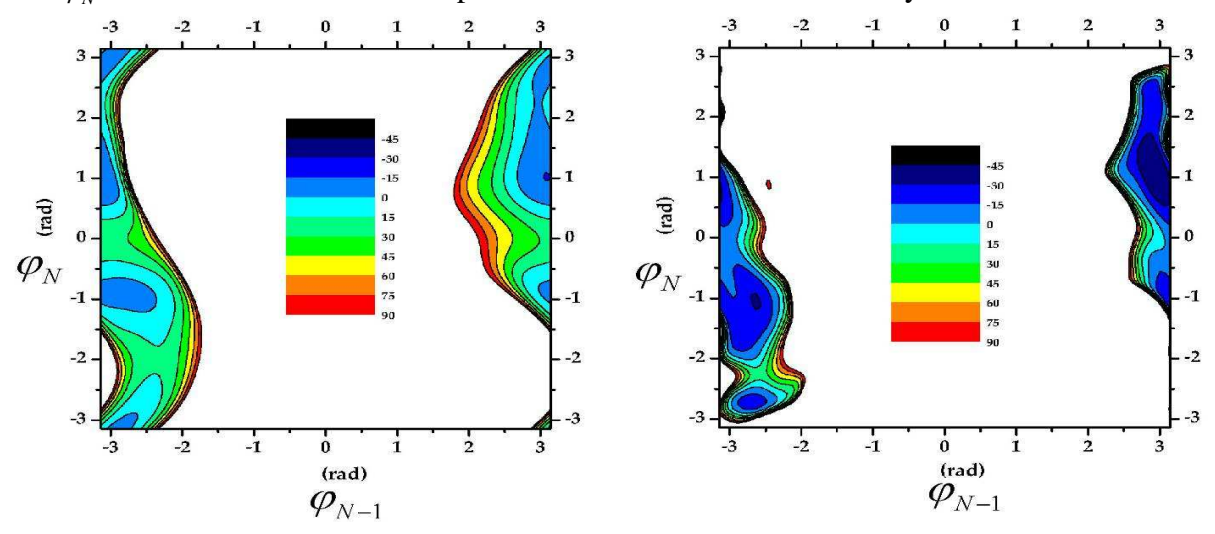


Figure 2.- Active degrees of freedom for a two-bond deep cut in a CCB trial move. Torsion angle φ_{N-1} drives site (N-1), torsion angle φ_N drives site (N).

The procedure just described univocally characterizes mappable domains in $\Omega^{(0)}$ and $\Omega^{(1)}$ with the same formal structure. Additionally, we have used a homotopical minimization procedure based in Watson and Haftka's HOM to perform the sequence of minimizations involved in the mutation process for the transitions in force field $(U_{non-bonded}^{(0)} \leftrightarrow U_{non-bonded}^{(1)}, U_{tors}^{(0)}(\varphi) \leftrightarrow U_{tors}^{(1)}(\varphi))$ and in geometrical parameters (bond lengths, bond angles and torsion angles).

Finally, the evaluation of restricted partition functions is carried out numerically by standard Monte Carlo integration¹, using a number k_{exc} of points uniformly distributed over $\Gamma^{(I)}$:

$$\int_{\mathbf{r}^{(1)}} \exp\left[-\beta U_{1}(\mathbf{r})\right] \sqrt{\left|\underline{\underline{g}}(\mathbf{r}^{(1)})\right|} d\mathbf{r} \propto \sum_{k=1}^{k_{exc}} \left\{ \exp\left[-\beta U_{1}(\mathbf{r}_{k}^{(1)})\right] \sqrt{\left|\underline{\underline{g}}(\mathbf{r}_{k}^{(1)})\right|} S^{(1)}(\mathbf{r}_{k}^{(1)}, \Gamma^{(1)}) \right\}$$
(4)

The selector functions convert integrals over $\Gamma^{(I)}$ in integrals over hyperspheres so that hypervolumes cancel and need never evaluated, hence the proportionality suffices.

Outlook

The min-map bias is general and can be combined with any type of proper MC move. It seems to be quite effective in alleviating the explicitness problem. Specifically, when combined with a CCB scheme and applied to an explicit description of eicosane, acceptance rates for trial moves were high enough for efficient and correct configuration space sampling.

The simple strategy behind min-map bias is that of carrying over the MC move from the original configuration space $\Omega^{(0)}$, where MC moves are almost always rejected, to a different configuration space, $\Omega^{(1)}$, where acceptances are high; performing the move in $\Omega^{(1)}$ and finally mapping back the resulting trial configuration to $\Omega^{(0)}$. Configurations are mapped between $\Omega^{(0)}$ and $\Omega^{(1)}$ and back using weights (bias) which are subsequently removed in the overall acceptance criterion.

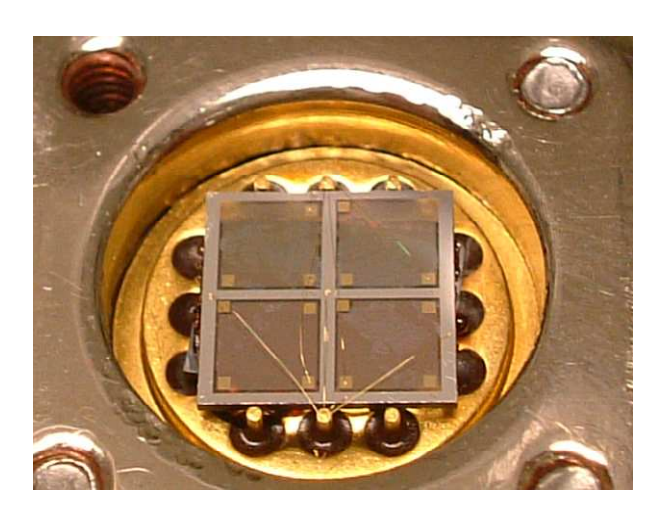
However, if the descriptions chosen in $\Omega^{(0)}$ and $\Omega^{(1)}$ are too different, the efficiency of the method will decline. The method is strictly applicable to configuration spaces $\Omega^{(0)}$ and $\Omega^{(1)}$ of the same dimensionality. It also has the potential to be applied to multiple "hopping" between more than just two configuration spaces, so that MC moves performed in a relatively simple molecular representation can be mapped stepwise onto complicated, possibly biological, molecules. Needless to say, although multiple hopping is a clearly legitimate extension of the present method (it reduces to a well-defined sequence of bijections, and to a concatenation of formally identical terms), its real usefulness and computational efficiency still remain to be demonstrated.

References

- D. N. Theodorou, Journal of Chemical Physics **124** 034109 (2006).
- D. A. Kofke, Fluid Phase Equilibria **228**, 41 (2005).
- B. Widom, Journal of Chemical Physics **39**, 2808 (1963).
- 4 B. S. Daan Frenkel, *Understanding Molecular Simulation* (Academic Press London, 2001).
- 5 J. I. Siepmann and D. Frenkel, Molecular Physics **75**, 59 (1992).
- 6 J. I. Siepmann, I. R. McDonald, and D. Frenkel, Journal of Physics-Condensed Matter 4, 679 (1992).
- J. J. Depablo, M. Laso, and U. W. Suter, Journal of Chemical Physics 96, 2395 (1992).
- J. J. Depablo, M. Laso, and U. W. Suter, Abstracts of Papers of the American Chemical Society **203**, 533 (1992).
- 9 J. J. Depablo, M. Laso, and U. W. Suter, Journal of Chemical Physics 96, 6157 (1992).
- 10 M. Laso, J. J. Depablo, and U. W. Suter, Journal of Chemical Physics 97, 2817 (1992).
- P. V. K. Pant and D. N. Theodorou, Macromolecules 28, 7224 (1995).
- 12 V. G. Mavrantzas, T. D. Boone, E. Zervopoulou, et al., Macromolecules 32, 5072 (1999).
- 13 A. Uhlherr, V. G. Mavrantzas, M. Doxastakis, et al., Macromolecules 34, 8554 (2001).
- 14 N. C. Karayiannis, V. G. Mavrantzas, and D. N. Theodorou, Physical Review Letters 88 (2002).

7 RESEARCH PROJECTS





AlGaN/GaN HEMT transistor for high temperature, high power microwave applications. Upper picture:

Four GaN/InGaN MQW photodetectors fabricated to sense flame optical emissions from a gas domestic Lower picture:

combustion boiler

7.1 International Public Funding

Europe:

- "GalnAsN-based semiconductor heterostructures for 1.5µm Optoelectronics (GINA)"

ESPRIT IST-2000-23678 (2001-2004).

Principal Investigator (PI): Enrique Calleja

- "New Generation of GaN-based sensor arrays for nano and picofluidic systems for fast and reliable biomedical testing (GANANO)"

STREP NMP4-CT-2003-505641 (2003-2006).

PI: Elías Muñoz

- "A novel technology for ultra sensitive reliable integrated magnetic sensors: a new era in magnetic detection (SENPIMAG)"

STREP NMP2-CT-2003-505265 (2003-2006).

PI: José Luis Prieto

- "Polymer Molecular Modeling at Integrated Time/Length Scales (PMILS)"

GROWTH G5RD-CT-2002-00720 (2002-2006).

PI: Manuel Laso

- "Multiscale Modeling of Nanostructured Interfaces for Biological Sensors (MNIBS)"

STREP NMP-NSF-1 EU-NSF Coordinated activities in Computational materials research FP6-016375 (2005-2008).

PI: Manuel Laso

- "Key Organisation for Research on Integrated Circuits in GaN Technology (KORRIGAN)"

European Understandings for Research Organisation, European Defense Agency

Programmes and Activities Memorandum of Understanding (EUROPA MOU); Contract nº 04/102.052/032. CA Nº 2157 V7.(2005-2009).

PI: Elías Muñoz

 "Ultrahigh sensitivity Slot-wAveguide BlOsensor on a highly integrated chip for simultanous diagnosis of multiple diseases (SABIO)"

European Comission STREP; Contract nº 026554 (2006-2009)

PI: Carlos Angulo Barrios

USA:

- "P-type doping of GaN and AlGaN layers grown by MBE"

ONR-NICOP-WIDEBANDGAP; N00014-011-0828 (2001-2004).

PI: Enrique Calleja

Integrated Actions (travel and stage funding):

 "Estudio de las propiedades morfológicas de estructuras láser de pozo cuántico de InGaAsN crecidas por MBE"

HISPANO-ALEMANA (Paul Drude Institut, Berlín) HA2002-0004 (2003-2005).

PI: Álvaro de Guzmán Fernández

- "Chemical and Biochemical Sensors based on group III-nitrides"

HISPANO-ALEMANA (Walter Schottky Institüt, Munich) HA2002-0005 (2003-2004).

PI: Fernando Calle

7.2 National and Regional Public Funding

- "Sensores planares y materiales nanoestructurados para su integración en dispositivos magnéticos"

Min. Ciencia y Tecnología MAT 2001-3554-C02-02 (2001-2004).

PI: Claudio Aroca

"Emisores en 510 nm para aplicaciones de alta temperatura"

Min. Ciencia y Tecnología TIC 2000-1887-CE (2001-2004).

PI: Enrique Calleja

"Tecnologías y Aplicaciones de Microsistemas Activos Inteligentes"

Min. Ciencia y Tecnología TIC 2001-3838-C03-01 (2001-2004).

PI: Fernando Aldana/Elías Muñoz (ISOM)

- "Crecimiento Epitaxial por Haces Moleculares de Aleaciones de InGaAsN. Aplicación a láseres en el rango 1.3 a 1.5 μm"
- Min. Ciencia y Tecnología TIC 2001-3849 (2001-2004).
- PI: Enrique Calleja
- "Tecnología de Fabricación de Dispositivos de alta frecuencia/alta temperatura basados en Nitruros"

Min. Ciencia y Tecnología, TIC 2001-2794 (2001-2005).

PI: Fernando Calle

· "Detectores de radiación infrarroja (4.2-4.7 μm) y ultravioleta-C (260-290 nm) para la rápida detección de incendios forestales"

Com. de Madrid. CAM 07M-0110/2002 (2002-2004).

PI: Miguel Ángel Sánchez

"Heteroestructuras semiconductoras basadas en GalnNAs para optoelectrónica en 1,5 micras"

Min. Ciencia y Tecnología, TIC-2001-4950-E (2002-2004).

PI: Enrique Calleja

- "Sensores magnetométricos fluxgate miniaturizados. Aplicación en lectores de tarjetas inteligentes sin contactos".

Min. Ciencia y Tecnología TIC2002-04132-C02 (2002-2005).

PI: Pedro Sánchez

- "Desarrollo de sensorización basada en fotodetectores GaN para monotorización de combustión"

ORKLI-MCYT (PROFIT) FIT-020100-2003-411 (2003-2004).

PI: Elías Muñoz

- "Desarrollo de Amplificadores de Potencia (HPAs) en banda ancha, utilizando Transistores HEMT de Nitruro de Galio"

INDRA-MITYC, FIT-330100-2004-83 (2004-2005).

PI: Elías Muñoz

- "Sistema de medida de impedancias en RF en componentes semiconductores en oblea"

Min. Educación y Ciencia UNPM05-33-003. FEDER 2004-2005.

PI: Fernando Calle

 "Crecimiento por MBE de detectores de IR de punto cuántico para su utilización a alta temperatura e incidencia normal"

Min. Educación y Ciencia, TEC2004-04965-C02-01/MIC (2004-2005).

PI: Álvaro de Guzmán Fernández

 "Crecimiento y caracterización de heteroestructuras de nitruros-III e integración con materiales magnéticos para su aplicación de dispositivos híbridos magnético-semiconductor"

Min. Educación y Ciencia, TIC2004-05698-C02-01 (2004-2006).

PI: Miguel Ángel Sánchez

- "Desarrollo de Dispositivos Emisores y Detectores en el rango Ultravioleta para Aplicaciones en Comunicaciones, Generación de Luz Blanca, Detección de Contaminación y Bio-Fotónica"

Min. Educación y Ciencia, MAT 2004-02875 (2004-2006).

PI: Enrique Calleja

- "Equipo Láser con emisión en modo continuo a 244 nm"

Min. Educación y Ciencia UNPM05-34-004 FEDER (2005).

PI: Adrián Hierro

- "Heteroestructuras semiconductoras basadas en GalnNAs para optoelectrónica en 1,5 micras"

Min. Educación y Ciencia, TEC2004-21202-E (2005).

PI: Enrique Calleja

"Desarrollo de Nanoestructuras Semiconductoras basadas en Nitruros-III para la Fabricación de Dispositivos Multifuncionales"

Com. de Madrid. GR/MAT/0042/2004 (2005).

PI: Enrique Calleja

- "Desarrollo de un dispositivo magnético para control e identificación de vehículos"

Com. de Madrid. GR/MAT/0041/2004 (2005).

PI: Claudio Aroca

"Sensores selectivos de infrarrojo basados en nanoestructuras cuánticas"

Com. de Madrid. GR/MAT/0249/2004 (2005).

PI: Álvaro de Guzmán Fernández

 "Nueva Generación de matrices de sensores basados en GaN para sistemas nano y pico-fluídos para análisis biomédico rápido y fiable"

Min. Educación y Ciencia, TEC2004-0004-E (2005-2006)

PI: Elías Muñoz

 "Nueva Tecnología para sensores magnéticos integrados ultrasensibles y fiables: Abriendo una Nueva Era en la detección magnética"

Min. Educación y Ciencia MAT2004-0005-E (2005-2006)

PI: Claudio Aroca

- "Red Nacional para el Desarrollo Multidiscioplinarde Dispositivos Biosensores"

Acción Complementaria del P.N. Biotecnología,

Min. Educación y Ciencia, (2005-2006)

Pl. L. Lechuga (coordinador), Fernando Calle (UPM)

-- "Fabrication of AlGaN/GaN High Mobility Transistors grown on Si(111) and SiC/Si(111) Substrates"

CSIC-CNM-BARNA, Acuerdo Hispano-Canadiense NRC-SEPOCYT (2005-2007)

PI: Elías Muñoz (ISOM)

- "Mejora y acceso de las grandes instalaciones científicas GIC-ISOM"

Min. Educación y Ciencia, GIC 05-10 (2005-2007).

PI: Pedro Sánchez (ISOM)

 "Desarrollo de láseres horizontales y de cavidad vertical para la banda de 1.35 a 1.55 micras basados en pozos cuánticos de GalnNAs/GaAs"

Min. Educación y Ciencia, TEC2005-03694/MIC (2005-2008).

PI: Adrián Hierro

"Nanoestructuras de Semiconductores como Componentes para la Información Cuántica (NANIC)"

Min. Educación y Ciencia, -9062. Acción Estratégica en Nanotecnología. NAN2004-09109-C04-02. (2005-2008).

PI: Enrique Calleja (Coordinado).

 "(Bio)sensores químicos avanzados para medida in-situ de la calidad de aguas basados en elementos específicos de reconocimiento y lectura "multifuncional integrada"

Com. de Madrid. S-0505/AMB/0374 (2005-2009)

PI: Guillermo Orellana (coordinador) / Miguel Angel Sáchez (UPM)

- "Adquisición e instalación de un sistema de nanolitografia de ultra alta resolución por haz electrónico"

Min. Educación y Ciencia, TEC 2005-24733-E (2006)

PI: Elías Muñoz

- "Obtención de nanopartículas magnéticas por pulverización catódica"

Com. de Madrid - Univ. Politécnica Madrid, R05-11885 (2006)

PI: Marco Maicas

- "Programa de Infraestructura y Calidad de la CAM 2006"

Com. de Madrid - Univ. Politécnica Madrid, Resolución 29/04/2006

PI: Jose Luis Pau

- "Demostrador de un conmutador electromecánico operando en altas frecuencias"

Ministerio de Industria, Turismo y Comercio, PN TEC, FIT-330100-2006-184, con INDRA SISTEMAS S.A. (2006).

PI: Fernando Calle

 "Fabricación de substratos nanoestructurados de SiO2 para crecimiento epitaxial de emisores eficientes de Luz Blanca con Nitruros del Grupo-III"

Min. Educación y Ciencia, -PROFIT- 2006. FIT-330100-2006-139 (2006-2007).

PI: Enrique Calleja

 "Ayuda financiera para la mejora de las Infraestructuras Científicas y Tecnológicas Singulares y para el acceso a las mismas"

Min. Educación y Ciencia, ICTS-2006-01 (2006-2008)

PI: Pedro Sánchez

"Nanoestructuras de semiconductores como componentes para la información cuántica" (NANOCOMIC)

Com. de Madrid. (IV PRICYT)- S-0505/ESP-0200 (2006-2009)

PI: Enrique Calleja

"Tecnologías de Información Basadas en Optica Cuántica"

Programa Consolider-Ingenio CSD2006-19. Solicitud: 7120. Aceptado. (2006-2011).

Pl.: Jürgen Eschner. Fundación Privada Instituto de Ciencias Fotónicas. Invest. : Enrique Calleja

7.3 Funding from companies and institutions:

- "Desarrollo de un sensor UV para monitorización de combustión"

IKERLAN- Univ. Politécnica Madrid, (2003-2004).

PI: Elías Muñoz

- "Desarrollo de matrices de detectores QWIP tri-color"

CIDA- Univ. Politécnica Madrid, 1053830042 (2003-2004).

PI: Álvaro de Guzmán Fernández

" Desarrollo de Transistores GaN de potencia para amplificadores de radiofrecuencia"

CIDA- Univ. Politécnica Madrid, 1053830118 (2003-2004).

PI: Elías Muñoz

- "Desarrollo de Transistores GaN de potencia para amplificadores de radiofrecuencia"

CIDA- Univ. Politécnica Madrid, 1053840076 (2004-2005).

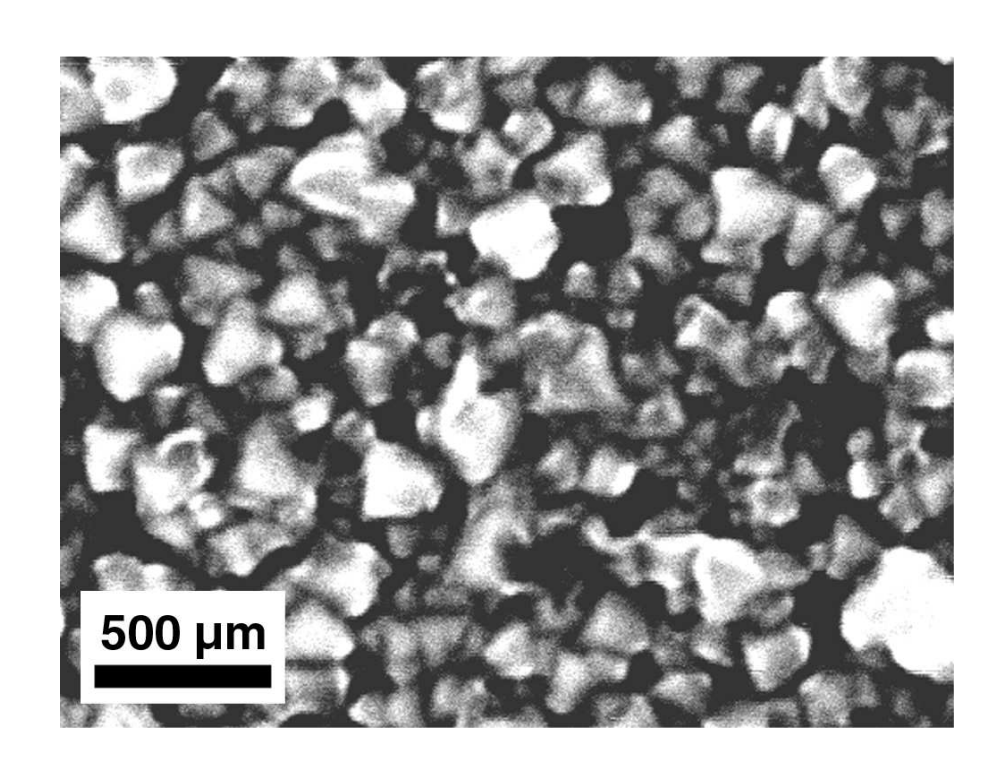
PI: Elías Muñoz

- "Asistencia técnica para la optimización de la tecnología de detectores Qwip tricolor para la banda de 3 a 5 micras"

CIDA- Univ. Politécnica Madrid, 10538400345 (2004-2005)

PI: Álvaro de Guzmán Fernández

8 DISEMINATION OF THE SCIENTIFIC ACTIVITY



Scanning Electron Microscope image of Co nanoparticles produced by electrochemical deposition in liquid cathode. The mean particle size is approximately 200nm with a quite homogeneous size distribution. After biocompatibilization with Dextran, these nanoparticles will be used as magnetic markers for medical imaging.

8.1 Papers in Scientific Journals and Books

2004

F. CALLE, J. GRAJAL, J. PEDRÓS

"Active SAW filters using 2DEG AlGaN/GaN heterostructures"

Electronic Letters, 40, 1384-1385 (2004)

D. CIUDAD, C. AROCA, M.C. SÁNCHEZ, E. LÓPEZ, P. SÁNCHEZ

"Modeling and fabrication of a MEMS Magnetostatic Magnetic Sensor"

Sensors and Actuators A, 115 (2-3), 408-416 (2004)

D. CIUDAD, L. PEREZ, P.SÁNCHEZ, M.C.SÁNCHEZ, E.LÓPEZ, C.AROCA,

"Ultra low frequency contactless smart cards "

Journal of Electrical Engineering, 55, 58-61 (2004)

D. CURCÓ, M. LASO, C. ALEMÁN

"Generation-Relaxation Algorithms to Construct Representative Atomistic Models of Amorphous Polymers: Influence of the Relaxation Method"

Journal of Physical Chemistry B, 108, (52) 20331-20339 (2004)

R. CUSCÓ, L. ARTÚS, E. PASTOR, F. NARANJO, E. CALLEJA

"Local Vibrational Modes of H-Complexes in Mg-doped GaN Grown by Molecular Beam Epitaxy"

Applied Physics Letters 86, 897-899 (2004)

M. GONZÁLEZ-GUERRERO, L. PÉREZ, C. AROCA, M. C. SÁNCHEZ, E. LÓPEZ, P. SÁNCHEZ

"Hybrid Ferrite-Amorphous Planar Fluxgate"

Journal of Magnetism and Magnetic Materials, 272-276, 777-779, (2004)

M. LASO, J. RAMIREZ

"Implicit Micro-Macro Methods"

Journal of Non-Newtonian Fluid Mechanics, 122, 215-226 (2004)

M. LASO, U. VON STOCKAR

"Absorption"

Chapter 4 in Kirk-Othmer's "Encyclopedia of Chemical Technology",

Wiley-Interscience, 4th edition ISBN 0471646865, New York, (2004)

M. MAICAS

"Current-driven magnetization switching in circular magnetic nanodots"

Physica B 343, 247-25 (2004)

M. MAICAS, D. CIUDAD, D. CIUDAD, C.AROCA, P. SANCHEZ, M.C SÁNCHEZ, E. LÓPEZ

"Magnetic properties and magnetoelastic coupling measurement in layered Fe-Co-B thin films"

Journal of Electrical Engineering, 55, 10/S, 35-37 (2004)

J. MIGUEL-SÁNCHEZ, A. GUZMÁN, J.M ULLOA, A. HIERRO, E. MUÑOZ

"Effect of nitrogen on the optical properties of InGaAsN p-i-n structures grown on misoriented (111)B GaAs substrates" Applied Physics Letters 84, 2524-2526 (2004)

J. MIGUEL-SÁNCHEZ, A. GUZMÁN, E. MUÑOZ

"The role of N ions on the optical and morphological properties of InGaAsN quantum wells for 1.3 -1.5 micron applications"

Applied Physics Letters, 85 (11), 1940-1942 (2004)

- J. MIGUEL-SÁNCHEZ, M. HOPKINSON, M. GUTIERREZ, P. NAVARETTI, H.Y. LIU, A. GUZMÁN, J.M. ULLOA, A. HIERRO, E. MUÑOZ
- "Structural and optical quality of InGaAsN Quantum Wells grown on misoriented GaAs (111) B substrates by MBE" Journal of Crystal Growth, 270, 62-68 (2004)
- J. MIGUEL-SÁNCHEZ, A. GUZMÁN, J. M. ULLOA, A. HIERRO, E. MUÑOZ
- "Influence of substrate misorientation and growth temperature on N incorporation in InGaAsN/GaAs quantum wells grown on (1 1 1)B GaAs"

Physica E, 23, 356-361 (2004)

E. MUÑOZ, J.L. PAU, C. RIVERA

"Nitride Photodetectors in UV biological effects studies"

M.S. Shur and A. ZU.K.auskas (eds), *ŪV Solid-State Light Emitters and Detectors*, 161-177. Kluwer Academic Publishers, Printed in The Netherlands, ISBN: 1-4020-2034-1 (2004)

F.B. NARANJO, E. CALLEJA, Z. BOUGRIOUA, A. TRAMPERT, X. KONG, K.H. PLOOG

"Efficiency Optimization of p-type Doping in GaN:Mg Layers Grown by Molecular Beam Epitaxy" Journal of Crystal Growth, 270, 542-546 (2004)

H.C. ÖTTINGER, M. LASO

"CONNFFESSIT: Simulating Polymer Flow"

"Simulation Methods for Modeling Polymers" Kotelyanski, M.J. and Theodorou, D.N. (eds.) 511-559, ISBN 0-8247-0247-6 (2004)

- T. PALACIOS, F. CALLE, J. GRAJAL
- "Remote Collection and Measurement of Photogenerated Carriers Swept by Surface Acoustic Waves in GaN" Applied Physics Letters, 84, 3166-3168 (2004)
- J.L. PAU, C. RIVERA, E. MUÑOZ, E. CALLEJA, U. SCHÜHLE, E. FRAYSSINET, B. BEAUMONT, J.P. FAURIE, P. GIBART. "Response of Ultra-Low Dislocation Density GaN photodetectors in the near-and vacuum-UV"

 Journal of Applied Physics 95, 8275-8279 (2004)
- J.L PAU, C. RIVERA, J. PEREIRO, E. MUÑOZ, E. CALLEJA, U.SCHÜHLE, E. FRAYSSINET, B. BEAUMONT, J.P. FAURIE, P. GIBART
- "Nitride-based photodetectors: from visible to X-ray monitoring"

Superlattices and Microstructures 36, 807-814 (2004)

- J. PEDRÓS, F. CALLE, J. GRAJAL, R. J. JIMÉNEZ RIOBÓO, C. PRIETO, J.L. PAU, J. PEREIRO, M. HERMANN, M. EICKHOFF, Z. BOUGRIOUA
- "Anisotropic propagation of surface acoustic waves on nitride layers"

Superlattices and Microstructures. 36, 815-823 (2004)

- L. PÉREZ, C. AROCA, P. SÁNCHEZ, E. LÓPEZ, M.C. SÁNCHEZ
- "Planar fluxgate sensor with an electrodeposited amorphous core"

Sensors and Actuators A109, 208-211(2004)

J. RAMIREZ, M. LASO

"Micro-macro 3D calculations of viscoelastic flows"

Modelling and Simulation in Materials Science and Engineering 12 (6) 1293-1306 (2004)

J. RISTIĆ, E. CALLEJA, M.A. SÁNCHEZ-GARCÍA, A. TRAMPERT, K.H. PLOOG, J. SÁNCHEZ-PÁRAMO, J.M. CALLEJA "Self-organized molecular beam epitaxial growth of AlGaN/GaN Nanostructures on Si(111) substrates for optoelectronic applications"

Future Trends in Microelectronics: The Nano, the Giga, and the Ultra, Ed. S. Luryi, J. Xu, A. Zavslavski, Wiley Interscience, New York, p. 226, ISBN: 0-471-48405-9 John Wiley & Sons (2004).

C. RIVERA, J.L. PAU, F.B. NARANJO, E. MUÑOZ

"Novel photodetectors based on InGaN/GaN multiple quantum wells"

Physica Status Solidi (a) 201, No. 12, 2658 –266 (2004)

C. RIVERA, J.L. PAU, J. PEREIRO, E. MUÑOZ

"Properties of Schottky barrier photodiodes based on InGaN/GaN MQW structures"

Superlattices and Microstructures 36, 849-857 (2004)

M. A. RIVERO, M. MAICAS, E. LÓPEZ, C. AROCA, M.C. SÁNCHEZ, P. SÁNCHEZ

"Magnetostatic interactions in bilayer films"

European Physical: J. Appl. Phys. 28, 305-311 (2004)

A. TRAMPERT, J-M CHAUVEAU, K. PLOOG, E. TOURNIÉ, A. GUZMÁN

"Correlation between interface structure and light emission at 1.3-1.55 μm of (Ga,ln)(N,As) diluted nitride heterostructures on GaAs substrates"

Journal of Vacuum Science and Technology B 22 (4), 2195-2200 (2004)

J.M. ULLOA, A. HIERRO, J. MIGUEL-SÁNCHEZ, A. GUZMÁN, E. TOURNIÉ, J.L. SÁNCHEZ-ROJAS, E. CALLEJA "Dominant Carrier Recombination Mechanisms in GalnAsN/GaAs Quantum Well Light Emitting Diodes" Applied Physics Letters, 85, 40-42 (2004)

2005

- C. ALEMAN, E. ARMELIN, J.I. IRIBARREN, F, LIESA, M, LASO, J. CASANOVAS.
- "Structural and Electronic Properties of 3,4-Ethylenedioxithiophene, 3,4-Ethylenedisulfanylfurante and Thiophene Oligomers: A Theoretical Investigation"

Synthetic Metals 149, (2-3)151–156 (2005)

- Z. BOUGRIOUA, M. AZIZE, A. JIMENEZ, A. F. BRAÑA, P. LORENZINI, B. BEAUMONT, E. MUÑOZ, P. GIBART "Fe doping for making resistive GaN layers with low dislocation density; consequence on HEMTs" *Physica Status Solidi* (c) 1–5 / DOI 10.1002 (2005)
- F. CALLE, J. PEDRÓS, T. PALACIOS, J. GRAJAL
- "Acoustic wave devices on III-V nitrides"

Physica Status Solidi (c) 2, 976-983 (2005)

- B. DAMILANO, J. BARJON, J-Y. DUBOZ, J. MASSIES, A. HIERRO, J. M. ULLOA, E. CALLEJA
- "Growth and in situ annealing conditions for long-wavelength (Ga,ln)(N,As)/GaAs lasers Applied Physics Letters, **86**, 071105-071105-3 (2005)
- S. DHAR, L. PÉREZ, O. BRANDT, A. TRAMPERT, K.H. PLOOG, J. KELLER, B. BESCHOTEN
- "Gd-doped GaN: A very diluted ferromagnetic semiconductor with a Curie temperature above 300 K" *Physical Review B* **72**, 245203 (2005)
- S. FERNÁNDEZ, R. CUSCÓ, D. PASTOR, L. ARTÚS, K.P. O´DONNELL, R.W. MARTIN, I.M. WATSON, Y. NANISHI, E. CALLEJA "Raman-scattering study of the InGaN alloy over the whole composition range"

 Journal of Applied Physics, 98, 013511-013515 (2005)
- J. GRANDAL, M.A. SÁNCHEZ-GARCÍA, F. CALLE, E. CALLEJA
- "Morphology and Optical Properties on InN Layers Grown by Molecular Beam Epitaxy on Silicon Substrates" *Physica Status Solidi* (c), **2**, 7, 2289-2292 (2005)
- J. GRANDAL, M.A. SÁNCHEZ-GARCÍA
- "InN layers grown on Silicon substrates: effect of substrate temperature and buffer layers" *Journal of Crystal Growth* **278** (1-4), 373-377 (2005)
- A. HIERRO, J. M. ULLOA, E. CALLEJA, B. DAMILANO, J. BARJON, J-Y. DUBOZ, J. MASSIES
- "Room temperature perfomance of low threshold 1.34-1.44 mm GalnNAs/GaAs quantum-well lasers grown by molecular beam epitaxy"

IEEE Photonics Technology Letters, 17 (1),1142-1144, (2005)

M. HUGUES, B. DAMILANO, J. BARJON, J.Y. DUBOZ, J. MASSIES, J-M. ULLOA, M. MONTES, A. HIERRO

"Perfomance improvement of 1,52 1.52 µm (Ga,In)(N,As)/GaAs quantum well lasers on GaAs substrates" *Electronics Letters* (a), 41, 595-596 (2005)

S. LAZIC, M. MORENO, J.M. CALLEJA, A. TRAMPERT, K.H. PLOOG, F. NARANJO, E. CALLEJA

"Resonant Raman Scattering in strained and relaxed InGaN(GaN) Quantum Wells"

Applied Physics Letters, 86, 061905 (2005)

E. LÓPEZ CABARCOS, A. F. BRAÑA, B. FRICK, F. BATALLÁN

"Thermal hysteresis loop in the elastic incoherent scattering function of vinilydene fluoride and trifluoraethylene ferroelectric copolymers"

Physical Review B, 71, 184304/1-7 (2005)

I. LUCAS, L. PEREZ, C. AROCA, E. LÓPEZ, P. SÁNCHEZ, M.C. SÁNCHEZ

"Magnetic properties of Co-P Alloys electrodeposited at room temperature

Journal of Magnetism and Magnetic Materials 290-291, 1513-1516 (2005)

E. LUNA, A. GUZMÁN, E. MUÑOZ

"Offset in the dark current characteristics of photovoltaic double barrier quantum well infrared photodetectors" *Infrared Physics & Technology*, **47**, 22-28 (2005)

E. LUNA, A. TRAMPERT, A. GUZMÁN, E. CALLEJA,

"Correlation between the performance of double-barrier quantum-well infrared photodetectors and their microstructure: On the origin of the photovoltaic effect"

Journal of Applied Physics 98, (1-4), 44510 (2005)

- J. MIGUEL-SÁNCHEZ, A. GUZMÁN, J.M. ULLOA, A. HIERRO, M. MONTES, E. MUÑOZ
- "Room temperature laser emission of InGaAsN/GaAs quantum wells grown on GaAs (111) B" *IEEE Photonics Technology Letters*, **17**,11, 2271-2273 (2005)
- J. MIGUEL-SÁNCHEZ, A. GUZMÁN, J.M. ULLOA, A. HIERRO, E. MUÑOZ "InGaAsN on GaAs (111)B for telecommunication laser application"
- Journal of Crystal Growth, 278, 234-238 (2005)
- D. MORECROFT, B.B. VAN AKEN, J. L. PRIETO, D.-J.KANG, G. BURNELL, M.G. BLAMIRE "In situ magnetoresistance measurements during nanopatterning of pseudo-spin-valve structures" *Journal of Applied Physics* **97**, 054302 (2005)
- D. MORECROFT, J.L. PRIETO, M.G. BLAMIRE
- "Study of the size dependence of exchange bias using in situ magnetoresistance measurements" *Journal of Applied Physics* **97**, 10C518 (2005)
- D. PASTOR, R. CUSCÓ, L. ARTÚS, G. GONZÁLEZ-DÍAZ, S. FERNÁNDEZ-GARRIDO, E. CALLEJA, "Effect of the Implantation Temperature on Lattice Damage of Be+-Implanted GaN" Semiconductor Science and Technology, **20**, 374-377 (2005)
- J.L. PAU, J. PEREIRO, C. RIVERA, E. MUÑOZ
- "Plasma-assisted molecular beam epitaxy of nitride-based photodetectors for UV and visible applications" Journal of Crystal Growth, **278**, 718-722 (2005)
- J. PEDRÓS, F. CALLE, J. GRAJAL, R. J. JIMÉNEZ RIOBÓO, C. PRIETO, Z. BOUGRIOUA Anisotropy-induced polarization mixture of surface acoustic waves in GaN/c-sapphire heterostructures *Physical Review B* **72**, 075506-12 (2005)
- J.L. PRIETO, B.VAN AKEN, J.I. MARTIN, A. PÉREZ-JUNQURA, G. BURNELL, N.D. MATHUR, M.G. BLAMIRE "Absence of spin scattering of in-plane spring domain walls" *Physical Review B* **71**, 214428 (2005)
- J. RAMIREZ. M. LASO
- "Size reduction methods for the implicit time-dependent simulation of micro.macro viscoelastic flow problems" Journal of Non Newtonian Fluid Mechanics, 127,1, 41-49 (2005)

- R. RANCHAL, M. BIBES, A. BARTHÉLÉMY, K. BOUZEHOUANE, S. GUYARD, E. JACQUET, J. P. CONTOUR. "Substrate influence on the growth of Co-doped La0.5Sr0.5TiO3-d epitaxial thin films" *Journal of Applied Physics*, **98**, 013514 (2005)
- J. RISTIC, C. RIVERA, E. CALLEJA, S. FERNÁNDEZ-GARRIDO, M. POVOLOSKYI, A. DI CARLO "Carrier confinement effects in Nanocolumnar GaN/AlGaN Quantum Discs Grown by Molecular Beam Epitaxy" *Physical Review B* 72, 085330-085335 (2005)
- J. RISTIC, E. CALLEJA, A. TRAMPERT, S. FERNÁNDEZ-GARRIDO, C. RIVERA, U. JAHN, K.H. PLOOG "Columnar AlGaN/GaN Nanocavities with AlN/GaN Bragg Reflectors Grown by Molecular Beam Epitaxy on Si(111)" Physical Review Letters, 94, 146102 (2005)
- J. RISTIC, E. CALLEJA, S. FERNÁNDEZ-GARRIDO, A. TRAMPERT, U.JAHN, K.H. PLOOG, M. POVOLOSKYI, A. DICARLO "GaN/AlGaN Nanocavities with AlN/GaN Bragg Reflectors Grown in AlGaN Nanocolumns by Plasma-assisted MBE" *Physica Status Solidi* (a) **202**, nº 3, 367-371 (2005)
- E. SILLERO, F. CALLE, M.A. SÁNCHEZ-GARCÍA "Reactive ion etching of GaN using SiCl4: Ar: SF6 chemistry" Journal of Materials Science: Materials in Electronics, 16,7-8,409-413(2005)
- H. TEISSEYRE, I. GORCZYCA, N.E. CHRISTENSEN, A. SVANE, F.B. NARANJO, E. CALLEJA "Pressure Behavior of Beryllium Acceptor Level in Gallium Nitride"

 Journal of Applied Physics, 97, 043704 (2005)
- J.M. ULLOA, A. HIERRO, M. MONTES, B. DAMILANO, M. HUGUES, J. BARJON, J.-Y. DUBOZ, J. MASSIES "Impact of N on the lasing characteristics of GalnNAs/GaAs quantum well lasers emitting from 1.29 to 1.52 mm" Applied Physics Letters 87, 251109 (2005)
- B. B. VAN AKEN, J.L. PRIETO, NEIL D. MATHUR "Ground state and constrained domain walls in Gd/Fe multilayers" *Journal of Applied Physics.* **97**, 063904 (2005)
- M. ZAMFIRESCU, M. ABBARCHI, M. GURIOLI, A. VINATTIERI, J. RISTIĆ, E. CALLEJA "Carrier Dynamics and Recombination in GaN Quantum Discs Embedded in AlGaN Nanocolumns" *Physica Status Solidi* (c) **2**, nº 2, 822-825 (2005)
- M. ZAMFIRESCU, M. GURIOLI, A. VINATTIERI, J. RISTIĆ, E. CALLEJA "Study of piezoelectric field in GaN Quantum Discs embedded in AlGaN Nanocolumns" *Physica Status Solidi* (c) **2**, nº 11, 3847-3850 (2005)

2006

C.A. BARRIOS

"Ultrasensitive Nanomechanical Photonic Sensor based on Horizontal Slot-Waveguide Resonator," *IEEE Photonics Technology Letters*, **18**, no. 22, 2419-2421, (2006)

C.A. BARRIOS, M. LIPSON

"Silicon photonic read only memory,"

IEEE Journal of Lightwave Technology, 24, no. 7, 2898-2905, (2006)

C.A. BARRIOS

"Electrooptic Modulation of Multi Silicon-on-Insulator Photonic Wires," *IEEE Journal of Lightwave Technology*, **24**, no. 5, 2146-2155, (2006)

A. BONITO, M. LASO, M. PICASSO

"Numerical Simulation of 3D Viscoelastic Flows with Free Surfaces" Journal of Computational Physics, 215 (2) 691-716 (2006) L. CERUTTI, J. RISTIĆ, S. FERNÁNDEZ-GARRIDO, E. CALLEJA, A. TRAMPERT, K.H. PLOOG, S. LAZIC, J.M. CALLEJA

"Wurtzite GaN Nanocolumns Grown on Si (001) by Molecular Beam Epitaxy: an Open Door to Optoelectronics Integration on Si"

Applied Physics Letters 88, 213114 (2006).

O. DE ABRIL, M.C. SÁNCHEZ, C. AROCA

"New closed flux stripe domain model for weak perpendicular magnetic anisotropy films"

Applied Physics Letters 89, 172510-(1-3) (2006)

O. DE ABRIL, M.C. SÁNCHEZ, C. AROCA

"The effect of the in-plane demagnetizing field on films with weak perpendicular magnetic anisotropy"

Journal of Applied Physics 100, 063904-(1-8) (2006)

S. DHAR, T. KAMMERMEIER, A. NEY, L. PÉREZ, K.H. PLOOG, A. MELNIKOV, A.D. WIECK

"Ferromagnetism and colossal magnetic moment in Gd-focused ion-beam-implanted GaN"

Applied Physics Letters 89, 062503 (2006)

M. LASO, J. RAMIREZ

"Implicit Micro-Macro Methods"

in "Multiscale modelling for polymer properties", E.A. Perpète, M. Laso, eds.,

Computer-Aided Chemical Engineering, 22, 85-108, Elsevier ISBN 0444521879 (2006)

M. LASO, N. JIMENO, C. ALEMÁN

"Monomer Solubility and Diffusion in Confined Polyethylene by Mapping Atomistic Trajectories onto the Macroscopic Diffusion Equation"

in "Multiscale modelling for polymer properties", E.A. Perpète, M. Laso, eds.,

Computer-Aided Chemical Engineering, 22, 183-200, Elsevier ISBN 0444521879 (2006)

M. LASO , L.M. MUNETA, M. MÜLLER, V. ALCÁZAR, F. CHINESTA, A. AMMAR

"Hierarchical Approach to Flow Calculations for Polymeric Liquid Crystals"

in "Multiscale modelling for polymer properties", E.A. Perpète, M. Laso, eds.,

Computer-Aided Chemical Engineering, 22, 359-401, Elsevier ISBN 0444521879 (2006)

M. LASO, N. KARAYIANNIS, M. MÜLLER

"Min-map Bias Monte Carlo for Chain Molecules: Biased Monte Carlo Sampling Based on Bijective Minimum-to-Minimum Mapping"

Journal of Chemical Physics, 125, 164108 (2006)

M. LASO, N. JIMENO, L.M. MUNETA, M. MÜLLER

Determination of rotary diffusivity of poly-(n-propyl isocyanate) by molecular dynamics

Journal of Chemical Physics, 125, 244901 (2006)

J. MIGUEL-SÁNCHEZ, A. GUZMÁN, J. M. ULLOA, M. MONTES, A. HIERRO, E. MUÑOZ

"MBE growth and processing of diluted nitride quantum well lasers on GaAs(111)B"

Microelectronics Journal 37, 1442-1445 (2006)

J. MIGUEL-SÁNCHEZ, A. GUZMÁN, J.M. ULLOA, A. HIERRO, E. MUÑOZ

"New Challenges in the growth of diluted nitrides"

Focus on Crystal growth research, Editor: George Karas.

Nova Science Publishers, 2006. ISBN: 1-59454-540-5

J.MIGUEL-SANCHEZ, A. GUZMAN, U. JAHN, A. TRAMPERT, A. HIERRO, E.MUÑOZ

"Impact of nitrogen ion density on the optical and structural properties of MBE grown InGaAsn/Gaas (100) and (111) B quantum wells"

Dilute Nitrides: Physics & Applications (2006), Editor: Ayse Erol.

Research Signpost, 2006. In press, ISBN: 81-7895-249-1

J. MIGUEL-SANCHEZ, U. JAHN, A. GUZMÁN, E. MUÑOZ

"Cathodoluminescence investigations of GalnAs on GaAs(111)"

Applied Physics Letters 89, 231901 (2006)

- M. NIEBELSCHÜTZ, V. CIMALLA, O. AMBACHER, T. MACHLEIDT, J. RISTIC, E. CALLEJA,
- "Electrical performance of Group III nitride nanocolumns"

Physica E, (in press)

- D. PASTOR, R. CUSCÓ, L. ARTUS, G. GONZALEZ-DIAZ, E. IBORRA, J. JIMENEZ, F. PEIRÓ, E. CALLEJA "The effect of substrate on high-temperature annealing of GaN epilayers: Si vs sapphire" *Journal of Applied Physics* **100**, 043508 (2006).
- J. PEDRÓS, R. CUERDO, R. LOSSY, N. CHATURVEDI, J. WÜRFL, F. CALLE
- "High temperature characterization of Pt-based Schottky diodes on AlGaN/GaN heterostructures" *Physica Status Solidi (c)* c) **3**, 1709 (2006).
- B. PEREIRA LO, A. J. HASLAM, C. S. ADJIMAN, M.LASO
- "A method for the systematic estimation of parameters for a stochastic reptation model" in "Multiscale modelling for polymer properties", E.A. Perpète, M. Laso, eds., *Computer-Aided Chemical Engineering* **22**, 69-84, Elsevier ISBN 0444521879 (2006)
- L. PÉREZ, I. LUCAS, C. AROCA, P. SÁNCHEZ, E. LÓPEZ, M.C. SÁNCHEZ "Analytical model for the sensitivity of a fluxgate sensor" Sensors and Actuators A 130-131, 142-146 (2006)
- L. PEREZ, G.S. LAU, S. DHAR, O. BRANDT, K.H. PLOOG "Magnetic phases and anisotropy in Gd-doped GaN" *Physical Review B* **74**, 195207 (2006)
- M. PLAZA, L. PÉREZ, M.C. SÁNCHEZ "Reducing the losses in sintered permally by addition of ferrite" *Journal of Magnetism and Magnetic Materials* **309**, 207-211 (2006)
- J. RAMIREZ, M. LASO
- "Micro-macro 3D calculations of viscoelastic flow"
- in "Multiscale modelling for polymer properties", E.A. Perpète, M. Laso, eds., Computer-Aided Chemical Engineering, 22, 123-142, Elsevier ISBN 0444521879 (2006)
- J. RAMIREZ, M. LASO
- "Implicit Viscoelastic Calculations using Brownian Configuration Fields"
- in "Multiscale modelling for polymer properties", E.A. Perpète, M. Laso, eds., *Computer-Aided Chemical Engineering*, **22**, 161-180, Elsevier ISBN 0444521879 (2006)
- R. RANCHAL, C AROCA, M.C. SÁNCHEZ, P. SÁNCHEZ, E. LÓPEZ "Effective exchange-coupling in Py/Gd films"

 Physica Status Solidi (A) 203, 1415-1419 (2006)
- R. RANCHAL, C AROCA, M.C.SÁNCHEZ, P. SÁNCHEZ, E. LÓPEZ
- "Improvement of the structural and magnetic properties of Permalloy/Gadolinium multilayers with Mo spacers" Applied Physics A, 82, 697-701 (2006)
- R. RANCHAL, C. AROCA, E. LÓPEZ
- "In-plane magnetotransport properties of Permalloy/Gadolinium/Permalloy trilayers" Journal of Applied Physics **100**, 103903 (2006)
- C. RIVERA, J.L.PAU, E. MUÑOZ, T. IVE, O. BRANDT "Photocapacitance characteristics of (In,Ga)N/GaN MQW structures" Physica Status Solidi (c), 3, 1978-1982 (2006)
- C. RIVERA, J. L. PAU, E. MUÑOZ, P. MISRA, O. BRANDT, HT. GRAHN, K.H.PLOOG "Polarization-sensitive photodetectors based on M-plane GaN grown on LiAIO2 substrates" Applied Physics Letters, 88, 213507 (2006)

C. RIVERA, J.L. PAU, AND E. MUÑOZ,

"Photocurrent gain mechanism in schottky barrier photodiodes with negative average electric field", *Applied Physics Letters* **89**, 263505 (2006)

C. RIVERA, J.L PAU, A. NAVARRO, E. MUÑOZ

"Photoresponse of (In,Ga)N/GaN multiple-quantum well structures in the visible and UVA ranges" IEEE Journal of Quantum Electronics, **42**, 1, 51-58, (2006)

M.A. SANCHEZ-GARCIA, J. GRANDAL, E. CALLEJA, S. LAZIC, J.M. CALLEJA, A. TRAMPERT, "Epitaxial growth and characterization of InN nanorods and compact layers on silicon substrates" *Physica Status Solidi* (b), **243**, 7, 1490 (2006).

J.M. ULLOA, A. HIERRO, M. MONTES, B. DAMILANO, M. HUGUES, J. BARJON, J.-Y. DUBOZ, J. MASSIES "Correlation between quantum well morphology, carrier localization, and the opto-electronic properties of GalnNAs/GaAs light emitting diodes"

Semiconductor Science and Technology 21, 1047-1052 (2006)

8.2 Conferences and Meetings

2004

O. DE ABRIL, R. FERNÁNDEZ, C. AROCA, P. SÁNCHEZ, E. LOPEZ, M.C. SÁNCHEZ

"Surface magnetization reversal proceses in Co-P microstructures"

Joint European Magnetic Symposia (JEMS'04)

Dresden (Germany), 2004

A.R. BARNES, D. HAYES, M.J. UREN, T. MARTÍN, R.S. BALMER, D. WALLIS, K.P HILTON, J. POWELL, W.A. PHILLIPS, A. JIMÉNEZ, E. MUÑOZ, M. KUBALL, S. RAJASINGAM, J. POMEROY, N. LABAT, N. MALBERT. P. RICE, A. WELLS

"AIGaN/GaN HFETs for LNA and Power Applications"

IEEE MTT-S International Microwave Symposium.

Texas (USA), 2004

M. BIBES, A. BARTHÉLÉMY, M. GAJEK, U. LÜDERS, R. RANCHAL, K. BOUZEHOUANE, E. JACQUET, M. VARELA, J.-F. BOBO, J. FONTCUBERTA, J.-P. CONTOUR, A. FERT

"New strategies to design spin-polarized electrons sources with oxide layers"

11th International Workshop on Oxide Electronics

Kakone (Japón), 2004

F. CALLE, J. PEDRÓS, T. PALACIOS, J. GRAJAL

"Acoustic wave devices on III-V Nitrides"

European Materials Research Society 2004 Fall Meeting, E-MRS.

Warsaw (Poland), 2004

F. CALLE, T. PALACIOS, J. PEDRÓS, J. GRAJAL

"Surface acoustic waves controlled photodetectors"

2nd European Workshop on Optical Fibre Sensors, ed. JM López-Higuera, B. Culshaw, Proc. SPIE vol. 5502, 442 (SPIE, Bellingham, WA. 2004) Santander (Spain), 2004

E. CALLEJA, J. RISTIC, S. FERNÁNDEZ-GARRIDO

"Nanocavities and Nanoemitters with AIN/GaN Bragg Reflectors Grown by MBE in Nanopillar Arrays"

Trends in NanoTechnology" International Conference (TNT-2004)

Segovia (Spain), 2004

E. CALLEJA et al.

"Resonant Raman Study of Strain and Composition in InGaN Multi Quantum Wells"

27th Int. Conference on the Physics of Semiconductors (ICPS-27),

Flagstaff, Arizona (USA), 2004

D. CIUDAD, L. PÉREZ, P. SÁNCHEZ, M.C. SÁNCHEZ, E. LÓPEZ, C. AROCA

"Low frecuency contactless smart cards"

Magnetic Measurements

Prague (Czech Republic), 2004

R. FERNÁNDEZ, O. DE ABRIL. P. SÁNCHEZ

"Observación de dominios magnéticos en microcintas de CoP mediante microscopía de fuerzas magnéticas"

III Reunión Nacional de Física del Estado Sólido

San Sebastián (Spain), 2004

J. GRAJAL, F. CALLE, J. PEDRÓS, T. PALACIOS

"Voltage Controlled SAW filters on 2DEG AlGaN/GaN heterostructures"

IEEE MTT-S International Microwave Symposium. Proc. IEEE Microwave Theory and Techniques S Digest, 387-390 Texas (USA), 2004

J. GRANDAL, M.A. SANCHEZ-GARCÍA

"InN layers grown on Silicon substrates: effect of substrate temperature and buffer layers

13th International Conference of Molecular Beam Epitaxy

Edinburgh (U.K.), 2004

J. GRANDAL, M.A. SÁNCHEZ-GARCÍA, F. CALLE, E. CALLEJA

"Morphology and optical properties of InN layers grown by MBE on silicon substrates"

Int. Workshop on Nitrides Semiconductors, IWNS'04.

Pittsburgh (USA), 2004

A. GUZMÁN, J. MIGUEL-SÁNCHEZ, E. LUNA, E. MUÑOZ

"InGaAsN and GaAsN based quantum well lasers and detectors for optical sensing in 1.3 and 1.55 µm"

2nd European Workshop Optical Fibre Sensors (EWOFS 04), SPIE vol. 5502, 414-417 Santander (Spain), 2004

A. HIERRO, J.-M. ULLOA, J. MIGUEL-SÁNCHEZ, E. LUNA, A. GUZMÁN, E. CALLEJA

"Growth and Characterization of GalnNAs QWs and their Application to QWIPs and LDs"

2nd Int. Workshop on "Metastable Compound Semiconductors and Heterostructures" Philipps-University Marburg (Germany), 2004

A. JIMÉNEZ, A.F. BRAÑA, E. CALLEJA, E. MUÑOZ

"Electrón Transport in AlGaN/GaN two dimensional electorn gases grown by MBE"

WOCSDICE 2004

Smolenice (Slovakia), 2004

I. LUCAS, L. PEREZ, C. AROCA, E. LÓPEZ, P. SÁNCHEZ, M.C. SÁNCHEZ,

"Magnetic properties of Co-P alloys electrodeposited at room temperature"

Joint European Magnetic Symposium (JEMS' 04)

Dresden (Germany), 2004

B. LÜHMANN, T. DOLLASE, M. LASO

"Understanding and controlling product anisotropy and its evolution in hotmelt coating processing of pressure-sensitive adhesive materials"

PSTC TECH XXVII Global Conference

Orlando, Florida (USA), 2004

E. LUNA, A. GUZMÁN, A. TRAMPERT, E. MUÑOZ

"The photovoltaic effect in the double barrier structure QWIPs and its relation to the offset in the dark current"

QWIP 2004 Workshop on Quantum Well Infrared Photodetectors

Kananaskis (Canadá), 2004

M. MAICAS, D. CIUDAD, C.AROCA, P.SÁNCHEZ, M.C.SÁNCHEZ, E. LÓPEZ,

"Magnetic properties and magnetoelastic coupling measurements in layered Fe-Co-B thin films"

Magnetic Measurements

Prague (Czech Republic), 2004

M. MAICAS, E.LÓPEZ, C AROCA M.C.SÁNCHEZ, P.SÁNCHEZ

"Propiedades magneto-elasticas de aleaciones de Fe-Co-B

III Reunión Nacional de G.E.F.E.S. de la R.S.E.F.

San Sebastian (Spain), 2004

M.D. MICHELENA, M. MAICAS, C. AROCA, MC. SÁNCHEZ, P. SÁNCHEZ, E. LÓPEZ

"Magnetometric sensor based on a magnetostrictive FeCoB layer sputtered on a bimorph"

13th European Workshop on Heterostructure Technology

Crete (Greece), 2004

J. MIGUEL-SÁNCHEZ, A. GUZMÁN, J.M. ULLOA, A. HIERRO, E. MUÑOZ

"Effect of nitrogen ions in the properties of InGaAsN-based lasers grown by plasma assisted molecular beam epitaxy"

European Materials Research Society E-MRS 2004 Spring Meeting. IEE Proceedings of Optoelectronics, 151, 305-308 Strasbourg (France), 2004

J. MIGUEL-SÁNCHEZ, A. GUZMÁN, J.M. ULLOA, A. HIERRO, E. MUÑOZ

"InGaAsN on GaAs (111)B for telecommunications laser applications"

13th International Conference of Molecular Beam Epitaxy

Edinburgh (U.K.), 2004

T. MONTOJO, C. MÉNDEZ, A. ARTÉS-RODRÍGUEZ, Á. GUZMÁN

"Naval Missile Warning Research Platform Based on Multi-spectral IR Imaging"

International Symposium MISSILE DEFENCE'04. 2nd AAAF International Conference on Missile Defence "Challenges in Europe" Florence (Italy), 2004

F. B. NARANJO, S. FERNÁNDEZ-GARRIDO, E. CALLEJA, Z. BOUGRIOUA, A. TRAMPERT, X. KONG, K.H. PLOOG

"Effciency optimization of p-type doping in GaN:Mg grown by Molecular beam Epitaxy"

13th International Conference on Molecular Beam Epitaxy

Edinburgh (U.K.), 2004

J.L. PAU, C. RIVERA, J. PEREIRO, E. MUÑOZ, E. CALLEJA, U. SCHÜHLE, E. FRAYSSINET, B. BEAUMONT, J.P. FAURIE, P. GIBART

"Nitride-based photodetectors: from visible to x-ray monitoring"

European Materials Research Society E-MRS 2004 Spring Meeting Strasbourg (France), 2004

J.L. PAU, J. PEREIRO, C. RIVERA, E. MUÑOZ, E. CALLEJA

"Plasma-assisted molecular beam epitaxy of nitride-based photodetectors for UV and visible applications"

13th International Conference on Molecular Beam Epitaxy

Edinburgh (U.K.), 2004

J. PEDRÓS, F. CALLE, J. GRAJAL, R. J. JIMÉNEZ RIOBÓO, C. PRIETO, J.L. PAU, J. PEREIRO, M. HERMANN, M. EICKHOFF, Z. **BOUGRIOUA**

"Anisotropic propagation of surface acoustic waves on nitride heterostructures"

13th European Heterostructure Technology Workshop

Heraklion (Crete), 2004

J. PEDRÓS, F. CALLE, J. GRAJAL, R. J. JIMÉNEZ RIOBÓO, C. PRIETO, M. EICKHOFF, Z. BOUGRIOUA

"Anisotropic propagation of surface acoustic waves on nitride layers"

European Materials Research Society E-MRS 2004 Spring Meeting

Strasbourg (France), 2004

J. PRIETO, B.B. VAN AKEN, G. BURNELL, M.G.BLAMIRE, J.E. EVETTS

"Magnetoresistance of in-plane domain-wall like structures"

9th Joint MMM-Intermag Conference

Anaheimn, Los Angeles (USA), 2004

R. RANCHAL, A. BARTHÉLÉMY, K. BOUZEHOUANE, M. BIBES, S. GUYARD, A. HAMZIC, C. PASCANUT, P. BERTHET, N. DRAGOE, E. JACQUET, J.-P. CONTOUR, A. FERT.

"Optimisation of Co-doped La0.5Sr0.5TiO3 epitaxial thin films"

20th General Conference of the Condensed Matter Division of the European Physical Society

Prague (Czech Republic), 2004

J. RISTIC, E. CALLEJA, S. FERNÁNDEZ-GARRIDO, A. TRAMPERT, K.H. PLOOG, M. POVOLOVSKYI, A. DI CARLO,

"GaN/AIGaN Nanocavities with AIN/GaN Bragg Reflectors Grown in AIGaN Nanocolumns by Plasma-assisted MBE"

13th International Conference on Molecular Beam Epitaxy

Edinburgh (U.K.), 2004

J. RISTIC, E. CALLEJA, S. FERNÁNDEZ-GARRIDO, A. TRAMPERT, K.H. PLOOG, M. POVOLOSKYI, A. DICARLO

"GaN/AlGaN Nanocavities with AlN/GaN Bragg Reflectors Grown in AlGaN Nanocolumns by Plasma-assisted MBE"

4th Int. Conf. on Phys.of Light-Matter Coupling in Nanostructures

St. Petersburg (Russia), 2004

J. RISTIC, E. CALLEJA, S. FERNÁNDEZ-GARRIDO, A. TRAMPERT, K.H. PLOOG, M. POVOLOSKYI, A. DICARLO

"GaN/AlGaN Nanocavities with AlN/GaN Bragg Reflectors Grown in AlGaN Nanocolumns by Plasma-assisted MBE"

6th Conference of the Yugoslav Materials Research Society Yucomat 2004

Herceg-Novi (Montenegro), 2004

J. RISTIC, E. CALLEJA, S. FERNÁNDEZ-GARRIDO, A. TRAMPERT, K.H. PLOOG

"III-Nitride Nanocolumnar Structures Grown by MBE: Nucleation Steps"

13th International Conference on Molecular Beam Epitaxy

Edinburgh (U.K.), 2004

C. RIVERA, J. L. PAU, E. MUÑOZ, F. B. NARANJO, E. CALLEJA

"InGaN(AI)GaN-based multiple-quantum-well photodetectors"

5th International Symposium on Blue Laser and Light Emitting Diodes

Gyeongju (Corea), 2004

C. RIVERA, J. L. PAU, J. PEREIRO, E. MUÑOZ,

"Properties of Schottky barrier photodiodes based on InGaN/GaN MQW structures"

European Materials Research Society E-MRS 2004 Spring Meeting Strasbourg (France), 2004

C. RIVERA, J.L. PAU, J. PEREIRO, E.MUÑOZ

"Photoresponse of III nitrides detectors in the λ >360nm and λ <200nm regions"

11th Advanced Heteroestructure Worshop

Kohala Coast, Hawai (USA), 2004

E. SILLERO, F. CALLE, M.A. SÁNCHEZ-GARCÍA

"GaN Reactive ion etching of GaN using SiCl4:Ar:SF6 Chemistry"

Materials for Microelectronics and Nanoengineering, MFMN'04

Southampton (U.K.), 2004

E. SILLERO, F. CALLE, M.A. SANCHEZ-GARCÍA

"Plasma processing for GaN-based technology"

13th European Workshop on Heterostructure Technology

Crete (Greece), 2004

J.M. ULLOA, A.HIERRO, J. MIGUEL-SÁNCHEZ, A. GUZMÁN, J.-M CHAUVEAU, A. TRAMPERT, E. TOURNIÉ, J.L. SÁNCHEZ-ROJAS, E. CALLEJA

"Opto-electronic properties of 2D and 3D-grown GalnNAs/GaAs QW ligth emitting diodes"

European Material Research Soc. (EMRS) Spring Meeting. IEE Proceedings of Optoelectronics, 151, 421-424 (2004)

Symposium on "Dilute Nitride and Related Mismatched Semiconductor Alloys"

Strasbourg (France), 2004

M. ZAMFIRESCU, M. GURIDI, Z. VINATTERI, J. RISTIC, E. CALLEJA

"Carrier dynamics and recombination in GaN quantum discs embedded in AlGaN nanocolumns"

4th Int. Conf. on Phys.of Light-Matter Coupling in Nanostructures

St. Petersburg (Russia), 2004

2005

A. F. BRAÑA, A. JIMENEZ, Z. BOUGRIOUA, M. AZIZE, P.P. CUBILLA, Y. J. FDEZ. DE BOBADILLA, F. ROMERO, M.T. MONTOJO, M. VERDU, J. GRAJAL, E. MUÑOZ

"Improved AIGaN/GaN HEMTs using Fe doping"

5ª Conf. Dispositivos Electrónicos, Actas CDE'05,

Tarragona (Spain), 2005

E. CALLEJA, J. RISTIC, C. RIVERA, S. FERNÁNDEZ-GARRIDO, M. POVOLOSKYI, A. DI CARLO, A. TRAMPERT, K.H.PLOOG

"Self-assembled growth of AlGaN/GaN/AlGaN Nanocavities on Si(111) by MBE"

13th European Molecular Beam Epitaxy Workshop

Grindelwald (Switzerland), 2005

E. CALLEJA et al.

"On the origin of carrier localization in GalnNAs/GaAs quantum wells: relative influence of QW morphology, and In and N contents" 13th Euro MBE Workshop.

Grindelwald (Switzerland), 2005

E. CALLEJA et al.

"Substrate influence on the high-temperature annealing behavior of GaN: Si vs. sapphire"

Materials Research. Soc. Fall Meeting Symp. on "GaN and Related Compounds",

Boston (USA), 2005

R. CUERDO, J. PEDRÓS, F. CALLE

"Characterization of Schottky contacts on n-GaN at high temperature"

5ª Conf. Dispositivos Electrónicos, Actas CDE'05,

Tarragona (Spain), 2005

F. CHINESTA, D. RYCKELYNCK, A. AMMAR, M. LASO

"Improving efficiency in complex flow simulations"

European Materials Society 2005 Conference, Euromat

Prague (Czech Republic), 2005

S. FERNÁNDEZ-GARRIDO, J. RISTIC, E. CALLEJA, A. TRAMPERT, K.H. PLOOG

"InGaN and InGaN/GaN Nanocolumnar Heterostructures grown on Si(111) by Plasma Assisted Molecular Beam Epitaxy"

13th European Molecular Beam Epitaxy Workshop

Grindelwald (Switzerland), 2005

A. HIERRO, J.M. ULLOA, B. DAMILANO, J. BARJON, J-Y. DUBOZ, J. MASSIES, A. TRAMPERT

"Impact of N on lasing characteristics of Galn(N)As/GaAs heteroestructures emitting between 1.3 µm and 1.44 µm"

13th European Molecular Beam Epitaxy Workshop

Grindelwald (Switzerland), 2005

U. JAHN, T. FLISSIKOWSKI, HT. GRAHN, R. HEY, E. WIEBICKE, A. K. BLUHM, J. MIGUEL SÁNCHEZ, A. GUZMÁN

"Carrier diffusion lenghts of GaAs, (In,Ga)As and (In,Ga)(As,N) quantum wells studied by spatially resolved cathodoluminiscence" Microtechnologies for the New Millenium 2005. Photonic Materials Devices and Applications, Proceeding SPIE, Sevilla (Spain), 2005

E. LUNA, L. GONZÁLEZ, Y. GONZÁLEZ, R. HEY, A. TRAMPERT, D. LÓPEZ-ROMERO, A. GUZMÁN

"Critical role of the growth conditions on double barrier quantum well infrared photodetectors based on AlGaAs/AlAs/GaAs: comparison between coventional and atomic layer MBE"

13th European Molecular Beam Epitaxy Workshop Grindelwald (Switzerland), 2005

J. MIGUEL-SÁNCHEZ, A. GUZMÁN, J.M. ULLOA, A.HIERRO, E. MUÑOZ

"Effects of rapid thermal annealing on InGaAsN quantum well based devices grown on misoriented (111)B GaAs" Microtechnologies for the New Millenium 2005. Photonic Materials Devices and Applications, Proceeding SPIE, 5840, 766-773 Sevilla (Spain), 2005

J. MIGUEL-SÁNCHEZ, A. GUZMÁN, M. HOPKINSON, J.M. ULLOA, A. HIERRO

"Optimization of InGaAsN on GaAs (111)B for semiconductor laser devices"

Actas CDE 05, 5ª Conferencia de Dispositivos Electrónicos Tarragona (Spain), 2005

J. MIGUEL-SÁNCHEZ, U. JAHN, A. TRAMPERT, A. GUZMÁN, J.M. ULLOA, A. HIERRO, E. MUÑOZ

"Cathololuminesce and TEM studies of InGaAsN quantum wells"

13th European Molecular Beam Epitaxy Workshop Grindelwald (Switzerland), 2005

J.L. PAU, C. RIVERA, E. MUÑOZ

"Development of radiation detectors based on group III-N compounds"

COST action P7:X-ray and neutron optics Madrid (Spain), 2005

J.L. PAU, C.RIVERA, P.TAPIA, A. NAVARRO, E. MUÑOZ

"Radiation detectors based on III-N compounds"

10th European Symposium on Semiconductor Detectors

Kreuth (Germany), 2005

J.L. PAU, C. RIVERA, J. PEREIRO, A. NAVARRO, R. PECHARROMÁN, E. MUÑOZ

"III-Nitride Based Photodetectors for the Visible Range"

Workshop on Compound Semiconductor Devices & Integrated Circuits in Europe 2005. Cardiff School of Engineering Cardiff (U.K), 2005

J.L. PAU, C. RIVERA, J. PEREIRO, A. NAVARRO, E. MUÑOZ

"Ultraviolet and visible photodetectors: applications"

Conferencia de Dispositivos Electrónicos, CDE 2005

Tarragona (Spain), 2005

J. PEDRÓS, R. CUERDO, J. GRAJAL, E. SILLERO, Z. BOUGRIOUA, F. CALLE

"Gate-biased SAW devices on AlGaN/GaN heterostructure"

14th European Heterostructure Technology Workshop.

Smolenice (Eslovaquia), 2005.

J. PEDRÓS, R. CUERDO, R. LOSSY, N. CHATURVEDI, J. WÜRFL, F. CALLE,

"High temperature characterization of Pt-based Schottky diodes on AlGaN/GaN heterostructures"

6th International Conference on Nitride Semiconductors.

Bremen (Germany), 2005

J. PEREIRO, J.L. PAU, C. RIVERA, E.MUÑOZ

"InGaN-based photoconductors and photodiodes grown by Molecular Beam Epitaxy"

13th European Molecular Beam Epitaxy Workshop

Grindelwald (Switzerland), 2005

M. PLAZA, L. PÉREZ, E. LÓPEZ, M.C. SÁNCHEZ

"Reducción de pérdidas en Permalloy sinterizado mediante la adición de ferrita"

Orense (Spain), 2005

R. RANCHAL, C.AROCA, P. SÁNCHEZ, M.C.SÁNCHEZ, E. LÓPEZ

"Efective exchange-coupling in Py/Gd bilayers"

Trends in Nanotechnology

Oviedo (Spain), 2005

R. RANCHAL, C. AROCA, P. SÁNCHEZ, M.C. SÁNCHEZ, E. LÓPEZ,

"Acoplamiento de canje en bicapas Py/Gd"

Orense (Spain), 2005

J. RISTIC, S. FERNÁNDEZ-GARRIDO, E. CALLEJA, A. TRAMPERT, K.H. PLOOG

"Nucleation Mechanisms in Self-assembled GaN Nanocolumns Grown by Plasma-Assisted MBE"

13th European Molecular Beam Epitaxy Workshop

Grindelwald (Switzerland), 2005

J. RISTIC, C. RIVERA, S. FERNÁNDEZ-GARRIDO, E. CALLEJA, A. TRAMPERT, K.H. PLOOG, M. POVOLOSKYI, DI CARLO

"Carrier confinement effects in III-N Nanocolumnar Heterostructures and Nanocavities Grown by Molecular Beam Epitaxy"

6th International Conference on Nitride Semiconductors (ICNS6)

Bremen (Germany), 2005

C. RIVERA, J.L. PAU, E. MUÑOZ, T. IVE, O. BRANDT

"Photocapacitance characteristics of (In,Ga)N/GaN MQW structures"

6th International Conference on Nitride Semiconductors

Bremen (Germany), 2005

M.A. SÁNCHEZ-GARCÍA, J. GRANDAL, E. CALLEJA, S. LAZIC, J.M. CALLEJA, A. TRAMPERT

"Epitaxial growth and characterization of InN nanorods and compact layers on silicon substrates"

6th International Conference on Nitride Semiconductors (ICNS6)

Bremen (Germany), 2005

J.M. ULLOA, A. HIERRO, J. MIGUEL-SANCHEZ, A. GUZMÁN, A. TRAMPERT, J-M. CHAUVEAU, E. TOURNIE, E. CALLEJA

"On the origin of carrier localization in GalnNAs/GaAs quantum wells: relative influence of QW morphology, and In and N contents" 13th European Molecular Beam Epitaxy Workshop

Grindelwald (Switzerland), 2005

J.M. ULLOA, A. HIERRO, M. MONTES, J. MIGUEL-SÁNCHEZ, A. GUZMÁN, B. DAMILANO, J. BARJON, M. HUGUES, J.-Y. DUBOZ, J. MASSIES, A. TRAMPERT

"Influence of carrier localization on lasing characteristics of MBE grown GalnNAs/GaAs QW laser diodes"

Microtechnologies for the New Millenium 2005. Photonic Materials Devices and Applications, Proceeding SPIE,

Sevilla (Spain), 2005

M. ZAMFIRESCU, M.GURIOLI, A. VINATTIERI, J. RISTIC, E. CALLEJA

"Study of piezoelectric field in GaN Quantum Discs for estimating the residual strain in self assembled AlGaN Nanocolumns"

5th Int. Conf. on Phys.of Light-Matter Coupling in Nanostructures, (PLMCN5)

Glasgow, (U.K.), 2005

2006

C.A. BARRIOS, Q. XU, J. SHAKYA, C. MANOLATOU, M. LIPSON,

"Compact Silicon Slot-Waveguide Disk Resonator,"

Conference on Lasers and Electro-Optics (CLEO) 2006, paper CTuCC3,

Long Beach, California (USA), 2006.

E. CALLEJA et al.

"Self-assembled MBE growth of III-Nitride Nanocolumnar Heterostructures on Si substrates"

33rd Conf. on the Physics and Chemistry of Semiconductor Interfaces (PCSI),

Florida (USA), 2006

E. CALLEJA et al.

"Growth of III-Nitride Nanocolumnar heterostructures on Si(111) and Si(100) by MBE"

Japanese-Spanish-German Workshop,

Berlin (Germany), 2006

E. CALLEJA et al.

"Ill-Nitride Nanocolumnar Heterostructures on Silicon: Growth Mechanism and Application to Devices"

2006 International Conference on Blue Lasers and Light Emitting Diodes,

Montpellier (France), 2006

E. CALLEJA et al.

"Crystal damage assessment of Be+-implanted GaN by UV Raman scattering"

2006 International Conference on Blue Lasers and Light Emitting Diodes,

Montpellier (France), 2006

E. CALLEJA et al.

"GaN Nanocolumns Grown on Si by Molecular Beam Epitaxy for integrated nanophotonics"

14th International Conference on Molecular Beam Epitaxy (MBE2006),

Tokyo (Japan), 2006

F CALLEJA et al.

"Coupled Longitudinal Optical Phonon-Plasmon Modes in InN Nanocolumns"

28th International Conference on the Physics of Semiconductors (ICPS),

Vienna (Austria), 2006

E. CALLEJA et al.

"Growth and characterization of InN and In-rich (Al,Ga)InN quantum well heterostructures by PA-MBE"

International Workshop on Nitride Semiconductors (IWN 2006)

Kyoto (Japan), 2006

E. CALLEJA et al.

"Electrical performance of Gallium Nitride nanocolumns"

European Materials Research Society Spring Meeting (E-MRS)

Nice (France), 2006

E. CALLEJA et al.

"Self-assembled MBE growth of III-Nitride Nanocolumnar Heterostructures on Si substrates"

12th Advanced Heterostructure Workshop,

Hawaii (USA), 2006

E. CALLEJA et al.

"Growth, morphology, and structural properties of III-Nitride nanocolumns and nanodisks"

I Jornadas de Nanofotónica, Universidad Politécnica de Valencia

Valencia (Spain), 2006

E. CHO, E. SILLERO, D. PAVLIDIS, G. ZHAO, S. SEO, S.JATTA, B.KÖGEL, P. MEIBNER,

"GaN/Air Gap Based Micro Opto Electro Mechanical (MOEM) Fabry-Pérot Filters"

International Workshop on Nitride Semiconductors 2006,

Kyoto (Japón), 2006

R. CUERDO, J. PEDRÓS, A. BRAÑA, F. CALLE, E. MUÑOZ,

"High temperature characterization of nitride-based HEMT and SAW devices"

15th European Workshop on Heterostructure Technology,

Manchester (U.K.), 2006

R. CUERDO, J. PEDRÓS, A. NAVARRO, A. BRAÑA, J.L. PAU, E. MUÑOZ, F. CALLE

"High temperature assessment of nitride-based devices"

6th International Conference on Materials for Microelectronics and Nanoengineering, Proc. 110-113. ISBN 10:0-9553082-1-6. Cranfield (U.K.), 2006

T. DOLLASE, M. LASO

"Product anisotropy in hotmelt coating processing of pressure-sensitive adhesive materials"

Swissbonding 2006

Rapperswil (Switzerland), 2006

S. LOURDUDOSS, F. OLSSON, C.A. BARRIOS, T. HAKKARAINEN, A. BERRIER, S. ANAND, A.AUBERT, J.BERGGREN, R. G. BROEKE, J. CAO. N. CHUBUN, S-W SEO, J-H BAEK, N. CHUBUN, K.AIHARA, ANH-VU PHAM, S.J.BEN YOO, M. AVELLA, J. JIMÉNEZ.

"Heteroepitaxy and Selective Epitaxy for Discrete and Integrated Devices,"

Conference on Optoelectronic and Microelectronic Materials and Devices (COMMAD 2006),

Perth (Australia), 2006.

I. LUCAS, L. PÉREZ, M.PLAZA, M.C. SÁNCHEZ

"Pinning field and coercivity in CoP alloys"

III Joint European Magnetic Symposia,

San Sebastian (Spain), 2006

J. MIGUEL-SANCHEZ, A. GUZMAN, J. M. ULLOA, M. MONTES, A. HIERRO, E. MUÑOZ

"MBE growth and processing of diluted nitride quantum well lasers on GaAs (111)B"

Sixth International Workshop on Epitaxial Semiconductors on Patterned Substrates and Novel Index Surfaces (ESPS-NIS) Nottingham (U.K.), 2006

M. MONTES, A. HIERRO, J.M. ULLOA, B. DAMILANO, M. HUGUES, M. AL KHALFIOUI, J.-Y. DUBOZ, J. MASSIES

"Thermal characteristics of 1.3-1.5 Im InGaAs(N)/GaAs quantum well laser diodes grown by molecular beam epitaxy" European Semiconductor Laser Workshop (ESLW) 2006

Nice (France), 2006

A. NAVARRO, C. RIVERA, R. CUERDO, J. L. PAU, J. PEREIRO, E. MUÑOZ

"Low-frequency noise in InGaN/GaN MQW-based photodetector structures"

SBLLED 2006

Montpellier (France), 2006

J. PEDRÓS, R. CUERDO, F. CALLE, J. GRAJAL, J. L. MARTÍNEZ-CHACÓN, Z. BOUGRIOUA

"Field-Effect-Modulated SAW Devices on AlGaN/GaN Heterostructures"

IEEE International Ultrasonics Symposium,

Vancouver (Canadá), 2006

R. RANCHAL, C. AROCA, M. MAICAS, E. LÓPEZ

"Temperature dependence of magnetic and electrical properties of Py/Gd/Py thin films"

Joint European Magnetic Symposia (JEMS'06)

San Sebastián (Spain), 2006

R. RANCHAL, C. AROCA, E. LÓPEZ,

"Influencia de la difusión de Ni en el acoplamiento magnético en la interfase Permalloy/Gadolinio"

IV Reunión Nacional de G.E.F.E.S. de la R.S.E.F.

Alicante (Spain), 2006

C. RIVERA, P. MISRA, J. L. PAU, E. MUÑOZ, O. BRANDT, H. T. GRAHN, K. H. PLOOG

"M-plane GaN-based dichroic photodetectors"

ISBLLED 2006

Montpellier (France), 2006

C. RIVERA, J. L. PAU, E. MUÑOZ

"Internal gain mechanisms in III-nitride based MQW photodetectors"

IWN 2006

Kyoto (Japan), 2006

C. RIVERA, P. MISRA, J. L. PAU, E. MUÑOZ, O. BRANDT, H. T. GRAHN, K. H. PLOOG

"Electrical and optical characterization of M-plane GaN films grown on LiAlO2 substrates"

IWN 2006

Kyoto (Japan), 2006

B. SCHMIDT, C. A. BARRIOS, M. LIPSON,

"Si₃N₄-SiO₂-Si slot-waveguide disk resonators in a silicon photonic platform"

Materials Research Society (MRS)

Boston, Massachussets (USA), 2006.

J. SEGURA, N. GARO, A. CANTARERO, J. MIGUEL-SÁNCHEZ, A. GUZMÁN, A. HIERRO

"Photoluminescence and magneto-photoluminescence studies in GalnNAs/GaAs quantum wells"

International Conference on Physics of Semiconductors (ICPS) 2006

Viena (Austria), 2006

E. SILLERO, F. CALLE, D. LÓPEZ-ROMERO, M. EICKHOFF, J. F. CARLIN, N. GRANDJEAN, M. ILEGEMS,

"Selective etching of AllnN/GaN heterostructures for MEMS technology "

32nd International Conference on Micro and Nano Engineering (MNE2006),

Barcelona (Spain), 2006

E. SILLERO, F. CALLE, M. EICKHOFF, J. F. CARLIN, N. GRANDJEAN, M. ILEGEMS

"Etching procedures for III-N microsystems technology"

6th Int Conf. Materials for Microelectronics and Nanoengineering, Proc. 41-44. ISBN 10:0-9553082-1-6. Cranfield (U.K.), 2006

I. TANARRO, C. DOMINGO, M.CASTILLO, T. DE LOS ARCOS, M.M. SANZ, V.J. HERRERO

"FTIR Spectroscopic Diagnosis of Cold Reactive Plasmas generated in Hollow Cathode Discharges".

1st International Workshop on Infrared Plasma Spectroscopy

Greifswald (Germany), 2006

8.3 Invited Talks

F. CALLE, J. PEDRÓS, T. PALACIOS, J. GRAJAL

"Acoustic wave devices on III-V nitrides"

European Materials Research Society 2004 Fall Meeting, EMRS.

Warsaw (Poland), 2004

E. CALLEJA, J. RISTIC, S. FERNÁNDEZ-GARRIDO

"Nanocavities and Nanoemitters with AIN/GaN Bragg Reflectors Grown by MBE in Nanopillar Arrays"

"Trends in NanoTechnology" International Conference (TNT-2004)

Segovia (Spain), 2004

C. RIVERA, J. L. PAU, J. PEREIRO, E. MUÑOZ

"Photoresponse of III-nitrides detectors in the λ >360nm and λ <200nm regions"

11th Advanced Heterostructure Workshop

Kohala Coast, Big Island of Hawai'i (USA), 2004

E. MUÑOZ, E. LUNA, J. MIGUEL SÁNCHEZ, C. RIVERA, A. GUZMÁN, A. HIERRO, J.L. PAU, E. CALLEJA

"Quantum well photodetectors based on nitrides. Operation in the near IR, visible and UV"

Japan-Germany-Spain Joint Workshop on advanced Semiconductor Optoelectronic Devices and Materials Yufuin, Oita (Japan), 2004

E. CALLEJA

"III-Nitrides: Growth by MBE and Applications"

Universidad de Roma "Tor Vergata",

Roma (Italia), 2005

E. CALLEJA, J. RISTIC, C. RIVERA, S. FERNÁNDEZ-GARRIDO, M. POVOLOSKYI, A DI CARLO, A. TRAMPERT, K.H. PLOOG "Self-assembled growth of Algan/Gan/Algan Nanocavities on Si(111) by MBE"

13th European Molecular Beam Epitaxy Workshop

Grindelwald (Switzerland), 2005

A. GUZMÁN, E. LUNA, D. LÓPEZ-ROMERO, E. MUÑOZ

"Quantum well infrared detectors based on dilute nitrides"

Workshop on Compound Semiconductor Devices & Integrated Circuits in Europe 2005. Cardiff School of Engineering. 2005 Cardiff (U.K), 2005

E. MUÑOZ, J.L. PAU, C. RIVERA, J. PEREIRO, A. NAVARRO, R. PECHARROMÁN

"Al,In,GaN)N-based UV and VIS Photodetectors"

18th Annual Meeting of the IEEE Lasers & Electro-Optics Society

Sydney (Australia), 2005

J.L. PAU, C. RIVERA, J. PEREIRO, A. NAVARRO, R. PECHARROMÁN, E. MUÑOZ

"Ultraviolet and visible photodetectors: applications"

Conferencia de Dispositivos Electrónicos, CDE 2005

Tarragona (Spain), 2005

M. LASO, N, JIMENO

"Polymers in confined geometries: PE in a zeolite catalyst"

ECOREP III

Lyon (France), 2005

MIASO

"Ergodic Generation of Amorphous Cell Structures in Atomisitic Simulations of Polymers"

XIII Congreso de Física Estadística

Madrid (Spain) 2005

E. CALLEJA et al.

"Self-assembled MBE growth of III-Nitride Nanocolumnar Heterostructures on Si substrates"

33rd Conf. on the Physics and Chemistry of Semiconductor Interfaces (PCSI), Florida (USA), 2006

E. CALLEJA et al.

"Growth of III-Nitride Nanocolumnar heterostructures on Si(111) and Si(100) by MBE"

Japanese-Spanish-German Workshop,

Berlin (Germany), 2006

E. CALLEJA et al.

"Ill-Nitride Nanocolumnar Heterostructures: Growth, Properties and Application to Devices"

Monte Verita Summer School on "Wide Bandgap Semiconductor Quantum Structures",

Ascona (Switzerland), 2006

E. CALLEJA et al.

"Growth, morphology, and structural properties of III-Nitride nanocolumns and nanodisks"

I Jornadas de Nanofotónica, Universidad Politécnica de Valencia.

Valencia (Spain) 2006

A. HIERRO, M. MONTES, J.M. ULLOA, B. DAMILANO, M. HUGUES, M. AL KHALFIOUI, J.-Y. DUBOZ, J. MASSIES

"Carrier recombination mechanisms in MBE-grown InGaAsN/GaAs laser diodes"

European Semiconductor Laser Workshop (ESLW) 2006

Nice (France), 2006

M. LASO

"Short Course on Multiscale Modelling Techniques"

Annual European Rheology Cconference 2006 FORTH, Institute of Electronic Structure & Laser Heraklion (Greece), 2006

E. MUÑOZ

"Recent advances in III-N-based photodetectors"

2006 Japanese-Spanish-German Joint Workshop on Advanced Semiconductor Optoelectronic Materials Devices Berlín (Germany), 2006

E. MUÑOZ,

"Ill-nitrides photodetectors for the VIS and UV regions"

Research Institute of Electronics, University of Shizuoka

Hamamatsu (Japan), 2006

L. PÉREZ

"Synthesis of GaN: Gd by MBE"

Workshop on Gd-doped Nitride Semiconductors Gainesville, FL (USA) 2006

R. RANCHAL, C. AROCA, M. MAICAS, E. LÓPEZ

"Temperature dependence of magnetic and electrical properties of Py/Gd/Py thin films"

Joint European Magnetic Symposia (JEMS'06)

San Sebastián (Spain), 2006

8.4 Ph.D. Thesis

Title: "Diseño y fabricación de reflectores Bragg para diodos LED de cavidad resonante"

Autor: Susana Fernández Ruano

Director: Enrique Calleja Pardo - Fernando Calle Gómez

University: Universidad Politécnica de Madrid, E.T.S., Ing. de Telecomunicación, 2004

Grade: Sobresaliente "Cum Laude"

Title: "Desarrollo de detectores de infrarrojo fotovoltaicos, de pozocuántico y doble barrera

para la banda de 3-5 µm"

Autor: Esperanza Luna García de la Infanta

Director: Álvaro de Guzmán Fernández González - José Luis Sánchez Rojas Aldavero University: Universidad Politécnica de Madrid, E.T.S,. Ing. de Telecomunicación, 2004

Grade: Sobresaliente "Cum Laude

Title: "Estudio de Dispositivos Magnetométricos. Aplicación al Proyecto NANOSAT"

Autor:: Marina Díaz Michelena

Director: Pedro Sánchez Sánchez - Claudio Aroca Hernández-Ros

University: Universidad Politécnica de Madrid, E.T.S., Ing. de Telecomunicación, 2004

Grade: Sobresaliente "Cum Laude"

Title: "Materiales magnéticos blandos obtenidos por electrodeposición: aplicaciones en sensores

integrados"

Autor: Lucas Pérez García

Director: María del Carmen Sánchez Trujillo- Claudio AROCA Hernández-Ros University: Universidad Complutense de Madrid, Facultad de C.C. Físicas, 2004

Grade: Sobresaliente "Cum Laude"

Title: "Diseño, fabricación y caracterización de diodos láser basados en pozos cuánticos de

InGaAs(N)/GaAs"

Autor: José María Ulloa

Director: José Luis Sánchez-Rojas Aldavero - Adrián Hierro Cano

University: Universidad Politécnica de Madrid, E.T.S., Ing. de Telecomunicación, 2005

Grade: Sobresaliente "Cum Laude"

Title: "Crecimiento y caracterizacion de estructuras nanocolumnares de nitruros del grupo III"

Autor: Jelena Ristic

Director: Enrique Calleia Pardo

University: Universidad Politécnica de Madrid, E.T.S., Ing. de Telecomunicación, 2006

Grade: Apto "Cum Laude" por unanimidad

Title: "Crecimiento por MBE de pozos cuánticos de InGaAsN sobre GaAs (111)B y (100) para su

aplicación a láseres de semiconductor"

Autor: Javier Miguel-Sánchez

Director: Álvaro de Guzmán Fernández González

University: Universidad Politécnica de Madrid, E.T.S., Ing. de Telecomunicación, 2006

Grade: Sobresaliente "Cum Laude"

Title: "Microestructuras magnéticas obtenidas mediante procesos electroquímicos"

Autor: Oscar de Abril Torralba

Director: Mª del Carmen Sánchez Trujillo - Claudio Aroca Hernández-Ros University: Universidad Complutense de Madrid, Fac. Ciencias Físicas, 2006

Grade: Sobresaliente "Cum Laude"

Title: "Optimización de las propiedades magnéticas y de transporte en multicapas metálicas y

heteroestructuras magnéticas diluidas"

Autor: Rocío Ranchal Sánchez

Director: Eloísa López Pérez - Claudio Aroca Hernández-Ros

University: Universidad Complutense de Madrid, Fac. Ciencias Físicas, 2006

Grade: Sobresaliente "Cum Laude"

8.5 B.Sc. Thesis

Title: "Desarrollo de matrices de detectores cuánticos tricolor en el infrarrojo medio utilizando ataque por

iones reactivos (RIE)"

Autor: Raquel Gargallo Caballero
Director: Álvaro de Guzmán Fernández

University: Universidad Politécnica de Madrid, E.T.S,. Ing. de Telecomunicación

Date: September 7th, 2004 Grade: Matrícula de Honor, 10 p.

Title: "Desarrollo de sistemas electrónicos de detección de ultravioleta visible basados en sensores de

Nitruros del Grupo III""

Autor: Álvaro Navarro Tobar
Director: Elías Muñoz Merino

University: Universidad Politécnica de Madrid, E.T.S,. Ing. de Telecomunicación

Date: October 14th, 2004 Grade: Matrícula de Honor, 10 p.

Title: "Tecnologías de Dispositivos basados en Nitruros: diodos Schottky y filtros SAW

Autor: Roberto Cuerdo Bragado Director: Fernando Calle Gómez

University: Universidad Politécnica de Madrid, E.T.S,. Ing. de Telecomunicación

Date: September 23th, 2005 Grade: Matrícula de Honor, 10 p.

Title: "Desarrollo de Tecnologías de procesado asistido por plasma para nitruros III-V: RIE, y PECVD"

Autor: Eugenio Sillero Herrero Director: Fernando Calle Gómez

University: Universidad Politécnica de Madrid, E.T.S., Ing. de Telecomunicación

Date: September 23^{th,} 2005 Grade: Matrícula de Honor, 10 p.

Title: "Automatización de la medida del efecto Hall y aplicación a medidas de transporte electrónico"

Autor: José María Gutierrez Director: Adrián Hierro Cano

University: Universidad Politécnica de Madrid, E.T.S,. Ing. de Telecomunicación

Date: September 30th, 2005 Grade: Matrícula de Honor, 10 p.

Title: "Diseño e implementación de un sistema prototipo antirrobo de detección de etiquetas comerciales

para tiendas y centros comerciales"

Autor: José Miguel Díaz Maroto
Director: Claudio Aroca / Pedro Sánchez

Universidad Universidad Politécnica de Madrid, E.T.S,. Ing. de Telecomunicación

Date: October 19th, 2005 Grade: Matrícula de Honor, 10 p. Title: "Sistema y Control y Monitorización para reactor de epitaxia de haces moleculares (MBE)"

Autor: Gerardo Martinez Bernat
Director: Miguel Ángel Sánchez-García

University: Universidad Politécnica de Madrid, E.T.S,. Ing. de Telecomunicación

Date: December 22nd, 2005 Grade: Matrícula de Honor, 10 p.

Title: ""Análisis térmico mediante emisión infrarroja de transistores basados en Nitruro de Galio""

Autor: Andrés Tallos Tanarro Director: Elías Muñoz Merino

University: Universidad Politécnica de Madrid, E.T.S,. Ing. de Telecomunicación

Date: February 15th, 2006 Grade: Matrícula de Honor, 10 p.

Title: "Desarrollo de un Sistema de Adquisición y Procesado de Imágenes de Corriente Inducida por Haz de

Electrones (EBIC)"

Autor: Javier Carretero Moya Director: Adrián Hierro Cano

University: Universidad Politécnica de Madrid, E.T.S., Ing. de Telecomunicación

Date: September 18^{th,} 2006 Grade: Matrícula de Honor, 10 p.

Title: "Desarrollo de sistemas optoelectrónicos integrados basados en Nitruros del Grupo III para

aplicaciones en Biofotónica"

Autor: Iciar Sarasola
Director: Elías Muñoz Merino

University: Universidad Politécnica de Madrid, E.T.S,. Ing. de Telecomunicación

Date: December 20th, 2006 Grade: Matrícula de Honor, 10 p.

8.6 Patents

Inventors: David Ciudad Río-Pérez, Claudio AROCA Hernández-Ros, Pedro Sánchez Sánchez, Mª. del

Carmen Sánchez Trujillo, Eloísa López Pérez.

Title: Low frequency emitter – receptor system for intelligent contactless cards.

Number of Request: P200402437
Country of Priority: Spain
Date of Priority: 2.004

Entidad titular: Universidad Politécnica de Madrid

Countries to which it has spread: Spain

Inventors: Carlos Angulo Barrios.

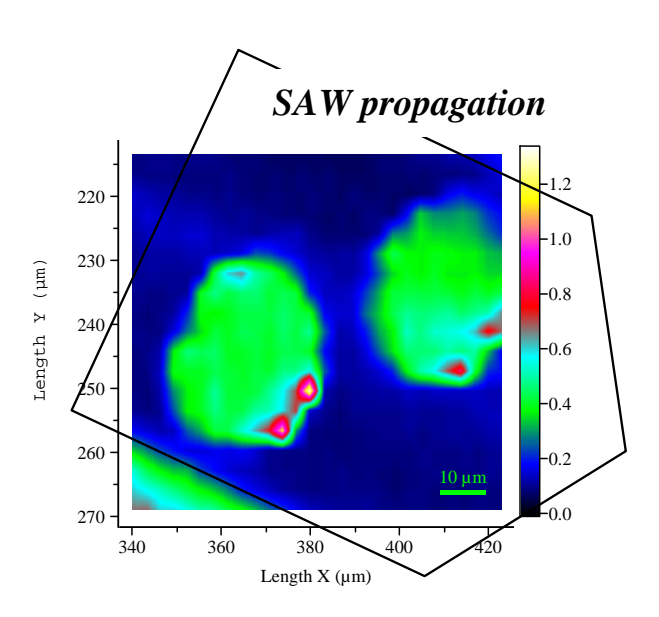
Title: Nuevo sensor óptico integrado de deflexión mecánica de ultra-alta sensibilidad

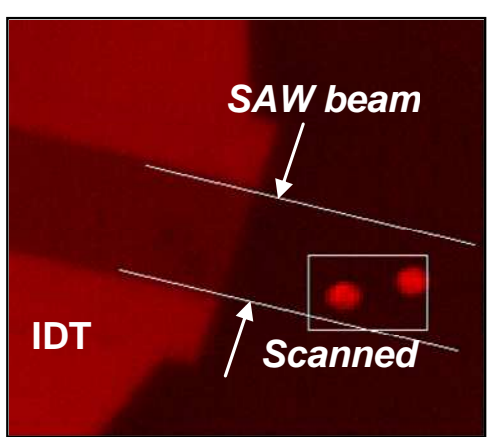
Number of Request: P200602724
Country of Priority: Spain
Date of Priority: 2.006

Entidad titular: Universidad Politécnica de Madrid

Countries to which it has spread:

9 R&D COLLABORATIONS, SERVICES AND SEMINARS





Top: Imaging of the photoluminescence (PL) quenching in an homogeneous GaN surface with sparse Ga-droplet footprints under the propagation of a SAW. The acoustic transport of photocarriers is partially disrupted at the outgoing boundary of the footprint, as shown by the local enhanced recombination.

Bottom: Experimental configuration of the PL mapping; the interdigital transducer (IDT) launches a SAW which propagates across the scanned area shown in the top figure.

[In collaboration with the Paul-Drude-Institut für Festkörperelektronik (Germany)]

9.1 International

- Centre de Recherche sur L'Hétéro-epitaxie et ses Applications, CRHEA-CNRS, (Valbonne, France)
- Cornell University (USA)
- Ghent University (Ghent, Belgium)
- INTEC/IMEC (Leuven, Belgium)
- Laboratoire d'Analyse et Aplications des Systèmes LAAS-CNRS, (Toulouse, France)
- Massachusetts Institute of Techonology, M.I.T (USA)
- Northwestern University, (USA)
- Paul Drude Institute (Berlin, Germany)
- Technische Universiteit Eindhoven (The Netherlands)
- Thales (Thomson CSF), (France)
- The University of Sheffield (U.K.)
- The University of Cambridge (U.K.)
- The University of California, Santa Bárbara (USA)
- University of Colorado at Boulder (USA)
- Walter Schottky Institut Technical University of Munich (Germany)
- West Virginia University (USA)
- University of Wisconsin-Madison (USA)
- Eidgenössische Technische Hochschule (ETH), Zürich (Switzerland)
- Friedrich-Alexander University Erlangen-Nurember (Germany)
- University of Surrey (U.K.)
- Ecole Politechnique Federale de Lausane (Switzerland)
- University of Darmstadt (Germany)
- Wake Forest University (USA)
- Purdue University (USA)

9.2 National

- Centro Nacional de Microelectrónica Instituto de Microelectrónica de Barcelona IMB-CNM. CSIC
- Centro Nacional de Microelectrónica Instituto de Microelectrónica de Madrid IMM-CNM-CSIC
- CIDA (Centro de Investigaciones de la Armada)
- CIEMAT (Centro de Investigaciones Energéticas y Medio Ambientales)
- INDRA Sistemas, S.A.
- Instituto de Física Aplicada Centro de Tecnologías Físicas «Torres Quevedo » CSIC
- Instituto de Estructura de la Materia- Centro de Física « Miguel Antonio Catalán »-CSIC
- INTA (Instituto Nacional de Tecnología Aeroespacial)
- Mondragón Corporación Cooperativa (Ikerlan, Orkli
- SIMAVE S.A.
- TUDOR-EXIDE
- Universidad Autónoma de Madrid
- Universidad Carlos III de Madrid
- Universidad Complutense de Madrid
- Universidad de Barcelona, Dpto. Electrónica
- Universidad de Cádiz, Centro de Microscopía Electrónica
- Universidad de Oviedo.
- Universidad de Valencia
- Universidad Politécnica de Madrid, SSR Department (ETSI. Telecomunicación)
- Universidad Rey Juan Carlos.

9.3 Cooperation and Services

- Centre de Recherche sur L'Hétéro-epitaxie et ses Applications, CRHEA-CNRS (Valbonne, Francia)

Researchers: Dr. P. Gibart and Dr. P. de Mierry

Research line: Reflectivity Measurements for Bragg reflectors for LEDs

Researcher: Dr. F. Omnes

Research line: Materials for UV detectors and HEMT transistors.

Researcher: Dr Z. Bougrioua.

Research line: Wafers for HEMT transistors.

Researcher: Dr B. Damilano
Research line: GalnNAs laser diodes

Centro de Investigación y Desarrollo de la Armada, CIDA

Researchers: Dr. M.T. Montojo and Dr. G. Vergara

Research Line: Far IR detectors

Centro de Investigaciones Energéticas y Medio Ambientales, CIEMAT

Researcher: Dr. J. Cárabe

Research Line: Surface Measurements by SEM

Researcher: Dr. M.T. Gutiérrez

Research Line: Hall Measurements at different temperatures

Resistivity Measurements

Researcher: Dr. A. Martínez

Research Line: SEM Measurements and compositional analysis by means of EDS

Researcher: Dr. F.L. Tabarés

Research Line: Plasma fusion wall interactions

European Synchrotron Radiation Facility (ESRF), Grenoble (France)

Researcher: Dr. G. Martínez Criado

Research Line: Lithography

FTIR measurements.

Instituto de Energía Solar (UPM)

Researcher: Dr. C. Algora

Research Line: PL measurements on materials for solar cells

X-Ray diffraction measurements on materials for solar cells

C-V characterization for solar cells

Hall measurements

Researcher: Dr. I. Rey-Stolle

Research Line: Rocking-Curve Measurements

Researcher: Dr. B. Galiana
Research Line: Hall Measurements

Researcher: Dr. C. del Cañizo Nadal
Research Line: Ellipsometry Measurements

Instituto de Estructura de la Materia (CSIC).

Researcher: Dr. V.J. Herrero
Research Line SEM Measurements.

Instituto de Física Aplicada (CSIC).

Researcher: Dr. I. Sayago
Research Line Lithography

Instituto de Microelectrónica (CSIC).

Researcher: Dr. L. González Sotos

Research Line Processing of Semiconductor Nanostructures as components for Quantum

Information.

Universidad Complutense de Madrid, Facultad de Ciencias Físicas,

Researcher: Dr. G. González

Research Line Metallization processes

Researchers: Dr. M.E. López Pérez and Dr. M.C. Sánchez Trujillo

Research Line: Photolitography processes

Surface and Structural Characterization

Magnetic sensors

Researcher: Dr. E. San Andrés

Research Line: Ellipsometry measurements

Universidad Miguel Hernández

Researcher: Dr. S. Fernández de Ávila

Research Line: Metallization and Characterization of hybrid polymers-nanoparticles systems to be

used in photodetectors and photovoltaic devices.

Universidad de Oviedo, Dpto. Química Analítica

Researcher: Dr. R. Badía

Research Line: Polimers Deposition for Chemical Sensors.

Researcher: A. Fernández González

Research Line: Imprinted sol-gel films characterization by means of FTIR, AFM, SEM and

ellipsometry.

Universidad del País Vasco.

Researcher: Dr. F. Plazaola

Research Line Metallization processes and Hall measurements

Universidad Politécnica de Madrid, Dpto. Ciencia de Materiales, ETSI Caminos

Researcher: Dr. M. Elices, Dr. J.M. Atienza.

Research Lines: Metallic evaporations

SEM measurements

Universidad Rey Juan Carlos, Madrid.

Researcher: Dr. A.L. Álvarez

Research Line Pulsed I-V measurements.

Thickness measurements for organic films

Universidad de Salamanca

Researcher: E. Diez Fernández

Research Line Processing of InGaAs/InAlAs quantum wells grown by MBE and AlGaAs/GaAs

superlattices

Universidad de Valladolid

Researcher: Dr. M.L. Rodríguez Méndez

Research Line Gas sensors based on magnetostrictive cantilevers and organic semiconductors.

University of Surrey (U.K.)

Researcher: Dr. P. Sellin

Research line: Fabrication of ionising radiation detectors

9.4 Stays abroad of ISOM members

D. Jorge Pedrós Ayala <i>"Ferdinand-Braun-Institut fü</i> Berlín	r Höchstfrequenztechnik " Germany	2004	9 weeks
D ^a . Jelena Ristic " Paul Drude Institut für Fest Berlín	körperlektronik" (PDI) Germany	2004	4 weeks
D. Carlos Rivera de Lucas "Paul Drude Institut für Fest Berlín	körperlektronik" (PDI) Germany	2004	9 weeks
D. Jorge Pedrós Ayala "Paul Drude Institut für Fest Berlín	körperlektronik" (PDI) Germany	2004	8 weeks
D. Fernando González Posada "Institute for Microstructural Ottawa		2005	12 weeks
D. Álvaro de Guzmán Fernánd "Paul Drude Institut für Fest Berlín		2005	8 weeks
D. Javier Miguel Sánchez "Paul Drude Institut für Fest Berlín	körperlektronik" (PDI) Germany	2005	2 weeks
D. Juan Pereiro Viterbo "Institute of High Pressure F Warsaw	Physis Polish Academy of S Poland	Sciences " 2005	8 weeks
D. Jorge Pedrós Ayala "Paul Drude Institut für Fest Berlín	körperlektronik" (PDI) Germany	2005	13 weeks
D. Enrique Calleja Pardo "Paul Drude Institut für Fest Berlín	körperlektronik" (PDI) Germany	2005	1 week
D. Eugenio Sillero Herrero "University of Darmstadt" Darmstadt Germany	ı	2006	13 weeks
D. Roberto Cuerdo Bragado "Walter Schottky Institut", To Munich	echnical University of Muni Germany	i ch 2006	3 weeks
Lucas Pérez García " <i>Paul Drude Institut für Fest</i> Berlín	körperlektronik" (PDI) Germany	2005-2006	78 weeks

9.5 Programme Committees Membership

Fernando Calle

Member of Steering Committee, Sessions Chairman

European Heterostructure Technology Workshop, HETECH Crete, Greece (2004)

Fernando Calle

Member of International Advisory Committee, Session Chairman

International Conference on Materials for Microelectronics & Nanoengineering, MFMN Southampton, UK (2004)

Elías Muñoz

Member of the International Committee

5th International Symposium on Blue Laser and Light Emitting Diodes (ISBLLED-2004) Gyeongju, Korea (2004)

Enrique Calleja

Member of the Conference Committee Board

27th International Conference on the Physics of Semiconductors (ICPS-27) Flagstaff, USA (2004)

Enrique Calleja

Session Chairman

4th International Conference on Physics of Light-Matter Coupling in Nanostructure St. Petersburg, Russia (2004)

Enrique Calleja

Member of the Conference Committee Board

5th International Symposium on Blue Laser and Light Emitting Diodes (ISBLLED-2004) Korea (2004)

Enrique Calleja

Member of the Conference Committee Board

International Conference on Molecular Beam Epitaxy (MBE-2004) Edimburg, UK (2004)

Fernando Calle

Member of Jury Committee

COIT Prizes for Thesis and Career Projects Madrid, Spain (2005)

Fernando Calle

Chairman of the Organizing Comittee, Session Chairman

2nd Research and Technological Development Meeting at ETSIT-UPM Madrid, Spain (2005)

Fernando Calle

Member of Steering Committee

European Heterostructure Technology Workshop, HETECH Smolenice, Slovakia (2005)

Fernando Calle

Member of the Program Committee

Spanish Meeting on Telecommunication (Telecom I+D) Málaga-Madrid, Spain (2005)

Elías Muñoz

Member of the International Advisory Committee

WOCSDICE 2005 Cardiff, U.K. (2005)

Elías Muñoz

Member of the International Advisory Committee

International Conference on Nitride Semiconductors, ICNS-6 Bremen, Germany (2005)

Elías Muñoz

Member of the Programme Committee

International Symposium on Compound Semiconductors ICSC Fribourg, Switzerland (2005)

Enrique Calleja

Session Chairman

13th European Workshop on Molecular Beam Epitaxy Grindelwald, Switzerland (2005).

Enrique Calleja

Member of the Conference Committee Board

13th European MBE Workshop on Molecular Beam Epitaxy Switzerland (2005)

Enrique Calleja

Member of the Conference Committee Board

6th International Conference on Nitride Semiconductors (ICNS-6) Bremen, Germany (2005)

Fernando Calle

Member of Jury Committee

COIT Prizes for Thesis and Career Projects Madrid, Spain (2006)

Fernando Calle

Member of the Program Committee

Spanish Meeting on Telecommunication (Telecom I+D) Madrid, Spain (2006)

Fernando Calle

Session chairman

Amena Chair Meeting Madrid, Spain (2006)

Fernando Calle

Member of Steering Committee, Sessions Chairman

European Heterostructure Technology Workshop, HETECH Manchester, UK (2006)

Fernando Calle

Member of International Advisory Committee, Session Chairman

International Conference on Materials for Microelectronics & Nanoengineering, MFMN Cranfield, UK (2006)

Elías Muñoz

Member of the International Advisory Committee

6th International Symposium on Blue Laser and Light Emitting Diodes (ISBLLED-2006) Montpellier, France (2006)

Elías Muñoz

Member of the International Advisory Committee

EWN-2006

Crete, Greece (2006)

Elías Muñoz

Member of the International Advisory Committee

International Workshop on NItrides

Kyoto, Japan (2006)

Enrique Calleja

Member of the Conference Committee Board

6th International Symposium on Blue Laser and Light Emitting Diodes (ISBLLED-2006) France (2006)

Enrique Calleja

Member of the Conference Committee Board

8th Int. Workshop on Expert Evaluation & Control of Comp. Sem. Mat. Tech. (EXMATEC) Cadiz, Spain (2006)

Enrique Calleja

Member of the Conference Committee Board

International Workshop on Nitride Semiconductors (IWN 2006) Kyoto, Japan (2006)

9.6 Invited Seminars held at ISOM

D. Miguel Ángel Álvarez Bernardo

"Quantum Cascade Lasers - Multilayer Semiconductor Injection Lasers"

ETSIT

March 26th, 2004

D. Andrés Díaz Gil

"Un paseo por el Universo"

Departamento de Física Teórica. UAM

April 2nd, 2004

D. Fernando Rodríguez González

"Micro-electro-mechanical systems (MEMS)"

ETSIT

April 16th, 2004

Dr. Mark Hopkinson

"Dilute Nitrides"

Universidad de Sheffield (U.K.)

May 12th, 2004

Dr. Rafael J. Jiménez Riobóo

"Luz para medir el sonido. (Espectroscopía óptica y propiedades elásticas

Instituto de Ciencia de Materiales de Madrid (CSIC)

May 7th, 2004

D. Stephane Gouraud

"Tertiary-Butyl-Chloride assisted Selective MOVPE Growth of Semi-Insulating Fe-doped InP applied to the fabrication of Electroabsorption Modulators on InP substrate"

University of Clermont-Ferrand, Clermont-Ferrand, (Francia)

December 10th, 2004

Dr. Laurent Cerruti

"Sb-based VCSEL in the 2-2.5 micron wavelength range"

Center of Electronics and Micro-optoelectronics. University of Montpellier, Univ. of Montpellier; (Francia) December 17th, 2004

D. Antonio Bazan Sulzberger

"Desarrollo de Transductores Ultrasónicos de Potencia con Radiadores de Placa para Procesos Industriales en Líquidos"

Instituto de Acústica, Consejo Superior de Investigaciones Científicas, Madrid (Spain) July 1st, 2005

Dr. Martin Stutzmann

"III-Nitride research at the Walter Schottky Institut: an Overview"

Walter Schottky Institut, Munich (Germany)

October 25th, 2005

D. Francisco Javier Blanco

"Tecnologías Microfluídicas y sus Aplicaciones"

IKERLAN, Madrid (Spain)

December 2nd, 2005

Dr. Tomás Apóstol Palacios Gutiérrez

"Nuevos Transistores de Nitruros para Aplicaciones a 40, 60 y 94 GHz"

Electrical and Computer Engineering Department, University of California Santa Barbara (USA)

December 15th, 2005

Dr. Adriana Gil

"Microscopía de campo cercano, herramienta clave para la Nanotecnología"

NANOTEC ELECTRÓNICA, Madrid (Spain)

December 20th, 2005

Dr. Héctor Guerrero Padrón

"Nanotecnología para los Sectores Aeroespacial y Defensa"

Instituto Nacional de Técnica Aeroespacial, Madrid (Spain)

January 20th, 2006

Dr. Martin Eickhoff

"Biochemical Analytics with Group-III Nitrides"

Walter Schottky Institut, Technische Universität Manchen, Munchen (Germany) January 23th, 2006

Prof. T. Suski, M. Leszczynski

"Nitride semiconductors: Review on Research Carried on at the Institute of High Pressure Physics and TopGaN"

The Institute of High Pressure Physics and TopGaN (Poland), Varsaw (Poland)

February 03th, 2006

Dr. Isabel Tanarro

"Plasmas reactivos a baja temperatura: Caracterización y diagnóstico"

Instituto de Estructura de la Materia, CSIC, Madrid (Spain)

February 17th, 2006

Prof. Peter Kordoš

"Research activities of the Institute of Electrical Engineering, Slovak Academy of Sciences, particularly on GaAs-based QWIPs and GaN-based MOSHFETs"

IEE SAS, Bratislava (Slovakia)

May 10th, 2006

D. Jorge Julián Sánchez Martínez

"Fotónica para seguridad y defensa: Aplicaciones y tendencias"

Sistema de Observación y Prospectiva Tecnológica de Defensa SDG-TECEN (Ministerio de Defensa), Madrid (Spain)

May 26th, 2006

Prof. Pierre Lefebyre

"Some subtleties of GaN and ZnO based quantum wells and quantum dots"

Directeur de Recherche – CNRS. Groupe d'Etude des Semiconducteurs. Universite Montpellier II, Montpellier (France)

June 23th, 2006

Prof. Martin Spaeth

"The beneficial role of defects in digital radiography"

University of Paderborn, Paderborn (Germany)

October 20th, 2006

Prof. Holger Grahn

"Prospects of group-III nitrides with nonpolar surfaces"

Paul-Drude-Institut für Festkörperelektronik, Berlín (Germany)

November 29th, 2006

Dr. Fumitaro Ishikawa

"Molecular beam epitaxial growth window for high quality (Ga,In)(N,As) quantum wells for 1.55 mm emission"

Paul-Drude-Institut für Festkörperelektronik, Berlín (Germany)

December 01st, 2006

9.7 Internal Seminars by ISOM members

D. Jorge Pedrós Ayala

"Anisotropic surface accoustic wave propagation in GaN and AlGaN/GaN heterostructures grown on sapphire" February 23rd, 2004

D. Carlos Rivera de Lucas

"Detectores de visible y ultravioleta basados en pozos cuánticos de InGaN/GaN"

February 6th, 2004

D. David López-Romero

"Diseño y fabricación de redes de difracción submicrónicas para acoplo de luz QWIPs en el infrarrojo medio" February 3rd, 2004

D. Pedja Mihailovic

"Magnetic field and electric current measurements using Faraday effect"

February 20th, 2004

D. Javier Miguel Sánchez

""Crecimiento de InGaAsn sobre sustratos de GaAs por Epitaxia de Haces Moleculares"

February 23rd, 2004

D. Miguel Ángel Álvarez Bernardo

"Quantum Cascade Lasers - Multilayer Semiconductor Injection Lasers" "

March 25th, 2004

Dª. Jelena Ristic

"Crecimiento de nanoestructuras III-V: Estudio de nucleación"

April 24th, 2004

Dª. Esperanza Luna García de la Infanta

"Desarrollo de detectores de infarrojo fotovoltaicos, de pozo cuántico y doble barrera para la bandas 3-5 micras" April 30th, 2004

D. Eugenio Sillero Herrero

"Silicon Nitride by Plasma Enhanced CVD"

June 18th, 2004

D. José María Ulloa

"Dominant carrier recombination processes in GalnNAs/GaAs QW light-emitting diodes"

June 25th, 2004

D. Raúl Pecharromán Gallego

"Investigations of the luminiscence of GaN and InGaN/GaN quantum wells"

October 29th, 2004

D. Javier Grandal Quintana

"Indium Nitride layers grown on silicon substrates by PA-MBE"

November 5th, 2004

D. Alejandro Braña de Cal

"Seminario de seguridad y uso de la Sala Blanca del ISOM"

November 12th, 2004

D. Sergio Fernández Garrido

"GaN/AIGAN Nanocavities with AIN/GaN Bragg Reflectors Grown in AIGAN Nanocolumns by Plasma Assisted MBE for Ultraviolet Emitting Devices"

November 19th, 2004

Dª. Fátima Romero Rojo

"Tecnología de fabricación de HEMTs de AlGaN/GaN"

November 26th, 2004

D. Juan Pereiro Viterbo

"InGaN - based photoconductors and photodiodes grown by molecular beam epitaxy"

January 14th, 2005

D. Jorge Pedrós Ayala

"Interaction of surface acoustic waves with light in GaN heterostructures"

January 21st, 2005

D. Carlos Rivera de Lucas

"Strain-Confinement in Mesoscopic Devices: Application to Nanocolumnar GaN/AlGaN Quantum Discs Grown by MBE"

February 4th, 2005

D. Álvaro Navarro Tobar

"Desarrollo de sistemas electrónicos de detección de ultravioleta y visible basados en sensores de nitruros del Grupo III"

February 1st, 2005

D. Javier Miguel Sánchez

"Estudio de las propiedades ópticas y estructurales de defectos sobre GaAs (111)B bajo diferentes microscopías" February 8th, 2005

D. Sergio Fernández, D. Juan Pereiro, D.Javier Miguel Sánchez, D.Jose María Ulloa

"Presentación de pósters para el congreso EURO-MBE 2005"

March 3rd, 2005

Dª. Jelena Ristic

"Growth and fabrication of nanocolumnar GaN diode structures"

March 10th, 2005

D. José María Ulloa

"Impact of N on lasing characteristics of Galn(N)As/GaAs heterostructures emitting between 1.3 and 1.5 um" March 18th, 2005

Dª. Rocío Ranchal Sánchez

"Estudio y optimización de películas delgadas de La0.5Sr0.5TiO3-d"

April 1st, 2005

D. Miguel Montes Bajo

"Generación de pulsos cortos y ultra cortos en láseres de estado sólido mediante Q-Switch pasivo" April 8th, 2005

D. Oscar de Abril Torralba

"Estructuras magnéticas submicrométricas obtenidas mediante procesos electroquímicos" April 15^{th,} 2005

D. José María Ulloa

"Diseño, fabricación y caracterización de diodos láser basados em pozos cuánticos de InGaAs(N)/GaAs"
April 22nd ,2005

D. Álvaro Navarro Tobar

"Exactitud, precisión, y ruido electrónico en fotodetectores"

June 17th, 2005

Dª. Raquel Gargallo Caballero

"Diseño, crecimiento por MBE y caracterización de QDs de InAs o InGaAs orientados al desarrollo de QDIPs" June 24th, 2005

D. Juan Pereiro Viterbo

"Crecimiento y caracterización de filtros ópticos de InGaN para su posterior integración en fotodetectores basados en estructuras p-i-n de InGaN/GaN"

16/12/2005

D. Victor Gracia Verano

"Filtros Clásicos con Elementos Activos de Ganancia Unidad"

10/03/2006

Dr. Ana Bengoechea Encabo

"Magneto-óptica en redes periódicas ferromagnéticas"

17/03/2006

D. Roberto Cuerdo Bragado

"Caracterización de fotodetectores a alta temperatura"

24/03/2006

Dr. Lucas Pérez García

"Ferromagnetismo a temperatura ambiente en GaN dopado con Gd".

31/03/2006

D. Eugenio Sillero Herrero

"Selective etching of lattice matched AllnN/GaN structures for microsystem technology" 07/04/2006

D. Fernando González Posada-Flores

"SiC, Al2O3 and Si HEMT Structures Characterisation and Processing Impact on AlGaN Surface" 12/05/2006

Dª. Raquel Gargallo Caballero

"Crecimiento por MBE de patrones auto-organizados de GaAs sobre sustratos GaAs(111)B desorientados usando nitruros diluidos"

02/06/2006

D. Andrés Redondo Cubero

"Ion beam analysis of GaN-based heterostructures"

09/06/2006

D. Diego Alonso Álvarez

"Aplicación de AES y XPS al estudio de dispositivos electrónicos basados en GaN"

9/06/2006

Dr. José Luis Prieto Martin

"Introducción a la Spintrónica: ¿Qué podemos hacer en el ISOM"

30/06/2006

9.8 Scientific workshops and meetings organized by ISOM members.

On May 22, 2006, a meeting on Optoelectronics jointly organized by the National Science Council of Taiwan and UPM-ISOM took place at *ETSI Telecomunicación* premises. The event was promoted by the UPM Vicerector for Research and by the Taiwan Science and Technology Office in Paris. A total of 10 presentations were given by scientist from various scientific institutes and universities in Taiwan and by ISOM members. The event was held as one step to foster the cooperation between Taiwanese and UPM-ISOM scientists in the area of optoelectronics.

FUNDING INSTITUTIONS



Our institute has all the facilities for a clean and reliable optical lithography process. We have two mask aligners in our class 100 lithography room. In the same room we have two chemical benches, one with the spinner and two digital hot-plates and the other with all the developing facilities. Although the institute has plenty masks for many different processes and devices, new ideas or configurations require alternative masks that can be designed in our CRESTEC CAB-9500C nanolithography tool.

Companies and Public Institutions

- ORKLI., S.COOP.
- Comunidad Autónoma de Madrid
- Exide-Tudor
- European Regional Development Fund (ERDF)
- European Space Agency ESA-ESTEC
- Fifth and Sixth Framework Programme for Research and Technological Development (EU)
- INDRA SISTEMAS S.A.
- Ministerio de Educación y Ciencia
- Ministerio de Industria, Turismo y Comercio
- Ministerio de Defensa-CIDA
- Mondragón Corporación Cooperativa
- Office of Naval Research (ONR-USA)
- ONERA (France)
- SeCretería de Estado de Educación, Universidades, Investigación y Desarrollo. Plan Nacional de I+D
- Borealis A/S
- CapSolva-Integrated Process Solutions Aps
- DICE Technologies
- ExxonMobil Chemical Europe
- Beiersdorf AG/ TESA AG

11 MEMBERS

(at January 2007)

Senior Researchers

Aroca Hernández-Ros, Claudio (caroca@fis.upm.es)
Calle Gómez, Fernando (calle@die.upm.es)
Calleja Pardo, Enrique (calleja@die.upm.es)
Laso Carbajo, Manuel (laso@diquima.upm.es)
López Pérez, Eloísa (elolopez@fis.ucm.es)
Merino Muñoz, Elías (elias@die.upm.es)
Sánchez Sánchez, Pedro (psanchez@fis.upm.es)
Sánchez Trujillo, Mª del Carmen (santruji@fis.ucm.es)

Ph.D. Students

Bengoechea Encabo, Ana Ma (abengo@die.upm.es) Ciudad Río-Pérez, David (dciudad@fis.upm.es) Cuerdo Bragado, Roberto (rcuerdo@die.upm.es) Durán Retamal, José Ramón (irduran@die.upm.es) Fernández Garrido, Sergio (sfernandez@die.upm.es) Gargallo Caballero, Raquel (rgargallo@die.upm.es) Glez-Guerrero Bartolomé, Miguel (mgonzalez@fis.upm.es) González-Posada Flores, Fernando (fposada@die.upm.es) Grandal Quintana, Javier (jgrandal@die.upm.es) López Romero, David (dlromero@die.upm.es) Montes Bajo, Miguel (mmontes@die.upm.es) Navarro Tobar, Álvaro (anavarro@die.upm.es) Pedrós Ayala, Jorge (jpedros@die.upm.es) Pereiro Viterbo, Juan (jpereiro@die.upm.es) Plaza Domínguez, Manuel (manuel@material.fis.ucm.es) Prieto Ortiz, Juan Luis (juanluis.prietoortiz@gmail.com) Rivera de Lucas, Carlos (crivera@die.upm.es) Romero Rojo, Fátima (fromero@die.upm.es) Sillero, Eugenio (esillero@die.upm.es) Utrera López, María (mutrera@die.upm.es)

Doctors

Angulo Barrios, Carlos (cbarrios@die.upm.es) Braña de Cal, Alejandro F. (abranha@die.upm.es) Fernández González, Álvaro de G. (guzman@die.upm.es) Foteinopoulou, Katerina (katerina @diquima.upm.es) Fuentes Iriarte, Gonzalo (gfuentes@die.upm.es) Hierro Cano, Adrián (ahierro@die.upm.es) Jiménez Martín, Ana (ajimenez@depeca.uah.es) Jimeno Aguilar, Nieves (jimeno@diquima.upm.es) Karagiannis, Nikolaos (nikos@diquima.upm.es) Maicas Ramos, Marco C. (maicas@fis.upm.es) Miguel Sánchez, Javier (jmiguel@die.upm.es) Pérez García, Lucas (lucas.perez@fis.ucm.es) Prieto Martín, José Luis (joseluis.prieto@upm.es) Ristic, Jelena (jelena@die.upm.es) Sánchez García, Miguel Ángel (sanchez@die.upm.es) Sanz Lluch, Mª del Mar (mmsanz@die.upm.es)

Administration and Technicians

Contreras González, Fernando (fcontreras@die.upm.es) García González, Óscar (oscar@die.upm.es) Juárez Migueláñez, Montse (montse.isom@die.upm.es) Padilla González, Isidoro (jpadilla@die.upm.es) Pérez de Lama, Mª Teresa (maite.isom@die.upm.es)

BSc. D. Students

Eroles Matallana, Javier (javier.eroles@die.upm.es) Morán Gómez, Soraya (smoran@die.upm.es) Tapia Reyero, Pablo (ptapia@die.upm.es)

External Collaborators

Abril Torralba, Óscar (oscar.deabril@fis.ucm.es)
Ranchal Sánchez, Rocío (rociran@fis.ucm.es)

